

10

Genotoxicity and Carcinogenic Potential of Carbon Nanomaterials

Todd A. Stueckle, Linda Sargent, Yon Rojanasakul, and Liying Wang

10.1

Introduction

Engineered carbon nanomaterials (ECNMs) have undergone broad technological developments in fields such as electronics, energy storage, structural materials, cosmetics, environmental remediation, medical diagnostics, and drug delivery [1, 2]. With such widespread incorporation into numerous products and uses, ECNMs' potential human exposure is to be expected during manufacturing, incorporation into other products, use, disposal, and release into the environment [3–5]. Carbon nanotubes (CNTs), a major group of carbon nanomaterials, exhibit a fibrous morphology and biopersistence similar to asbestos, a known human carcinogen, and potentially harbor asbestos-like lung cancer and mesothelioma risks associated with their long-term exposure. Several ECNMs are known to induce irreversible damage to exposed tissue (e.g., fibrosis) in animal models or cause genetic damage (i.e., genotoxicity) upon exposure to sensitive tissues/cells, a key first step at initiating tumorigenesis [6–8]. In addition, ultrafine carbon black (UFCB) and multiwalled carbon nanotubes (MWCNTs) have been identified as potential human carcinogens [9]. It raises urgent occupational, public, and environment safety and health concerns, and therefore a critical need exists to understand specific carbon nanomaterial-induced carcinogenesis potential as well as screen and evaluate methods based on that knowledge.

Lung cancer is the leading cause of cancer-related mortality, and has been largely associated with smoking and environmental carcinogen exposures. With a decrease in the smoking population in developed countries as a result of increased regulations and better control of atmospheric industrial particulates, the incidence of squamous lung carcinoma in the developed countries has seen a decline. However, the rate of adenocarcinoma in these countries has continued to increase, suggesting the rise of unknown environmental factors contributing to such occurrence [10–12]. Outdoor air pollution, a byproduct of anthropogenic activity, is responsible for a significant fraction of ultrafine carbon particulates (PM 2.5), which are considered a human carcinogen [13] and may contribute to

lung adenocarcinoma. Furthermore, exposure to man-made nanomaterials such as ECNNs may contribute to this development.

ECNNs possess novel and unique physicochemical properties that provide technological advantage over conventional materials, but they may also generate unknown health consequences (e.g., carcinogenesis) following their exposure. Assessing the carcinogenic effect of nanomaterials is a huge undertaking due to their rapid growth and great variety of nanomaterials. Guidelines for establishing a material's carcinogenic potential rely on human epidemiological data, confirmed cases in clinical reports, and animal studies. Studies can be qualitative and explorative in nature (i.e., yes or no) or quantitative (i.e., dose-response) to identify the lowest observed and nonobservable effective concentrations (i.e., LOEC and NOEC, respectively). At present, there is no human case of ECNN-induced cancer, and ECNN carcinogenic studies in animal models have only been conducted on a case-by-case basis [14]. These animal studies have used historical data with similar particles (i.e., fine TiO_2 and asbestos fibers) to justify their assessment of nano-sized TiO_2 and MWCNT. Very few engineered nanomaterials (ENMs) have undergone qualitative assessment for their carcinogenic potential (i.e., nano- TiO_2 , MWCNT), and no published studies have assessed their quantitative risk through expected exposure routes. The U.S. National Institute for Occupational Safety and Health (NIOSH) is currently conducting dose-response studies with MWCNTs, a known lung cancer and mesothelioma tumor promotor, in a mouse model [15].

With the exponential increase in novel ECNN development, there is an overwhelming and critical need to assess emerging ECNNs for their carcinogenic potential. With very few documented cases of chronic disease in humans linked to prolonged ECNN exposure, the best datasets at present are in sensitive animal models of tumor development and relevant *in vitro* screening models to investigate the unique physicochemical characteristics of ECNNs that can result in specific interactions and detrimental effects in exposed tissues [16].

The *main objective* of this chapter is to provide an overview of ECNN genotoxicity, neoplastic transformation, and tumorigenic potential, and how future ECNN carcinogenesis risk assessment can use current and developing cancer cell biology techniques to quickly screen and assess emerging nanomaterials. Here, we highlight key findings that form the basis of our current understanding of ENM-induced carcinogenesis and raise important issues that need to be addressed in future research. Focus of this chapter is on the pulmonary targets and related pulmonary responses, since the majority of human exposures to ENMs are via inhalation. Secondary effects as a result of ENMs' translocation into other tissues are also discussed. Subsequently, we describe how advances in *in vitro* neoplastic transformation and *in vivo* carcinogenesis models may be employed to screen suspected ENMs for neoplastic transformation and carcinogenic potential. Such information could be used to promote safe-by-design and prevention-by-design strategies that eventually enhance protection for occupational and environmental exposures and for long-term protection of the nanotechnology industry.

10.1.1

Engineered Nanomaterials and Long-Term Disease Risk: An Introduction

Documented or expected exposures to ENMs include occupational (laboratory and industrial raw material synthesis), ENM-enabled product manufacturing, industrial, consumer goods manufacturing, and end-of-life activities including recycling and waste disposal (e.g., incineration). Based on the projected estimates of nanotechnology use, release of ECNMs into the environment is expected [14]. Identified primary routes of ECNM exposure include inhalation as well as dermal and ingestion exposures [17, 18]. Because of their extremely small size and low biodegradable properties, inhaled ECNMs, such as MWCNTs, can deposit and be retained in deep alveolar tissue up to 336 days post exposure [19]. As such, potential long-term health effects such as carcinogenesis might be expected.

Thus far, there is limited evidence for ENM carcinogenesis. However, ENMs, once in contact with biological tissues, can harbor similar responses to their micrometer-sized or bulk counterparts in their ability to induce lung disease. Examples include crystalline silica versus nano-metal oxides and asbestos versus CNTs, which induce similar biological effects, including reactive oxygen species (ROS) generation, inflammation, genotoxicity, and fibrosis [20]. Because of their smaller size and increased reactivity, ENMs are expected to be even more potent and cause unpredictable toxicokinetics (e.g., uptake route) and biological responses. The strongest evidence to date for ENM carcinogenesis is the high-aspect-ratio nanomaterials (HARNs), which suggests that the current fiber pathogenicity paradigm, with some modifications, can give guidance for ENM carcinogenic risk assessment.

At present, no consistent framework exists to screen and assess ENM carcinogenicity. A vast majority of the published literature reports on acute exposure studies in both *in vitro* and *in vivo* systems, with little attention focused on long-term continuous or occasional/repeated exposures in occupational or public health exposure scenarios. In addition, a majority of published ENM toxicology studies report on observed toxicity at doses 10- to 1000-fold greater than the reported or suspected exposure levels [2, 21, 22]. Lack of exposure characterization studies with sensitive ENM analytical detection techniques accounts for part of this lack of appropriate dosing in some toxicological studies. Acute exposure studies have attempted to identify how different physicochemical properties impact toxicology. A percentage of these studies, however, use non-standardized materials, either from commercial supplies or synthesized in-house, with no well-studied control particle to compare across labs and other studies with similar ENMs. The results have been conflicting reports on known initiators and promoters of tumorigenesis, such as genotoxicity, ROS, and inflammation [23]. In addition, no consensus has been reached on the appropriate dose metric. Although mass is an easy and simple metric to use, it is usually not predictive of the effect. Surface area or particle number typically shows increased accuracy and precision in predicting the effect, but these metrics are hard to assess or

impractical for field studies, do not correlate with toxicity for some ENMs (e.g., graphene), or are under-reported in published literature.

A useful screening and prioritization paradigm for ENMs' carcinogenic potential is to conduct systematic studies in assessing model ENMs with different physicochemical characteristics [24]. They should either occur or predicted to occur with high exposure prevalence throughout its life cycle. By linking physicochemical characteristics with known initiation (i.e., genotoxicity) and promotion (i.e., tumorigenesis) effects, these data can then be used in quantitative structure–activity relationship (QSAR)-like predictive models. For example, the International Agency for Research on Cancer (IARC)'s recent establishment of Mitsui #7 MWCNT as a possible carcinogen suggests that the diameter and length may correlate with its tumor-promoting effect [9]. Examples of such strategies in other noncarbon ENMs exist. For example, nano-TiO₂ was found to be a more potent carcinogen than fine TiO₂ [25]. A robust and effective future carcinogenesis assessment framework for ECNM will rely not only on 2 years of dose–response studies [26] but also incorporate standardized genotoxicity tests, early disease screening models, and incorporation of new advances in *in vitro* and tissue culturing models to screen, assess, and predict ECNM carcinogenesis.

10.1.2

Carcinogenesis: A Multistep Process

As molecular and cellular biology tools advance, the tumorigenesis and cancer paradigm continues to evolve. Early studies indicated that DNA damage was an initial hallmark of potential tumor initiation but was not a good predictor since mammalian cells have robust machineries to repair or remove such damage if it occurs. Our current understanding of cancer is that it represents a combination of diseases, each with its own etiology and genomic signatures that rely on multiple factors for its growth and metastasis including interactions with other cell types, epigenetic factors, micro-RNA, and the tumor microenvironment [27]. Here, we aim to give an overview of the current carcinogenesis paradigm to allow toxicologists, biologists, and other researchers evaluating ENMs to understand what types of effects and data should be collected and evaluated. ENM exposures in reported human cases and *in vivo* models and the resulting adverse effects, namely ROS generation, inflammation, and hyperplasia, do suggest that some ENMs may possess carcinogenic potential.

Although advanced-stage cancers have their own unique genotypes and phenotypes, the working carcinogenesis paradigm relies on three broad steps for tumor growth within the human body: *initiation*, *promotion*, and *progression* [28]. A *carcinogen* is defined as a substance, either natural or anthropogenic in origin, which directly or indirectly induces or promotes cancer by damaging DNA or by altering normal cellular metabolic processes. A *genotoxic substance* can initiate tumorigenesis by causing DNA, chromosomal damage, aneuploidy, or mutation. A *co-carcinogen* is not genotoxic and is not tumorigenic, but can either amplify a genotoxic agent's ability to damage DNA, thereby modifying initiation

or enhance the cellular proliferation and altered gene expression associated with tumor promotion. The co-carcinogenic agent must be present at the same time as the carcinogenic agent. A *tumor promotor* is nontumorigenic on its own, but can increase the growth of DNA-damaged cells [29–35].

10.1.2.1

Genotoxicity and Initiation

Genotoxicity describes the property of an agent to damage or alter the genetic information (either DNA or chromosomes) within a cell, which may cause mutations that lead to cancer. Repeated exposure to a genotoxin can initiate carcinogenesis by increasing the mutation frequency resulting in genome instability, which allows changes in programmed cell death and cell survival signaling (Figure 10.1a). Along with DNA damage, nongenotoxic agents can cause epigenetic changes (e.g., DNA methylation) that can serve as initiating events, potentially leading to cancer. Spontaneous errors in replication, not due to genotoxic substance exposure, can lead to mutations and other genetic errors. Mutations greatly influence key regulatory pathways in lung adenocarcinomas

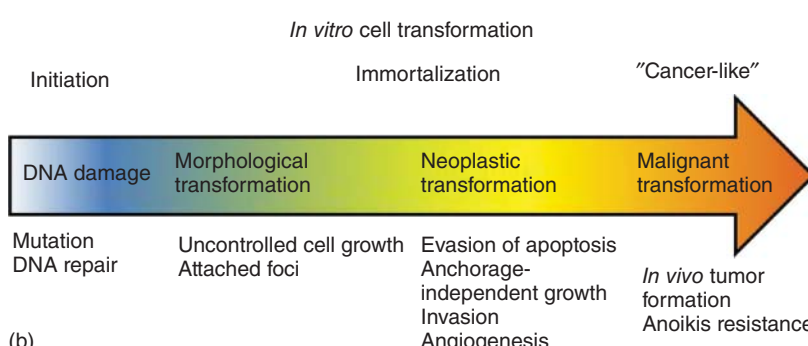
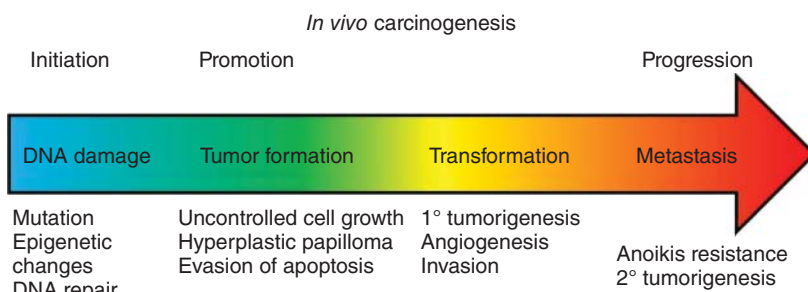


Figure 10.1 Evolution of carcinogenesis with key phenotypes following chromosome damage in mammalian cells. (a) *In vivo* carcinogenesis comprises three major stages, while

(b) *in vitro* cell culture transformation assays exhibit initiation and three separate stages of transformation. (Adapted and modified from [36].)

[37]. These mutations typically impact the signaling pathways involved in cell death, proliferation, DNA repair, and cell cycle. Initiation is the first step in the three-stage model of cancer development and is observed in both *in vivo* and *in vitro* models (Figure 10.1a and b). The end product of a tumor-initiating event is the inability to repair DNA damage, genomic instability, and potential survival advantage. However, a cell may still possess DNA repair ability. Since initiation is the result of permanent genetic change, any daughter cells produced from the division of the mutated cell will also carry the mutation [38]. Subsequent mutations and alterations in chromosome number and structure, which can occur during proliferation of a mutated population, can eventually lead to progression of the preneoplastic clone into frank neoplasms [31, 39].

Primary genotoxicity occurs through direct (i.e., DNA adduct) or indirect (i.e., ROS release from damaged mitochondria) mechanisms. Secondary genotoxicity occurs via other cell types interacting with a target cell. The inflammatory response, leukocyte recruitment, and respiratory burst ROS production from macrophages or polymorphonuclear leukocytes are typical and important responses to evaluate.

Numerous particles in the environment are known to induce direct and indirect mutations and oxidative damage of DNA [40]. Many studies report ROS generation from the particle surface itself (e.g., transition metal), interactions with cell components (e.g., altered mitochondrial membrane function), and inflammation response (i.e., neutrophils). Although studies report a dose–response of 8-oxo-7,8-dihydroguanine (8-oxodG) to numerous suspected mutagens, the chosen doses are usually extremely high and are not representative of known oral or inhalation exposures and modeled *in vivo* dose [40]. Depletion of antioxidant defenses (e.g., glutathione, catalase, superoxide dismutase) may also render exposed tissues susceptible to clastogenic DNA damage. Given the numerous direct and indirect genotoxicity modes of action, identifying both genotoxicity and epigenetic modifications to DNA must be a part of future efforts to effectively screen ECNMs for tumor initiation potential.

10.1.2.2

Promotion

Once a cell has been mutated or epigenetically modified by an initiator, it can experience greater sensitivity to the effects of promoters. These compounds promote the proliferation of the mutated cell, giving rise to a large number of preneoplastic or benign daughter cells containing the mutation created by the initiator. Briefly, cells that enter the promotion stage of carcinogenesis usually exhibit the inability to repair DNA damage, avoidance of cell death, enhanced proliferation through self-signals, resistance to tumor suppression factors, replicative immortality, and angiogenesis ability [27]. Clonal expansion of these cells *in vivo* results in the appearance of a papilloma-like tumor. Associated with these changes, late in the promotion phase is a *transformation* that impacts the visual appearance of both a single cell and a mass of cells, which is observable in both *in vitro* and *in vivo* carcinogenesis models. It is a continuous process

that contributes to various steps in the carcinogenic and metastatic processes. *Morphological transformation* relies on numerous cell signaling pathways (e.g., epithelial-to-mesenchymal transition, development signaling pathways) that remodel the neoplastic cell's cytoskeleton, resulting in changes in cell morphology, disorganized patterns in colony growth, and *in vitro* anchorage-independent growth (Figure 10.1) [36, 41]. *Neoplastic transformation* of an *in vitro* cell culture is characterized by the acquisition of most cancer cell hallmarks mentioned above, including invasion and angiogenesis. *Malignant transformation* describes a cell culture that has acquired the tumorigenic ability *in vivo* [36]. A large amount of research findings also support the role of chronic inflammation, inherent reprogramming of cell metabolism, and immune system evasion. Cells experiencing promotion will (i) undergo advancement toward progression and eventual cancer, (ii) continue to grow with no signs of aggression (e.g., benign growth), (iii) persist without further phenotypic advancement or reversal, or (iv) regress [42]. Few chronic ECNM *in vivo* exposures (e.g., MWCNT) show carcinogenesis or continued or arrested hyperplasia [15].

For preneoplastic cells to accelerate their proliferation, escape from tumor suppressor genes and death signaling pathways must occur. Decreased expression or post-transcriptional alterations to p53, p16, check point kinases, and RB1 can result in unregulated, accelerated growth. Conversely, activation of pro-survival signaling, including Ras, MAPK/ERK, Akt, and vascular endothelial growth factor (VEGF) pathways, promotes downstream enhancement of cell proliferation, apoptosis resistance, and angiogenesis. Many of these pro-survival/proliferation pathways are sensitive to changes in ROS/reactive nitrogen species (RNS) balance [43].

In vivo neoplastic growths and neoplastic transformation in cells *in vitro* usually involve not one single morphology or cell type. Rather, there is diverse clonal heterogeneity associated with most neoplasms, consisting of genetically damaged cells that drive and promote growth, while other associated cells experience the influence of these genetically damaged cells [42]. Out of the clonal heterogeneity has arisen the theory of cancer stem cells (CSCs). These cells are thought to have experienced genetic damage that has reversed differentiation and gained stem-cell-like properties including self-renewal, de- and differentiation into stem- and non-stem cell types, aldehyde dehydrogenase (ALDH) overexpression, overactive drug pumps (e.g., ABCG2), and apoptosis resistance signaling, which assist in the promotion and progression of precancerous growth [44].

Research studies routinely depict mixtures of different cell populations with evidence of phenotypic equilibrium within the tumor [45]. As with any other living system, a tumor consists of subpopulations of cells that can undergo population differences over time. Numerous aggressive cancers exhibit a small number of cancer cells with stem-cell-like properties, including the abilities to undergo self-renewal, resistance to death signals, and differentiation into other cell types. CSCs along with other non-stem-like cells exhibit unique surface markers that change over time as the tumor grows, encounters chemotherapeutics, and moves toward metastasis.

Our increased understanding of the tumor microenvironment has greatly impacted the view of cancer as not a single tumor cell type, but rather a unique mixture of primary tumor cells with CSCs, supported by other cell types including cancer-associated fibroblasts, leukocytes, endothelial cells (i.e., angiogenesis), and the extracellular matrix [42]. The broad diversity of heterogeneity, both histological and molecular, implies that cancers grow and evolve through a wide range of phenomena including differences in genetic abnormalities, promotion signaling, interaction with the tumor microenvironment, and epigenetic influences [42].

At present, carcinogenesis is not a simplistic view of one cell type growing to a large mass and metastasizing on its own. Rather, the carcinogenesis process and the resulting aggressive tumor are dependent on the tumor microenvironment: a collection of cancer cells, numerous non-cancer cells that support cancer cell growth, and the extracellular matrix. As our understanding of epigenetics and the tumor microenvironment evolves, the opportunities to develop carcinogenesis screening models early in the developmental process will potentially allow for effective ENM screening and prioritization for long-term carcinogenesis risk assessment studies.

10.1.2.3

Progression

This last stage of carcinogenesis is distinct from the promotion stage. Tumor progression involves more aggressive behaviors of tumor growth away from the site of the primary tumor and includes distinct morphology from preneoplastic hyperplasia, invasion, anoikis resistance, and metastasis (Figure 10.1) [27, 28]. Malignant tumors possess multiple heritable changes over the course of initiation and promotion, which collectively result in aggressive behaviors. It is important to note that several known human carcinogens do not cause initiation or promotion but may act as tumor progressors. A recent study showed that SWCNTs, at the least, have the ability to increase metastatic growth of lung carcinoma [46]. Use of early disease screening assays or models would not detect this phenomenon. ECNM carcinogenesis assessments must evaluate each major step of the carcinogenesis process using appropriate initiation, promotion, and progression models.

10.1.3

Current Knowledge and Challenges in Carcinogenesis Studies

Our understanding of carcinogenesis is continually evolving. This is partially based on key advancements in chemical, biological, and computational technologies that allow rapid development of new tools to study this complex disease. In the past, intracellular research has dominated oncology research in attempts to characterize and understand signaling pathways that control numerous cancer hallmarks. At the DNA regulation and genotoxicity level, evaluating how epigenetics, microRNA, and noncoding RNA influence carcinogenesis will dominate research in the coming years. By identifying additional tumor initiation

mechanisms, genomic biomarkers for early disease detection, screening, and preventive strategies can be developed.

Currently, a transition is under way, shifting from intracellular signaling to investigating carcinogenesis at the extracellular, tissue, and systems-biology levels. Tumor heterogeneity and the different cell types found in the tumor microenvironment may unlock key carcinogenesis mechanisms and identify the preventative targets. Key cell types under study include CSCs, cancer-associated fibroblasts, and several different leukocytes. From these studies, some of the first approved immunotherapies now show promising results in extending patient survival.

Lastly, the role of other health issues, namely environmental pollutants, nutrition, metabolism, and endocrine signaling impacting carcinogenesis, have taken the forefront in evaluating cancer at the systemic or exposome level. Environmental factors along with environmental xenobiotic exposures greatly influence the impact of neoplasm initiation events and the evolution of tumor growth [47, 48]. In addition, occupational exposure to known and suspected carcinogens greatly increases the duration and repeated exposure to documented DNA-damaging initiation agents, thereby greatly escalating the risk of carcinogenesis [48]. Understanding how ECNM exposure impacts the genetic tumor microenvironment and affects long-term health risk is a major challenge over the next few decades. Promising new techniques and models associated with these advances should be utilized in evaluating ECNM carcinogenesis.

10.2

Carbon Nanomaterials: Genotoxicity and Carcinogenic Potential

10.2.1

Physicochemical Properties of ECNMs

Nanotechnology development and research on the effects of ENMs within biological systems have largely focused on how distinct physicochemical properties impact the desired or adverse outcome. Identifying how changes in each property impact ENM bioactivity is the key to developing predictive models for effective and safe-by-design nanotechnology. Genotoxicity and carcinogenesis studies have and should further expand upon this strategy by developing systematic screening assays for each step of the carcinogenesis process.

Certain physicochemical properties of ECNMs such as CNTs, for example, their aerosolizability, biopersistence, and structural similarity to asbestos, which is a Group I human carcinogen [49, 50], may pose asbestos-like lung cancer and mesothelioma risk [20, 51]. According to the major U.S. think tank (RAND Corporation), widespread exposure to asbestos has been described as the worst occupational health disaster in U.S. history and the cost of asbestos-related diseases is expected to exceed \$200 billion. Predicting and preventing potential ENM-induced lung cancer has thus become a critical and urgent public health issue.

Size, shape, surface area, surface charges, and agglomeration/dispersion are all physicochemical properties of ECNMs that provide unique and novel technological applications. These same properties, however, can harbor unknown adverse health effects, including chronic diseases such as cancer, as described in this section for each major ECNM discussed. In addition to ECNMs' physicochemical characteristics, particle toxicokinetics (i.e., uptake, biopersistence, elimination/clearance and ultimate fate) must be evaluated since they will determine the internal dose. Translocation within the body away from the primary area of exposure must be considered given ECNMs' small size, surface charge, protein corona, and other physicochemical characteristics (e.g., hydrophobicity) that greatly impact toxicokinetics. Movement of ECNMs into blood circulation or lymphatic system may impact sensitive tissues and organs away from the exposed organs [52]. For example, several studies have reported ECNM presence in the liver, kidney, spleen, and bone marrow following pulmonary or other routes of exposure.

Furthermore, comparative studies within and across classes or groups of ECNMs are vital to identify those physicochemical properties that harbor enhanced genotoxic and cell transformation effects. These types of studies, however, are costly and, at present, do not fully consider vitally needed toxicokinetic and toxicodynamic effects following exposure. For example, a recent study performed a gastrointestinal exposure comparison of diesel exhaust, Printex 90 UFCB, fullerenes, and SWCNT [53]. Both oral instillation to rats and *in vitro* cell culture exposure of diesel exhaust elicited the largest amount of 8-oxodG followed by Printex 90, probably associated with oxidative damage from ROS generation. SWCNT and C60 fullerene showed little effect. Although informative in ranking different ECNMs against a particle exposure with robust literature, this did not report potential uptake differences or the potential role of other xenobiotics [e.g., metals or polycyclic aromatic hydrocarbons (PAHs)] on diesel exhaust effects. Here we highlight recent advances, findings, and short comings in assessing how differences in physicochemical properties impact ECNM carcinogenesis potential.

10.2.2

Ultrafine Carbon Black

Nano-scaled UFCB is widely and primarily used in rubber, plastics, inks, and paints. Occupational exposures usually consist of UFCB with known low levels of sorbed PAHs and metals [54, 55], and therefore its primary physicochemical property leading to adverse effects is its insoluble nature. Ultrafine particles with carbon core from combustion processes are known to cause lung damage following inhalation [56]. At present, carbon black is a Group 2B [57, 58] carcinogen, supported by numerous human epidemiology, *in vivo*, and *in vitro* studies. Its primary basis as a possible human carcinogen is due to elevated rates of lung cancer in workers in the carbon black manufacturing setting, although the available datasets are inconsistent at best. Most *in vivo* data conclude that UFCB is negative for mutagenicity. Prevailing theory for UFCB is indirect genotoxicity via oxidative damage caused by ROS release from infiltrating inflammatory cells.

DNA breaks, oxidized bases, and lipid peroxidation are frequently observed post exposure. Prevailing hypothesis for poorly soluble particles involves particle deposition, uptake via phagocytizing cells, improper clearance, release of pro-inflammatory cytokines and growth factors, inflammation, cell injury and proliferation, ROS release, oxidative damage, and DNA mutation leading to tumorigenesis [58, 59]. Ultrafine carbon particles are routinely found to harbor greater inflammation and ROS generating ability than fine and bulk carbon [60, 61]. Several studies have suggested that ROS [59, 62] generation occurs via direct generation on carbon core or other sorbed ROS-promoting xenobiotics. PAHs are usually tightly bound to the carbon core and pose reduced risk relative to free PAHs [54]. Regardless of other sorbed xenobiotics, long-term *in vivo* exposure studies with pristine carbon black have shown increased tumor incidence above unexposed controls [58].

10.2.2.1

In Vivo Studies

Extensive research and description of UFCB deposition, retention, and effects in murine models is available (reviewed by IARC [58]). DNA adducts are not frequently observed above control levels. If they do occur, they are usually particle/cell type-specific [54, 58, 59]. UFCB inhalation results in pro-inflammatory response in rats that is greater than with its fine particle counterpart [63]. A recent low-dose study (7 µg per dose) using multiple aspiration dosing in mice found massive macrophage infiltrate, increased phospholipids, collagen production, and enhanced IL-6 production [64]. Post-exposure chronic inflammation results in oxidized DNA [65, 66]. Additional studies have reported DNA strand breaks in lung and liver tissues following inhalation exposure of UFCB [67–70]. Recent dose–response research at doses below levels known to induce ROS from the inflammatory response indicates that UFCB can damage DNA in the bronchoalveolar lavage (BAL) and lung tissue cells [71]. Although inflammation was not present, low-dose Printex 90 could still generate intracellular ROS in target cells resulting in oxidative damage.

Several long-term inhalation and intratracheal (i.t.) instillation studies have reported that prolonged UFCB exposure causes a positive dose–response tumorigenesis in exposed lung tissue in rats at high doses but not in mice. The majority of these studies reported proliferating cysts with squamous cell morphology following exposure; however, its importance to lung cancer is unclear [58]. Rat lung tumor incidence at 30 months following a 24-month inhalation exposure ranged from 28% to 39% [72]. Conversely, a 9.5-month inhalation exposure study in mice found no difference compared to controls in lung tumor incidence [73]. Two separate groups of rats, exposed for 43 and 86 weeks, displayed 18% and 8% incidence above controls, respectively [74, 75]. The main difference in tumor rate between mice and rats is that mouse models are naturally resistant to particle-induced tumorigenesis [76, 77]. In addition, it has been suggested the rat's response is driven by the “overload phenomenon,” where particle number overloads the clearance ability, thus provoking inflammation, excessive ROS,

and lung tumor response [78]. In summary, the size and presence of the carbon core in carbon black are driving factors at moderate to high doses resulting in inflammation and ROS generation. Based on recent evidence of positive direct genotoxicity at doses well below inflammation, long-term inhalation studies should consider the potential absence of a robust inflammatory response in assessing tumorigenesis risk. This would also address issues associated with “overload” in sensitive *in vivo* tumorigenesis models.

10.2.2.2

In Vitro Studies

In general, *in vitro* studies suggest that UFCB (e.g., Printex 90) exposure causes ROS generation and is weakly to moderate mutagenic. Acute and subchronic exposure studies with murine cell lines resulted in increased mutation frequency in lacZ and cll transgenes, oxidized purines, strand breaks [79], induction of micronuclei (MN) and cytoskeleton disruption [80], hypoxanthine phosphoribosyltransferase (HPRT) mutations [81], and sister chromatid exchange accompanied by cell transformation [82]. Incubation of epithelial cells with activated neutrophils resulted in oxidative DNA lesions [83]. Human cell line exposures result in strand breaks and oxidative damage, although lung surfactant could mitigate these adverse effects [84, 85]. UFCB with sorbed benzo[a]pyrene (BaP) caused single strand breaks and cell cycle changes, NF-κB and AP-1 activation, and altered p53 phosphorylation [86]. Nanoparticles including urban dust are known to induce single and double strand breaks with subsequent p53 activation, similar to other known carcinogens [87]. The mutation spectrum associated with UFCB exposure suggests an ROS-mediated mechanism [88]. Prolonged UFCB exposure caused dose- and time-dependent proliferation due to stimulation of several ROS-sensitive signaling pathways in human bronchial epithelial cells [89]. A low-dose ($0.02 \mu\text{g cm}^{-2}$) 6-month UFCB exposure (Elftex 12) to small airway epithelial cells (SAECs) resulted in slow-growing cells with a pre-senescent transcriptome signature [90].

10.2.3

Carbon Nanotubes

As one of the most promising classes of ECNMs for use in numerous industrial, consumer, and biomedical applications, CNTs are poised for wide production and distribution over the next few decades. Although they possess favorable strength as well as electrical and mechanical properties, they have received some of the most skepticism due to concern regarding their striking similarities to asbestos fibers, a well-established human carcinogen. SWCNTs, double-walled carbon nanotubes (DWCNTs), and multiwalled carbon nanotubes (MWCNTs) possess high aspect ratio (HAR), fiber morphology, high surface area, and limited amount of transition-metal catalysts that contribute to their toxicity in exposed tissues. In addition to these asbestos-like qualities, they vary in their length, width, chirality, structural defect, surface charge, and functionalization, which impact their

toxicokinetics (i.e., protein corona formation and lipid partitioning), tissue distribution, and biopersistence. Upon exposure and deposition in deep airways and terminal bronchioles, CNTs elicit varying degrees of inflammation and ROS generation, resulting in granulomas and fibrosis, all with striking similarity to asbestos (reviewed below). Even though numerous similarities with asbestos exist, some *in vivo* and *in vitro* evidence suggests that CNTs may possess their own unique modes of action for long-term health consequences (i.e., fibrosis and cancer). Assessment of genotoxicity has shown that CNTs can damage DNA *in vitro* and *in vivo* [91]. CNTs disrupt mitosis by interrupting proper centrosome function, and create mono- and poly-polar centrioles, chromosome breaks, mutations, *in vitro* cell transformation, and *in vivo* tumor promotion. Recent IARC review labeled Mitsui #7 MWCNT (Hodogaya, Inc.) as a Group 2B carcinogen (possibly carcinogenic), while other SWCNTs and MWCNTs were placed in Group 3 (not classifiable) due to insufficient evidence [9]. Present research efforts strive to understand those physicochemical properties that influence adverse biological effects (i.e., fibrosis, tumor promotion) to provide information for “safe-by design” and/or “prevention-through-design” strategies for safe technological implementation of these unique ENMs. Here we review studies showing CNT-induced inflammatory and ROS generation, genotoxicity, and carcinogenic potential (Figure 10.2).

10.2.3.1

In Vivo Studies

A continuously evolving and published literature details pulmonary toxicological responses to CNTs upon i.t. exposure, pharyngeal aspiration, or inhalation exposure. Upon exposure, CNTs elicit macrophage activation, transient inflammation, neutrophil recruitment, ROS generation, partial clearance, interstitial penetration, biopersistence, epithelial Type II and fibroblast cell proliferation, onset of pulmonary fibrosis, immune suppression, DNA damage, and hyperplasia [17, 22, 92, 93].

Although no clear ENM-driven tumorigenesis mechanism has been described, we highlight those studies that point to potential initiation and promotion mechanisms that drive CNT exposure-associated tumorigenesis. In general, prolonged CNT exposure activates several known and possibly unknown mechanisms that may initiate and promote carcinogenesis. Mechanisms of HAR fiber carcinogenesis include mitotic disruption and DNA breaks, free-radical generation (i.e., ROS and nitric oxide synthase, NOS), stimulation of tumor-promoting cell signaling pathways, and chronic inflammation [17, 92, 94, 95]. It may be decades before ENM-fiber-associated human cancer is observed, if ever. The long latency period between asbestos exposure and mesothelioma development is possibly due to the multiple steps in genetic and cellular changes during carcinogenesis [96].

In consideration of the projected CNT life cycle, the highest risk exposure and the resulting adverse health effects, including potential tumorigenesis, are during CNT manufacturing, handling, and incorporation into other products [5, 22, 92]. Dry CNTs exhibit high dispersion into the air, suggesting that pulmonary

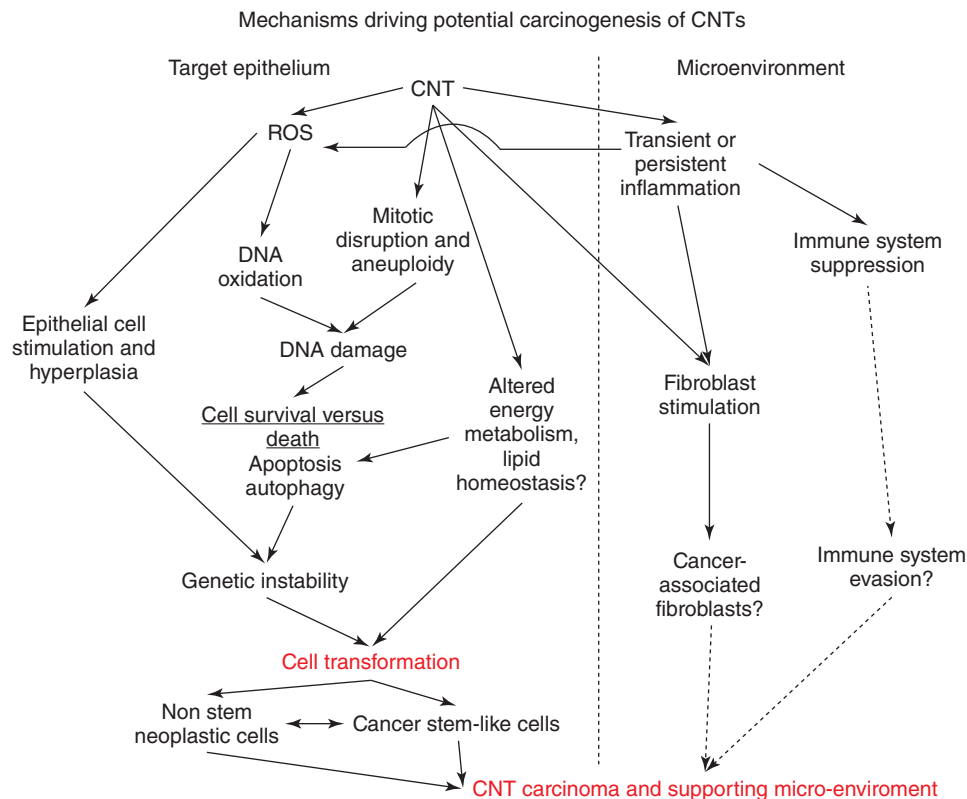


Figure 10.2 Mechanisms driving carbon nanotube carcinogenesis potential.

inhalation and dermal exposures are most likely. Several CNT occupational exposure studies report airborne concentrations and personal breathing zone of worker exposures of $>1 \mu\text{g m}^{-3}$ [21, 97, 98]. Airborne CNT concentrations in several U.S. manufacturing facilities average $10.6 \mu\text{g m}^{-3}$, with a majority near the NIOSH-recommended exposure limit of $1 \mu\text{g m}^{-3}$ [21]. These recent field studies show that $\geq 75\%$ of airborne CNTs are inhalable, but not respirable [21, 97, 98]. Administration of dispersed CNTs in either pharyngeal aspiration or inhalation exposure to model respirable fraction exposures results in deep lung deposition, primarily in terminal bronchioles and in the bronchiole/alveolar duct (BAD) region [99–101]. Alveolar macrophages, lung epithelial cells, and fibroblast cells are the first group of cells to interact with CNTs with different potential routes of cell uptake and interaction. CNTs interact with cells through either passive diffusion (i.e., random motion) or active uptake (i.e., phagocytosis). Each uptake route has implications for the overall effect and downstream signaling processes, leading to development of potential long-term health consequences.

Passive uptake of CNTs is due to Van der Waals forces and CNT surface–lipid membrane interactions (e.g., hydrophobicity) resulting in CNTs puncturing the

cells and persisting in the cytoplasm of cells. Direct interaction with cytoplasm and cellular structures has several important toxicological consequences for the affected cells. First, sorption and desorption of proteins to and from the protein corona may impact cell signaling and metabolic processes. Second, graphene surface may participate in redox reactions by either sequestering or assisting in the generation of ROS, thereby affecting ROS-sensitive signaling and/or cell damage. Lastly, CNTs show morphology similar to that of microtubules, suggesting that mimicry or interference of microtubule-associated processes may occur. Dinu *et al.* [102] demonstrated that tubulin associates with CNTs and that kinesin activity is impacted in the presence of CNTs. Both SWCNTs and MWCNTs were shown to integrate into the mitotic spindle and centrosome apparatus in human SAECs. Similar to asbestos [103], CNTs are able to disrupt mitosis, causing mono- or poly-polar centrosomes, resulting in chromosome breakage and aneuploidy [6, reviewed later].

Phagocytosis of CNTs can result in complete uptake and compartmentalization of CNTs within phagolysosomes. Several enzymes are capable of breaking down CNTs; however, their occurrence is cell-type-specific and is an extremely slow process. Rigid and long CNTs, however, are unable to undergo complete phagocytosis resulting in “frustrated phagocytosis” [104]. This phenomenon is also observed with asbestos fibers where macrophages are unable to completely engulf the HAR fibers. Phagosome rupture can cause cathepsin B release from damaged membrane, activating NLRP3 inflammasome and caspase-1, which in turn activates IL-1 β , an important inflammatory cytokine.

Pulmonary exposure to respirable fractions of MWCNTs results in deep penetration, alveolar and interstitial deposition, and extra-pulmonary translocation to subpleura and other sensitive organs. CNTs are known to experience penetration to subpleural tissue [105–108]. At present, it is unclear what adverse health effects inhalable fractions of MWCNT possess [21, 98]. Several reports demonstrated MWCNTs possessing an asbestos-like biopersistence ranging from months to 1 year post exposure [6, 19, 100, 101, 107, 109] and possibly longer. For example, Mitsui #7 MWCNT fate was evaluated in pulmonary and extra-pulmonary tissues at 1 and 336 days after a 12-day whole-body inhalation to 5 mg m⁻³ MWCNTs (49 nm width). At 336 days post exposure, 4.2% of the initial lung burden was found in the airways and 95.8% of the initial lung burden remained in the alveolar region, including 4.8% in the subpleural tissue region [19]. Singlet MWCNT was observed in several extra-pulmonary organs including the chest wall, diaphragm, kidney, and liver. Lymph nodes were especially noted as a significant site of MWCNT accumulation. Notably, tracheobronchial lymph nodes experienced an increase in MWCNT burden going from ~1% at day 1 to 7.3% at day 336 post exposure. A similar increase in extra-pulmonary deposition of MWCNT was observed in the chest wall, other lymph nodes, and organs. In addition, this study suggested that small MWCNT aggregates (>4 fibers) disassociate over time *in vivo*, resulting in persistent singlets that increased 10-fold over the course of the study. These studies highlights the fact that CNTs are not static in tissues once deposited at their primary site of exposure. It appears that through their

biopersistence and novel properties, they exhibit dynamic translocation ability and experience wide systemic distribution and may impact other sensitive areas with known tumor susceptibility. A recent study with ^{14}C -labeled MWCNTs (40 nm width) highlights this fact by finding MWCNTs deposited in spleen, liver, and bone marrow of mice following pulmonary aspiration at an occupationally relevant dose (20 μg bolus \sim 38 working years, Figure 10.3) [110]. Given that liver is sensitive to toxicants and many physiological functions depend on bone

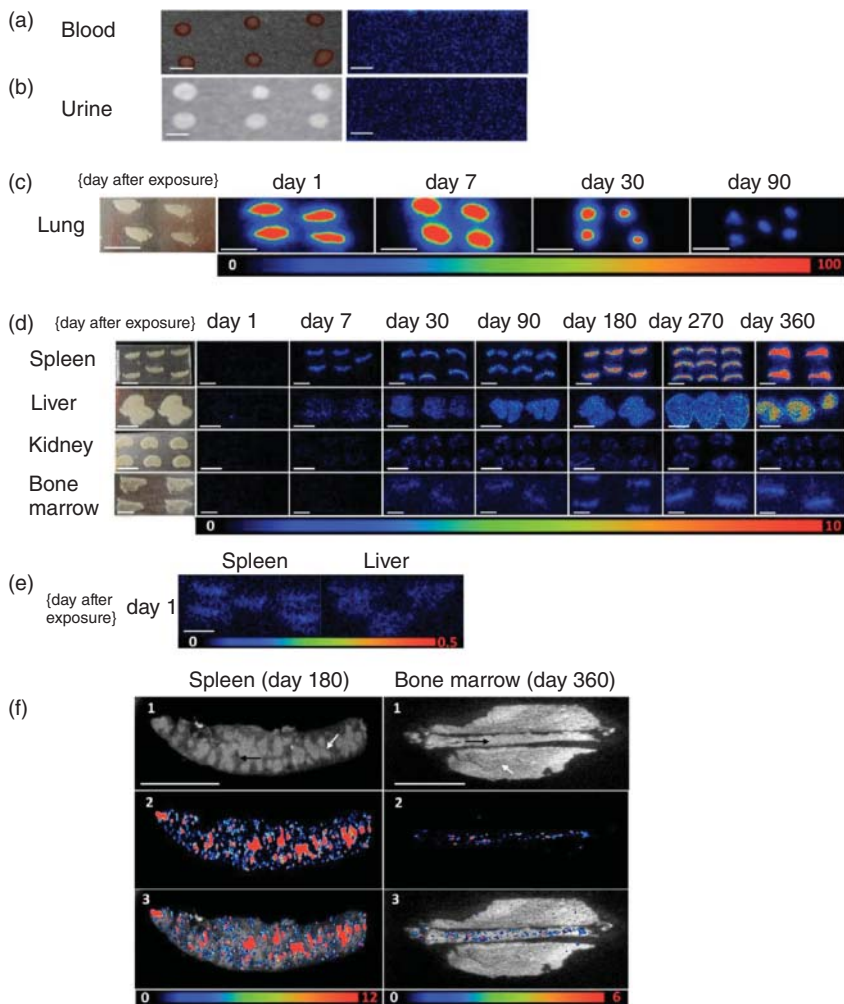


Figure 10.3 Systemic fate of ^{14}C -labeled MWCNTs following 20 μg per lung aspiration exposure in female mice. (a) Following exposure, MWCNTs were found to move out of the lung (b) and into several

organs. (c) High-resolution optical (top) and radioimaging (middle) of spleen and bone marrow. (Reprinted with permission from [110]. ©2014 American Chemical Society.)

marrow progenitor cells (e.g., stem and immune cells), this finding is, at least, worrisome. Future studies should evaluate the long-term health effects of CNT deposition and persistence in these sensitive tissues.

SWCNTs, although more difficult to identify, also exhibit this quality with slow degradation over time [111–113]. Alveolar macrophages phagocytose a significant portion of deposited CNTs and move them up the mucus ciliary escalator. It appears, however, that fiber morphology plays a role in macrophage recognition of CNT as a foreign particle. For example, alveolar macrophages only cleared 10% of SWCNTs compared to equal mass dose of well-dispersed MWCNTs [108]. This difference in clearance suggests that lower mass concentrations of SWCNT exposure elicit a response similar to that of higher MWCNT concentrations. The ability of SWCNTs to escape macrophage recognition, phagocytosis, and clearance allows for greater CNT reactivity with epithelium and penetration into the alveolar interstitium and subsequent interaction with lung fibroblasts. How this difference impacts *in vivo* carcinogenesis remains to be evaluated. Regardless, CNTs' ability to penetrate exposed tissue with prolonged biopersistence indicates that chronic CNT exposure at relatively low doses to sensitive tissues harbors increased risk for long-term health risks, potentially including cancer.

Physicochemical factors of CNTs that impact inflammatory and fibrotic effect in exposed lungs include length, width, surface charge, surface functionalization, surface area, dispersion stability, rigidity, and transition-metal content. Similar to asbestos, fiber length and dispersion in single fiber morphology are major factors determining biological responses. For example, well-dispersed SWCNTs and MWCNTs elicit potent inflammatory and fibrotic responses [99, 101, 114, 115], while CNT agglomerates are less reactive and mirror generalized response to large inhaled particles [116].

In early studies evaluating CNT-induced toxicity, several research groups reported data that would support early mechanisms of carcinogenesis. Inhalation exposure of SWCNTs caused a more robust ROS, inflammation, and KRAS mutation response than aspiration exposure using the same material [114]. This mutation is a known factor in increased risk of lung cancer associated with smoking and chemical-induced carcinomas [117]. In addition, several studies evaluating CNT inflammation and fibrosis via whole transcriptome array analyses have identified cancer signatures and known lung cancer prognostic markers in exposed mouse lung tissue [118, 119]. Interestingly, an identified lung cancer gene signature, including Bcl-2 and caveolin-1, has been implicated in CNT *in vitro* cell transformation studies [120, 121]. These genes may play a role in early CNT neoplastic transformation mechanisms. In a follow-up study by Guo *et al.* [122], using the same dataset, a 35-gene signature from MWCNT-exposed mice was able to predict human clinical lung cancer survival rates.

Given CNT's striking similarities to asbestos in subpleural translocation, as well as inflammatory and fibrotic reactions in the lung, recent concern has shifted to a potential for CNT induction of mesothelioma. HAR fiber-associated bioactivities include translocation out of alveoli to mesothelial tissues, biopersistence, epithelial and mesothelial cell injury, and activation of macrophage phagocytosis [123].

Several *in vivo* studies report that translocation of long CNTs from exposed lung to the parietal pleura impart inflammation, mesothelial hyperplasia, granulomatous lesions, and fibrosis [124–127]. The current CNT hypothesis for mesothelial disease closely mirrors that of asbestos in that long fibers tend to become trapped around parietal stomata in attempts to drain to the lymphatic system. This results in penetration, cell damage, and chronic inflammation, all likely key events promoting tumorigenesis [49, 128].

Although CNTs exhibit HAR fiber behavior with striking similarity to asbestos, several studies report deviations of CNT behavior from that of asbestos including lung transport mechanisms, transient inflammation, rapid onset of fibrosis, and prolonged progression of fibrosis in the absence of persistent inflammation [100, 101, 106, 129]. Such differences in both toxicokinetics and toxicodynamics suggest that CNTs possess unique properties, resulting in unknown mechanisms with potential unpredictable effect.

Presently, CNTs are thought to harbor elevated risk of carcinogenesis compared to other ECNMs. Recently, a large number of *in vivo* studies evaluated specific CNTs (most notably Mitsui #7) for neoplastic lesions or tumorigenesis. Overall, based on one report of MWCNT promotion of lung adenocarcinoma [15] and several reports of mesotheliomas following intraperitoneal (i.p.) injection (discussed later), the IARC Working Group concluded that there was sufficient evidence of carcinogenesis of Mitsui #7 in experimental animals. Although the evidence for neoplasia in rats and mice was strong and mechanisms in model systems associated with neoplasia were demonstrated, no neoplastic outcome has been observed in humans. The IARC committee therefore classified the Mitsui #7 MWCNT as a Group 2B carcinogen. Although there were mechanisms of carcinogenesis in experimental models that would be reasonable in humans, the IARC Working Group noted there was no evidence for carcinogenicity in humans. They also cited the lack of systematic and coherent evidence to support generalization to other CNTs [9]. Given no evidence of excess human cancers, short CNT production history (~10 years), and expected latency for detectable HAR fiber-induced tumors, excess cancers may not be observed for another two decades. Rigorous dose–response studies evaluating how key physicochemical properties contribute to CNT lung adenocarcinoma and mesothelioma are urgently needed to form adequate risk assessment and contribute to further “safe-by-design” CNT technology development.

Injection of suspected carcinogens with HAR fiber morphology via i.p. administration is a well-established technique to screen for mesothelioma risk [130]. Several studies using different lengths, widths, morphologies, and dispersibilities of MWCNT have reported that the physicochemical properties of MWCNTs impact their ability to promote HAR fiber-like lesions and mesotheliomas. Four key features of HAR fibers for adverse effects are translocation out of alveoli to mesothelial tissue, biopersistence, epithelial and mesothelial cell injury, and activation of macrophage phagocytosis [123]. In one of the first studies, two short and two long MWCNTs with different fiber thickness were i.p. injected to evaluate inflammation (7-day) and granulomatous lesion (28-day) potential [124]. Long

CNTs ($>15\text{ }\mu\text{m}$) caused asbestos-like inflammation and lesions, while short and tangled CNTs ($\ll 15\text{ }\mu\text{m}$) showed minimal effect. A study by Muller *et al.* [131] reported that short MWCNTs ($<1\text{ }\mu\text{m}$) did not induce mesothelial tumors following i.p. injection to the peritoneal cavity in male Wistar rats over the course of 2 years. Intrascrotal injections of MWCNTs (Mitsui #7) into male F344 rats caused a robust mesothelioma response, stronger than positive asbestos fiber control, resulting in early death of the majority of animals (37–40 weeks) prior to the 52-week endpoint [132]. Mesotheliomas were noted as aggressive in nature and metastatic in lung tissue.

Injection (i.p.) of MWCNTs (Mitsui #7; 1–20 μm length) results in dose-dependent induction of mesothelioma in p53 heterozygous mice [133, 134]. Doses ranging from 106 to 108 fibers per mouse resulted in 25–95% mesothelioma incidence. Interestingly, in the latter study, the time to tumor onset was dose-independent. All exposed mice exhibited mesothelial hyperplastic lesions, widely considered preneoplastic, with underlying macrophage infiltrate with single MWCNT fibers. This study suggests that frustrated phagocytosis and the resulting inflammation in the mesothelial lining microenvironment promote early tumorigenic events. A significant subset of human population has somewhat faulty p53 behavior, and human cancers possess faulty p53 signaling, so heterozygous p53 models have relevance in carcinogenesis studies [135].

Next, Nagai *et al.* [136] compared thin versus thick MWCNTs using both *in vitro* and *in vivo* models. One month following i.p. injection at low and high doses, thin and crystalline MWCNTs caused fibrosis around most i.p. exposed organs. A 1-year follow-up study found that thin MWCNTs caused mesothelioma that harbored CDKN2A/2B homozygous deletions, a common feature in human and rodent mesothelioma. Thick and tangled MWCNTs were less inflammatory and carcinogenic. *In vitro* exposure studies found that thin, crystalline-like MWCNTs pierced cells and induced cytotoxicity. Two types of mesothelial cells *in vitro* did not experience active MWCNT uptake, while asbestos did associate with these cells. Further investigation found that thin, crystalline MWCNTs passively puncture the plasma and nuclear membranes *in vitro*, leading to their potent cytotoxic effects. The authors systematically ruled out other physicochemical factors contributing to the differences in effect including length, ROS generation, surface area, fiber number, and transition metals. Diameter may be a determining factor for carcinogenesis; however, more systematic evaluations are needed.

A 2-year carcinogenic study in rats was conducted to compare four different MWCNTs to asbestos-induced mesothelioma [137]. A total of 5×10^8 to 5×10^9 CNTs/animal were injected (i.p.) and compared with 108 asbestos fibers/animal. All MWCNTs ranged from 7.9 to 10.2 μm in length and 37 to 85 nm in width. Given their similar lengths, MWCNTs primarily differed on their widths and straight versus curved morphology. Tumor incidence and time to onset was dose- and CNT-particle dependent. Earliest onset was observed in animals exposed to straight MWCNTs with large diameter (85 nm). Curved and narrow width (37 nm) MWCNTs exhibited the longest time to tumor onset. A majority of

MWCNT mesotheliomas were either sarcomatoid or biphasic with high similarities to asbestos-induced mesothelioma. The authors concluded that aspect ratio and curvature of MWCNT appeared to influence mesothelioma potential, although width appeared to contribute to mesothelioma induction potency.

Although i.p. injections provide a model for mesothelioma screening, they do not consider the toxicokinetics and fate in a physiologically relevant exposure (i.e., inhalation). Recent studies have begun to assess the expected exposures, the chronic toxicokinetics of CNTs *in vivo*, and their carcinogenic risk in both lung epithelium and pleural/subpleural mesothelium. Although only a few CNT inhalation studies to date have been conducted, they indicate that CNTs are probably human carcinogens. Sargent *et al.* [15] conducted a classic initiation/promotion evaluation of inhaled MWCNTs' carcinogenic potential by evaluating their ability to affect tumorigenesis in the absence/presence of a well-known DNA-damaging agent and carcinogenic initiator, namely methylcholanthrene (MCA). First, B6C3F1 mice, a National Toxicology Program (NTP) wild-type model, were i.p. exposed to vehicle-only or 10 µg MCA per gram body weight. At 1 week, mice were exposed to filtered air or 5 mg m⁻³ of Mitsui #7 MWCNTs for 15 days, 5 h per day, via whole-body inhalation with a reported lung burden of 31.2 µg per lung. MWCNT-only exposed mice evaluated MWCNT's ability as a complete carcinogen, while MCA+MWCNT evaluated MWCNT's cancer promotion potential. Approximately 52% of MCA-only and 90.5% of MCA+MWCNT mice at 17 months post exposure showed bronchioloalveolar adenomas and adenocarcinomas. Conversely, 26.5% of MWCNT-only and 23% of filtered-air-only exposed mice possessed similar tumors. Interestingly, MWCNT-only exposed mice exhibited focal hyperplasia in lungs characterized by crowded alveolar cells spaced randomly along alveolar septa (Figure 10.4). These foci were termed "focal adenomatous hyperplasia" since atypical hyperplasia is a commonly observed preneoplastic lesion in humans exposed to numerous carcinogens. As expected, singlet and small loose agglomerates of MWCNTs were found in the lung tissue or in subpleural (e.g., diaphragm) tissues (Figure 10.4). Metastasis was observed and potentially contributed to early euthanasia in mice exposed to MCA+MWCNT (Figure 10.5). Nine percent of the MCA+MWCNT mice showed tumors consistent with sarcomatous mesothelioma, as indicated with positive podoplanin and marginal cytokeratin staining (Figure 10.5). Sargent *et al.* [15] concluded that inhaled dispersed Mitsui #7 MWCNT is a lung cancer promoter.

A small pilot study ($n = 6$ per group) performed 100 µg i.t. injection of pristine MWCNT (7 µm long) versus acid-treated MWCNT (0.57 µm long) into C57BL/6 male mice Yu *et al.* 2013 [138]. After 6 months, more potent autophagy accumulation, hyperplastic adenoma, and adenocarcinoma regions response were observed with pristine MWCNT compared to acid-treated MWCNT in exposed mouse lungs.

Xu *et al.* [139] compared MWCNT's and asbestos fiber's ability to induce mesothelial lesions in F344 rats. MWCNT was found to translocate to pleural cavity, resulting in mesothelial hyperplasia following five different i.t. sprayings

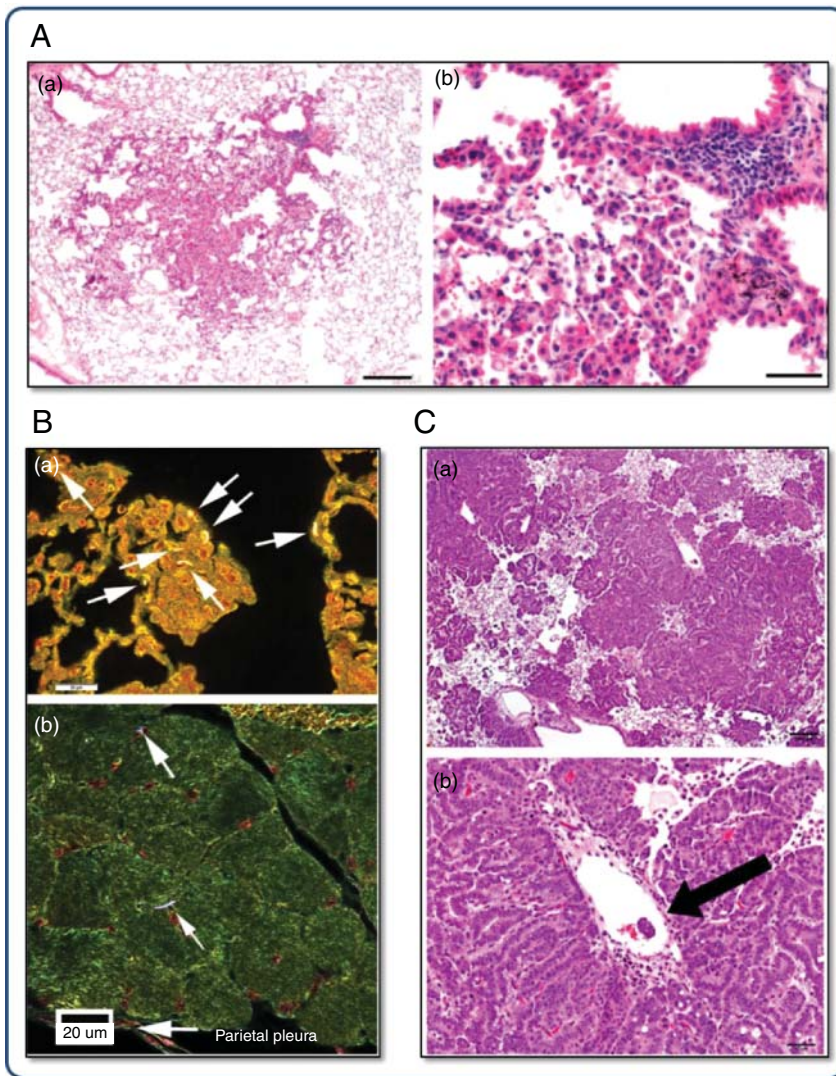


Figure 10.4 Promotion of lung adenocarcinoma and mesothelioma following MWCNT inhalation exposure. (a) MWCNT-only-exposed mice possess regions of focal adematous hyperplasia with unique morphological characteristics. (b) Enhanced dark-field imaging at 17 months post exposure, showing deposited MWCNTs (white

arrows) in alveolar (top) and extra-pulmonary (diaphragm) regions. (c) Lung adenocarcinoma (top) and metastatic tumor in pulmonary blood vessel (bottom) in mice exposed to MCA+MWCNT. (Reprinted with permission from [15]. ©2014 Particle and Fibre Toxicology.)

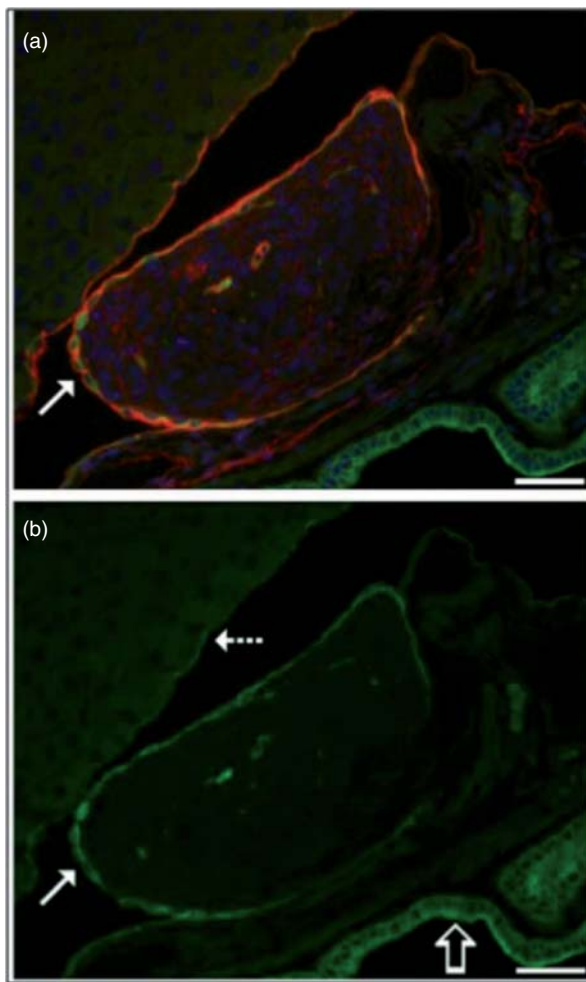


Figure 10.5 Sarcomatous mesothelioma in mice exposed to MCA+MWCNT. Co-staining of (a) podoplanin (red) and (b) cytokeratin (green) identified mesothelioma (white arrow, upper panel) between the gall bladder and

liver. (Bottom panel) Cytokeratin staining of mesothelial tissue. (Reprinted with permission from [15]. ©2014 Particle and Fibre Toxicology.)

over 9 days in Fisher rats. MWCNT hyperplastic lesions were associated with macrophage infiltration and inflammation-associated fibrosis. A majority of MWCNTs were found in alveolar macrophages and mediastinal lymph nodes. In addition, pleural macrophages were found to contain MWCNTs, with little to no nanomaterial in mesothelial tissue, thus suggesting that the observed hyperplasia was due to pro-inflammatory signaling. Conditioned medium from MWCNT-exposed macrophages confirmed an inflammation-driven mesothelial cell proliferation *in vitro*.

A follow-up study [127] evaluated the impact of the size and shape of MWCNTs on the fate, fibrosis, and mesothelial proliferation in F344 rats. Long and thick (8 μm) MWCNTs were compared to short, thin, and tangled (3 μm) material using a repeated dosing model comprised of 12 exposures over 24 weeks via transtracheal spray. Total administered MWCNT was 1.625 mg per rat. Long, well-dispersed MWCNTs reached the parietal pleura to induce fibrosis and mesothelial hyperplasia. Long MWCNTs also caused a stronger inflammation response in pleural cavity lavage. Interestingly, the short MWCNTs, which formed small aggregates, caused a more robust inflammation and oxidized DNA in exposed lung tissue than long MWCNTs. This study supports the growing hypothesis that long, thick, and rigid MWCNTs that are well dispersed can translocate to the pleural mesothelium and cause hyperplastic lesions and inflammation, consistent with the preneoplastic etiology observed in asbestos-induced mesothelioma. This study also raises the possibility that particle morphology impacts toxicokinetics and the eventual fate, and can still cause long-term risks in different tissues. Here, although no extra-pulmonary translocation occurred, short and tangled MWCNTs were highly inflammogenic and cytotoxic, in both *in vivo* and *in vitro* models. Although other studies suggest that shorter and tangled CNT exhibit less reactivity [126], it is still important to consider their adverse health effects given that a majority of CNTs in the occupational setting possess a tangled, agglomerated morphology [21].

SWCNTs, because of their single layer of graphene, are more flexible tube structures and can possess numerous morphologies including single fibers, nanoropes, and loose, tangled agglomerates. They do, however, possess significantly greater surface area compared to their DWCNT and MWCNT counterparts. This higher surface area has been implicated in producing greater potency than MWCNTs at equal mass dose. Two published studies with small sample sizes evaluating long-term effects of SWCNT exposure in rats found little tumor evidence after 6 months and 754 days post i.t. instillation [113, 140]. Several recent studies by Shvedova *et al.* [141] and others have suggested that SWCNTs promote carcinogenesis through several mechanisms including genotoxicity, altered cytokine signaling, and yet-undefined mode(s) of action. SWCNTs and carbon nanofibers (CNFs) were compared to asbestos via pharyngeal aspiration to evaluate long-term pulmonary effects, including inflammation, fibrosis, and genotoxicity in C57BL/6 mouse [112]. SWCNT aspiration data were then compared with a 4-day inhalation exposure to evaluate dosimetry. CNF and asbestos fibers were rigid and possessed 2- to 10-fold greater length than flexible SWCNTs. At 1-year post exposure, SWCNTs were still present in exposed lung tissue, primarily as nanoropes, with some detected in lymphatic tissue. SWCNTs were most fibrogenic and produced increases in MN, while CNFs and asbestos exhibited the largest inflammation response. Both SWCNT and CNF, but not asbestos, exposure increased KRAS oncogene mutation frequency. Although no tumors formed in this moderate tumor-resistant model, it is apparent that long, rigid HAR fibers contribute to a greater inflammatory response than the more flexible HAR fibers and that KRAS mutation may be a more common feature of prolonged exposure

to HAR carbon nanomaterials. This study also adds support to the hypothesis that CNT exposure may harbor a unique inflammation-independent mode of action in promoting chronic lung disease (i.e., fibrosis). A distinct CNT mode of action for bronchoalveolar epithelial carcinogenesis has yet to be defined, and is an area for future investigation.

Recently, two studies by Shvedova *et al.* [46] have raised the possibility that CNT exposure modulates immune cells, thus improving the tumor microenvironment and enhancing tumor growth. First, short SWCNTs (230 nm) were aspirated into mice (80 µg) followed by i.v. injection of Lewis lung carcinoma cells. At 21 days post i.v. injection, SWCNT-exposed lungs exhibited a 5-fold increase in weight and a 2.5-fold increase in number and size of lung metastases. Clearly, SWCNT pre-exposure enhanced the recruitment and proliferation of lung metastases. Further examination identified an increased number of recruited myeloid-derived suppressor cells (MDSCs), a cell type known to promote tumor growth, in SWCNT-treated lungs. MDSCs typically are found to suppress the immune response and enhance new blood vessel growth in tumors. Blockage of MDSCs in the mouse lung reduced lung cancer metastases. A second study reviewed the published literature and noted that overexpression of three signaling factors (M-CSF, GM-CSF, and TGF- β) was a common occurrence associated with lung cancer and SWCNT exposure, thus suggesting immune suppression in CNT-exposed lungs. Acute SWCNT aspiration exposure (80 µg) induced recruitment of MDSCs and TGF- β production, which in turn promoted an immunosuppressive microenvironment by suppressing T-cell activation and recruitment [141].

In summary, the length, width, surface functionalization, surface area, crystallinity, dispersion stability all appear to impact CNT toxicokinetics and the resulting genotoxicity and tumorigenesis *in vivo*. Long, straight, and thick MWCNTs appear to pose enhanced risk for mesothelioma due to their deep penetration and translocation ability, resulting in a chronic inflammatory response that drives mesothelial hyperplasia and eventual carcinogenesis. The fact that Mitsui #7 MWCNT agglomerates and similar fibers have the ability to dissociate to singlet fibers over time *in vivo* and systemically disperse [101] is alarming. Tangled MWCNTs typically observed in human occupational settings are potentially less likely to dissociate and translocate, and is an area of current research [21, 98]. NIOSH is currently evaluating carcinogenic dose–response following MWCNT inhalation in the hope of providing data for risk assessment criteria. Although tangled CNTs show little mesothelioma risk and reduced potency compared to well-dispersed fibers, they make up a significant portion of manufactured CNTs, retain some ability to induce a robust inflammatory response in exposed airways similar to other carbon-based particles, and may experience dispersion *in vivo*; therefore, they should not be overlooked as a potential carcinogen. At present, *in vivo* CNT carcinogenesis studies are expanding to consider other important physicochemical properties (e.g., surface functionalization) of these materials, which are projected to experience high manufacturing, wide use, and increased rates of exposure. Tier I *in vitro* genotoxicity/transformation and Tier

II short-term *in vivo* studies are paramount in identifying those properties with potential risk for CNT carcinogenesis.

10.2.3.2

In Vitro Studies

There is some evidence *in vitro* that ECNMs, such as CNTs, can gain access to the nucleus and genetic material, which can cause genetic aberrations by a primary mechanism additional to the inflammation or ROS-mediated one. These potential mechanisms require further study [20]. *In vitro* cell models remain and will continue to play a key role in screening novel ENMs for potential toxicity [24]. Recent advances in multicellular models hold vast promise in adding to the battery of available *in vitro* predictive models (reviewed below). Acute exposure to macrophage, epithelial, fibroblast, and endothelial cell results in passive or active uptake, plasma membrane damage, NLRF3 inflammasome activation, inflammatory cytokine release, ROS, proliferation, and enhanced collagen production [51, 142, 143]. Similar to *in vivo* findings, many of the same physicochemical properties of CNTs elicit cytotoxic and subtoxic effects leading to disease onset [144]. Size, surface functionalization, and surface charge impact the uptake route into the cells. COOH, OH, and other negatively charged functional groups repel the negatively charged phospholipid heads of the plasma membrane, thus making direct penetration less likely. Positively charged surfaces, such as N-containing groups, present a positive charge and may be more suitable for direct penetration and membrane disruption [145]. Functional groups and surface coatings may also interact with membrane-bound receptors, which may assist in endosomal uptake or initiate signaling cascades within exposed cells.

ROS generation, inflammation, genotoxicity, and the subsequent downstream signaling pathways and responses are all implicated in the early phases of CNT-associated neoplastic cell behavior and early stage tumor formation. For example, SWCNT exposure to human bronchial epithelial cells resulted in nitric oxide (NO) production, pro-inflammatory cytokine release, and autophagic cell death corresponding to cytoplasm damage and mitochondrial dysfunction [146]. The role of chronic inflammation following MWCNT exposure possibly plays a larger, critical role in mesothelial response, hyperplasia, and CNT tumorigenesis than epithelial cell response. MET5A mesothelial cells directly exposed to a panel of five different MWCNTs did not produce inflammatory cytokines. Rather, cytokines from CNT-exposed macrophages elicited pro-inflammatory cytokines from MET5A cells [128]. Another study reported distinct differences in oxidative responses between neutrophils and macrophages in response to MWCNT versus asbestos fibers. Neutrophils showed no response to MWCNTs, while two types of asbestos fibers elicited ROS and inflammatory responses. Macrophages responded to both particle types with ROS and inflammation [147]. Given the relatively small amount of macrophages in the pleural cavity compared to pulmonary airways, the presence of a positive feedback loop suggests that human mesothelial cells are sensitive to alterations in inflammation.

CNTs are known to cause increased ROS in exposed cells, but also harbor ROS quenching and sequestration ability. Generation or sequestration ability of ROS is most likely material-, impurity-, solution-, and assay-dependent. Residual transition metals from several CNT synthesis methods are known to participate in Fenton-like reactions and can cause greater ROS production than pristine, low-metal-content CNTs [95, 142, 148]. Alternatively, studies have suggested that structural defects and organic surface functional groups with available electrons can donate electrons to reactive radicals [149]. A recent systematic evaluation of MWCNTs in the absence and presence of a lung surfactant showed that MWCNTs, by nature, sequester free oxygen radicals [150]. On a $\mu\text{g cm}^{-2}$ basis, SWCNTs are more potent inducers of DNA strand breaks than MWCNTs *in vitro*. SWCNT exposure to both normal and malignant mesothelial cells resulted in ROS production, DNA damage, and activation of several signaling pathways including AP-1, NF- κ B, p38 MAPK, and Akt, all of which mirror events associated with asbestos-induced mesothelioma [142].

Although ROS generation in exposed tissues is known to occur and cause clastogenic damage, mounting evidence has identified direct genotoxic mechanisms that are ROS independent, echo other HAR fiber disruptions of mitosis, and have large implications for cellular fate. For example, exposure to low-iron-containing MWCNTs induced minimal ROS but DNA damage and apoptosis to both normal and malignant mesothelial cells. ERK and p38 MAPK also experienced enhanced activation [151].

A recent review of the *in vitro* genotoxicity literature identified the mitotic block MN, pH2AX, and comet assays as the most performed mammalian tests for CNT genotoxicity with positive results [152]. A wide range of human and mouse cell lines (e.g., Muta mouse epithelial cells, Balb/c mouse fibroblasts, BEAS-2B epithelial cells, RAW264.7 macrophages, normal human fibroblasts, and A549 cells) all show positive genotoxicity. Early genotoxicity studies employed high-dose CNT exposures with comet assay for hazard identification screening. Most exposures indicated DNA fragmentations with a potential role for oxidative stress damage. High-dose MWCNTs induced 8-nitroguanine lesions on DNA in A549 cells. Inducible nitric oxide synthase (iNOS) was also induced. DNA damage was suppressed by inhibitors of iNOS, NF- κ B, actin polymerization, and caveolae-mediated endocytosis, suggesting that uptake and the resulting inflammasome activation contributed to indirect DNA damage via nitrosative DNA damage [153].

A study evaluating both *in vitro* and *in vivo* lung models, however, reported that MWCNTs can induce both clastogenic and aneugenic effects, by using MN and fluorescence *in situ* hybridization (FISH) assays [7]. This suggested that CNTs themselves were either directly interacting with DNA or that CNTs were disrupting chromosome separation during mitosis. With better understanding of occupational exposure levels and potency of CNTs *in vivo*, more recent studies have focused on much lower dose and longer exposure time frames to assess genotoxicity.

CNTs can mimic microtubules *in vitro*, due to its carbon structure, size, and HAR morphology, which interfere with critical microtubule dynamics including proper chromosome separation during mitosis [6]. Dinu *et al.* [102] reported that tubulin can “self-assemble” onto MWCNTs to form tubulin-MWCNT hybrid structures. Alterations in the microtubule structure can impact not only cell division but also intracellular trafficking of proteins, lysosomes, and organelles. Sargent *et al.* [154] showed that high-dose SWCNT (HipCo) exposure caused fragmented centrosomes, multipolar spindles, anaphase bridges, and aneuploidy in two different human lung epithelial cell lines. SWCNTs were found to be associated with chromatin and tubulin, which are known to bind to G-C-rich areas of DNA. Carbon bridges formed during mitosis in SWCNT-exposed cells are reminiscent of asbestos bridges. Asbestos does not typically associate with centrosomes, but CNTs can, possibly due to their durability and flexibility [6]. Intercalation of SWCNTs would induce a DNA morphology change that could interfere with several vital processes including chromatin stability, replication, and transcription.

A follow-up study employing occupationally relevant doses to lung epithelial cells ($0.024\text{--}24\text{ }\mu\text{g cm}^{-2}$) of SWCNTs caused similar effects seen in high-dose exposures: fragmented centrosomes, disrupted mitotic spindles, and aneuploidy [155]. Subsequent clonal survival and proliferation assays found that SWCNT-exposed cells experienced increased colony formation and proliferation 7 days post exposure in surviving cells. These studies suggest that SWCNTs can disrupt chromosome integrity and enhance proliferation, which are two early characteristics in the cancer initiation/promotion etiology. Although a majority of cells harboring significant chromosome damage would not survive, it is possible that prolonged exposure would promote the survival of cells with chromosome damage, leading to genetic instability and early stages of carcinogenesis.

Subsequent studies reported similar outcomes for MWCNT exposure with some differences. MWCNTs (25 nm diameter) were found to disrupt cancer cell mitosis via microtubule mimicry [156]. MWCNT exposure (10–20 nm) was shown to cause dose–response ($0.024\text{--}24\text{ }\mu\text{g cm}^{-2}$) increases in the frequency of disrupted centrosomes, abnormal monopolar mitotic spindles, and aneuploidy chromosome number in BEAS-2B and primary human SAECs at 24 h (Figure 10.6) [157]. Primary SAECs exhibited decreased viability 72 h post exposure, while low-dose MWCNTs stimulated BEAS-2B cell proliferation. MWCNTs associated with DNA, centrosomes, and microtubules and were observed within the centrosomal structure. At the lowest dose tested, which approximates a 4-week exposure at the OSHA exposure limit, ~40% of the exposed cells exhibited these abnormal phenotypes. Aneuploidy was typically seen in cells with polyploidy, suggesting cytokinesis failure. Primary SAECs exhibited a strong colony-formation ability that was inverse dose-dependent. These worrisome results suggest that those surviving primary cells with genetic damage can expand. Secondly, aneuploidy and centrosome disruption are classically associated with tumor stage [158].

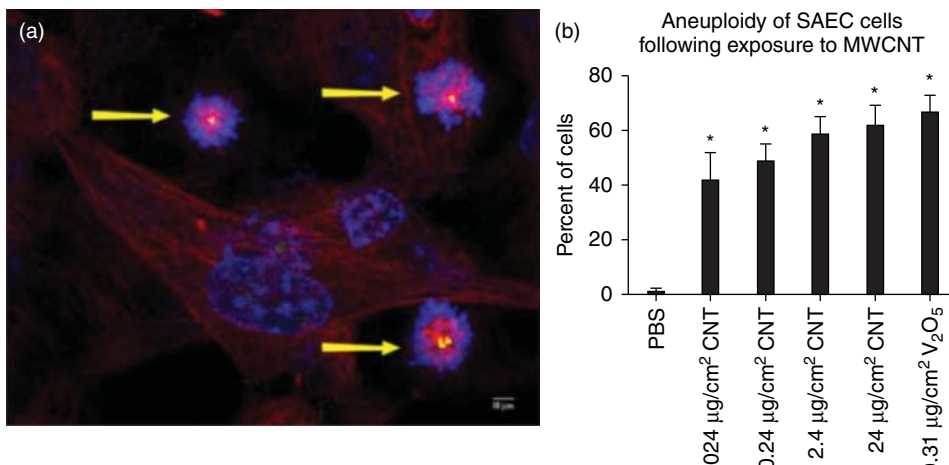


Figure 10.6 Mitotic disruption in MWCNT-exposed human small airway epithelial cells. (a) Monopolar mitotic spindles (yellow arrows) contribute to (b) chromosomal aneuploidy. (Reprinted with permission from [157]. ©2014 Particle and Fibre Toxicology.)

Clearly, CNTs of different physicochemical properties represent a genotoxic hazard to exposed pulmonary tissue. Although hazard clearly exists, very few studies have systematically evaluated specific physicochemical properties and their dose–response that is useful for risk assessment. Most recently, Jackson *et al.* [159] conducted a systematic *in vitro* evaluation of 15 different MWCNTs with different physicochemical properties including diameter, length, and surface functionalization. Although mass doses were high, mouse lung epithelial cells exhibited weak single strand breaks in the comet assay along with ROS and reduced cell proliferation. MWCNTs with large diameter appeared to show greater ability to induce single strand breaks. Studies like this highlight not only how useful systematic studies are but also how important using multiple genotoxicity assays for both direct and indirect genotoxicity can be. In addition, since a majority of *in vitro* and *in vivo* animal studies report positive genotoxic responses, both models should be used in tiered approaches to screen and assess CNT genotoxicity [e.g., 7, p. 159].

In vitro cell transformation studies have long been utilized to quickly screen and assess xenobiotics for genotoxicity and neoplastic transformation potential. Morphological transformation assays with these models are acknowledged as alternative, comparative models to the 2-year *in vivo* carcinogenesis assay [161, 162]. Although simplistic in nature, they possess merit in identifying the underlying molecular and cell mechanisms involved with early steps during carcinogenesis. These studies typically attempt to characterize several cancer hallmarks during promotion, including proliferation, apoptosis/anoikis evasion, anchorage-independent growth, migration, invasion, angiogenesis, and CSCs. The use of neoplastic cell transformation models, coupled with other analysis

platforms, has helped unlock the potential early stage mechanisms associated with tumorigenesis.

Using the Balb/3T3 cell model, Ponti *et al.* [163] evaluated nude and functionalized ($-\text{COOH}$, $-\text{OH}$ and $-\text{NH}_2$) MWCNTs for cytotoxicity, genotoxicity, and carcinogenesis potential. All MWCNTs possessed short lengths ($<1.5\text{ }\mu\text{m}$) and equal diameters (9.5 nm), which resulted in no observable cyto- or genotoxicity. Surprisingly, they all exhibited increased morphological transformation comparable to asbestos-exposed cells.

Although murine cell line assays are a useful screening tool for morphological transformation, they may harbor inherent differences in behavior compared to human cells in similar tissues. Using human cell lines for morphological and neoplastic transformation coupled with recent technological advances in evaluating genomic signatures and 3D models holds promise for future screening approaches for ENM- and other xenobiotic-associated carcinogenesis. For example, Wang *et al.* [164] found that subchronic, dispersed SWCNT exposure at an occupationally relevant dose ($0.02\text{ }\mu\text{g cm}^{-2}$) caused malignant transformation, as evidenced by several cancer hallmarks [27] including aggressive proliferation, attachment-independent growth, p53-mediated apoptosis evasion, invasion, angiogenesis, and *in vivo* tumorigenesis in the exposed cells. Decreased p-p53 (Ser15) expression was found to suggest that SWCNTs further destabilize p53 for proteosomal degradation. Similarly, repeated long-term MWCNT exposure to bronchial epithelial cells (BEAS-2B) resulted in oncogenic transformation [165]. Global comparative genomic hybridization identified chromosomal aberration at 2q31–32 near oncogenes HOXD9 and HOXD13, which regulate apoptosis, development, and cell proliferation. Other genes affected are associated with lung cancer, cell cycle, focal adhesion, and MAPK signaling. Conversely, prolonged MWCNT exposure caused increased ROS but had minimal effect on genotoxicity or promotion effect on human lung adenocarcinoma A549 cells [166].

Expansion of these studies [90] performed comparative subchronic HAR fiber exposure ($0.02\text{ }\mu\text{g cm}^{-2}$) to assess neoplastic transformation potential in human small airway epithelial cells. hTERT-immortalized SAEC cells with known loss of p16 expression after numerous continuous passages are a reasonable model since both asbestos- and CNT-induced mesotheliomas exhibit loss of CDKN2A/2B [136, 167]. After 6 months of exposure, both SWCNTs and MWCNTs caused increased proliferation, soft agar colony formation, migration, invasion, and angiogenesis above UFCB-exposed, asbestos-exposed, and unexposed control cells. Transcriptome profiling found that both SWCNTs and MWCNTs exhibited similar yet unique genome signatures characterized by proliferation, movement, cell death, and development signaling. Cancer-associated signaling was centered on overexpressed MYC, PPARG, COL18A1, PDGFRB, and CASP8. Asbestos-exposed cells, however, displayed a very different and distinct pro-inflammatory transcriptome signature centered on IL-1B, CCL2, and SPI1. Similar to the previous SWCNT-transformed BEAS-2B cells, loss of p-p53 (Ser15) expression was most prevalent in CNT-exposed cells, suggesting that p53 degradation may be a common mechanism in early stage CNT-associated tumorigenesis.

At present, the same group's preliminary analyses to identify CNT-specific *in vitro* gene markers to predict early disease effects *in vivo* [168] have been successful in identifying several genes associated with altered lipid metabolism following MWCNT exposure *in vitro* compared to genomic profiling data in MWCNT-exposed mouse lung [106, 122].

Establishing CNT-transformed cell models with neoplastic or malignant transformation phenotypes, coupled with whole transcriptome signature analysis, has allowed mechanistic studies to evaluate potential carcinogenic modes of action. Results of these studies have identified known signaling pathways and genes that exist in lung cancer, thus suggesting the usefulness of such studies to not only screen ENMs but also potentially use them for early disease biomarker identification. Transcriptome microarray analysis of the SWCNT-transformed BEAS-2B cells identified potential mechanisms for FLIP-mediated apoptosis resistance [169] and oncogenesis including the pAkt/p53/Bcl-2 signaling axis, Ras family cell cycle control, Dsh-mediated Notch1, and downregulated BAX and Noxa [121]. Further studies have identified the role of caveolin-1-mediated CSC induction by CNTs [120, 170]. Side population characterization in SWCNT-transformed bronchial epithelial cells identified CSC-like cells positive for Nanog, SOX2, SOX17, CD24 low/CD133 high, and E-cadherin surface markers. These p53-deficient CSCs possessed self-renewal properties, aggressive cancer behaviors, and *in vivo* tumorigenesis. Furthermore, CSCs were also found in the SWCNT-transformed small airway epithelial cells, suggesting that SWCNT induction of CSCs may be a widespread phenomenon in exposed lung epithelial tissue and that SV40 status does not dictate CSC formation.

Since well-dispersed MWCNT aspiration and inhalation exposure can result in extra-pulmonary translocation and pleural mesothelial exposure [19], similar subchronic neoplastic transformation studies on human mesothelial cells were performed by our group. Continuous subchronic exposure to both SWCNT (HipCo) and MWCNT (Mitsui #7) for 4 months to MET5A cells resulted in neoplastic transformation characterized by enhanced proliferation, cell mobility, and aggressive invasion phenotype [171]. Both sets of CNT-exposed cells exhibited greater cell movement and invasion ability than asbestos-exposed cells. Mechanistic studies, coupled with whole transcriptome profiles, identified distinct CNT invasion signaling pathways which differed substantially from those of asbestos. MMP2 overexpression was important to all three HAR fibers, while PLA2U, STAT3, AKT, and VEGFA were specific for CNT-exposed cells. A follow-up dose-response study with SWCNT-exposed mesothelial cells (MET5A and LP-9) identified activated HRAS/ERK, which contributed to cell invasion ability and cortactin overexpression [172].

10.2.4

Fullerenes and Derivatives

Fullerenes (C_{60} or C_{70}) and their water-soluble derivatives (e.g., fullerol) have attracted much attention due to their relatively small size, high surface

area/volume ratio, radical binding capacity, multiple functionalizations, and water solubility [173–175]. Their large diversity mainly rests on the ability to functionalize and/or use solvents to increase hydrophilicity, aqueous dispersion, and manipulation. For example, several manipulative strategies exist to surface-functionalize C₆₀ into water-soluble derivatives, including C₆₀(OH)₁₈ and C₆₀(OH)₂₄. The sum of all possible forms of fullerenes results in a wide array of potentially benign or toxic behaviors that are not completely understood. Dispersion in air with the resulting inhalation exposure is, at present, restricted to manufacturing and industrial uses of fullerenes and fullerols. At the consumer level, dermal exposure is widely expected as a result of fullerene's presence in a wide variety of cosmetics. Known or expected fullerene exposure levels in an occupational or environmental setting are relatively small compared to other carbon ENMs (e.g., UFCB and CNTs). Exposures during manufacturing range from 36 to 150 µg m⁻³ for PM_{2.5} while fullerene-specific doses range from 0.0004 to 2 µg m⁻³ [174, 176].

Similar to other pristine carbon ENMs, as expected, fullerene exhibits ROS scavenging and generation activities [177–180]. Fullerene can exist either as a quencher or as a generator of oxygen radicals. The antioxidant property of fullerene has been aggressively pursued, especially within biomedical applications for disease treatment [reviewed by Johnson *et al.* 4]. Highly dispersed fullerene derivatives and fullerol show enhanced, dose-dependent radical sequestration ability following exposure to known pro-oxidant xenobiotics or therapeutic agents. Photosensitization of C₆₀ generates excited electrons, resulting in singlet or superoxide radicals [179]. Water-soluble fullerenes primarily act as antioxidants partially due to their dispersibility and the resulting high surface area [177]. Anionic, water-soluble fullerenes sequester more superoxide than cationic or pristine fullerenes [178]. In general, both *in vitro* and *in vivo* studies suggest that differences in chemical structure, surface functionalization, dispersion technique, residual solvents, and target cell/tissue all impact the toxicity of fullerene and its derivatives. Toxicity is largely associated with oxidation of sensitive targets, which would dictate an inflammatory and potential genotoxic response.

10.2.4.1

In Vivo Studies

Several studies with different pulmonary exposure methods for varying lengths of time reported minimal inflammation response. Both fullerene and fullerol were not toxic in rat lung at 3 months post i.t. exposure [181]. Baker *et al.* [182] reported that nanometer- and micrometer-sized fullerenes caused no significant response following inhalation exposure, with no detection of particles in blood stream, suggesting no or limited translocation out of the lung. No significant inflammation or lung damage was observed during a 4-week inhalation exposure or at 3 months post exposure. A microarray study reported minor inflammation, oxidative stress, and apoptosis response following a 4-week whole-body inhalation in rats [183]. A comparison of i.t. versus inhalation exposure to fullerene in Wistar rats showed no significant induction of neutrophilic inflammation [184]. Conversely, Park *et al.* [185] reported a dose-dependent increase in several

pro-inflammatory cytokines (e.g., IL-1, IL-6, and TNF- α) and minimal cell infiltrate in stained lung tissue sections from 7 to 28 days post i.t. exposure to water-soluble fullerene in ICR male mice. The positive inflammatory response in this study compared to the Sayes *et al.* [181] study may be due to the use of toluene versus tetrahydrofuran dispersant, smaller diameter of the primary particle, and different *in vivo* models. A high dose of fullerol caused an inflammatory response dominated by neutrophils and macrophages. The same study reported that lower doses of fullerol helped in reducing ROS elicited by quartz dust exposure [186]. This finding supports both acellular and *in vitro* studies showing that water-soluble fullerene derivatives quench ROS and raises the possibility that expected low-dose exposures may guard against ROS *in vivo*. Higher doses of well-dispersed particles may break a threshold and elicit an inflammatory response. Jiao *et al.* [187] reported that two different types of functionalized, water-soluble fullerenes provided ROS scavenging ability and reduced lipid peroxidation when exposed to mice with established lung carcinomas. The NTP study found histiocytic infiltration, a shift in inflammatory leukocyte populations, and moderate increases in MCP-1 and IL-1B in both the Wistar rat and B6C3F1 mouse models following a 90-day inhalation fullerene exposure [188, 189].

Fullerene fate studies showed that deposition within the mammalian body following either oral or i.p. injection occurs primarily in the liver, spleen, and lung [190, 191]. It is metabolized or excreted rapidly [190, 192] and might be transported via circulation. Pulmonary exposure studies report relatively short half-lives (26–29 days), BALF macrophages with particles, and little evidence of deep penetration, suggesting adequate clearance for fullerene-exposed lungs [176, 182].

Based on the limited number of published studies, little evidence exists for *in vivo* mammalian genotoxicity. Shinohara *et al.* [176] found little evidence of bone marrow clastogenicity of C_{60} fullerenes in ICR mice following oral exposure. Fullerene was observed to increase 8-oxodG in a gastric exposure to Fischer rats [193]. Increased comet tails and mutation frequencies were reported in gtp transgenic mice in an i.t. exposure at 200 μ g per mouse but not at 50 μ g per mouse [194]. Single and repeated i.t. instillation to male rat lungs resulted in an inflammatory response at 24 h, but no observable DNA damage was found in the comet assay in the collected lung cells [195] which coincided with positive inflammation and no DNA damage response [196]. The positive effect in the Totsuka study could potentially be explained as a generalized response to extremely high levels of particles in the exposed tissue. Although no evidence appeared in the exposed lung tissue, the 90-day NTP inhalation study found significant increases in micronuclei in peripheral blood samples at all tested doses in female B6C3F1 mice, while males experienced no effect [189].

At present, only three published studies have evaluated *in vivo* tumorigenesis. Fullerenes are more probably an anti-carcinogen than a pro-carcinogen, based largely on its radical sequestration properties and bioaccumulation potential in tumor tissue [reviewed by Aschberger *et al.* 174]. Intraperitoneal injection of fullerenes into heterozygous p53 (+/−) mice resulted in minimal adverse tissue

morphology (serosal plaques) with no tumor formation [133]. Liu *et al.* [197] reported that fullerol ($C_{60}(OH_{20})$) exposure reduced Lewis lung carcinoma *in vivo*, possibly due to increased TNF- α levels and elevated T-cell counts that enhanced the ability to eliminate abnormal cells. Conversely, Zogovic *et al.* [198] reported that *in vivo* fullerene exposure to melanoma xenograft tumors promoted tumor growth, while *in vitro* exposure reduced melanoma cell viability. An NTP study has been conducted, but no summary of the results has been reported. At present, no published *in vitro* cell transformation study has been conducted on fullerenes.

10.2.4.2

In Vitro Studies

Compared to other carbon ENMs, a decent knowledge base for screening fullerene's *in vitro* genotoxicity exists, most probably due to its perceived small size and wide use in biomedical and cosmetic applications. In general, fullerenes and derivatives show a limited ability to induce genotoxicity compared to other carbon ENMs [174, 196]. If genotoxicity is detected, it usually coincides with ROS-mediated effects associated with photosensitization. Evidence for genotoxicity is given by chromosomal damage, DNA strand breaks, and mutagenicity in multiple human and mouse cell lines. For example, Wang *et al.* [199] found that cyclodextrin-bicapped C_{60} cleaved DNA under light in presence of NADH. Zhao *et al.* [200] found similar phototoxicity with increased superoxide generation following cyclodextrin-capped pristine and water-soluble fullerene exposure. Studies using the Ames test reported mutagenicity, 8-OHdG adducts, and ROS generation, which correlated with the intensity and duration of light exposure to C_{60} and derivatives [201, 202]. Use of antioxidants reduced genotoxicity in these studies, suggesting indirect genotoxicity via ROS damage. Conversely, no mutagenesis occurred in mouse lung epithelial cells or CHO cells exposed to fullerenol [203]. Rather, fullerenol reduced the micronucleus frequency in these cells. Fullerene at $100\text{ }\mu\text{g ml}^{-1}$ caused some short-term damage observed in sensitive sites and increased oxidized purines in the comet assay in exposed mouse lung epithelial cells [196], similar to the SWCNT effect.

Although a handful of studies suggest moderate to low genotoxicity, recent studies report on the contrary showing low dose effects. C_{60} exposure to A549 cells caused increased micronuclei at $0.02\text{--}200\text{ }\mu\text{g ml}^{-1}$ [194]. Dose-dependent ONOO production correlated with increased deletion mutations in primary mouse fibroblast cells [204]. Dhawan *et al.* [205] reported that both aqueous and ethanol colloidal fullerenes exhibited genotoxicity in comet assay in exposed human lymphocytes as low as 2 ng ml^{-1} , most likely due to increased ROS. The authors do acknowledge that the dispersion method has a large impact on the observed genotoxicity. One study reported that chronic exposure at extremely low concentrations ($1\text{--}10\text{ }\mu\text{g ml}^{-1}$) of water-soluble fullerene elicited a positive micronucleus result along with increased cell proliferation in both normal embryonic kidney and HeLa tumor cells [206]. These low concentrations suggest an ROS-independent mechanism.

In vitro toxicity assessment of fullerenes, water-soluble derivatives, and fullerols have primarily focused on evaluating pulmonary, dermal, macrophage, and hepatic cell responses. Improved hydrophilicity of water-soluble fullerene derivatives, compared to fullerene, appears to reduce the aggregate size, reduce attraction to and interactions with lipid membranes, and reduce cell uptake, thereby reducing cytotoxicity. Improved dispersibility for a material that quenches oxygen radicals can further reduce particle toxicity. For example, a novel β -alanine C_{60} derivative was protective against hydrogen peroxide-induced cell damage [180]. Aggregated pristine fullerene, nano C_{60} , was more cytotoxic to human fibroblasts and liver carcinoma cells than fullerene derivatives because of superoxide production resulting in lipid peroxidation and cell membrane damage [207]. A follow-up study found that nano C_{60} elicited ROS-mediated cytotoxicity, lipid peroxidation, and membrane damage responses in several cell lines, with LC_{50} ranging from 2 to 50 ppb [208]. Unlike hydroxylation modification of the fullerene surface, amino acid-functionalized fullerene exposure caused increased production of pro-inflammatory mediators at moderate to high doses in epidermal keratinocytes ($>40\text{ }\mu\text{g ml}^{-1}$) [209]. Light exposure to some fullerenes causes phototoxicity through the release of singlet oxygen and superoxide [200]. This would suggest potential ROS damage to keratinocytes if workers were exposed. Similarly, exposure to both photosensitized fullerene and $C_{60}(\text{OH})_{18}$ caused ROS and lipid oxidation damage in rat liver microsomes [210]. Interestingly, fullerene toxicity was due to singlet oxygen release, while that of $C_{60}(\text{OH})_{18}$ was due to several radical species resulting in a wider array of lipid and protein oxidation. Conversely, fullerol exposure elicited little response in macrophages (RAW 264.7), but evidence of mitochondrial perturbation via Ca^{2+} ion release was identified [211].

In summary, compared to other ENMs, acute and subchronic fullerene family data suggest low risk for direct genotoxicity or indirect genotoxicity via oxidative stress. The *in vitro* and *in vivo* genotoxicity data, however, are limited. Further research efforts should focus on relevant fullerene and fullerol exposure concentrations, *in vivo* toxicokinetics and translocation, primary and secondary genotoxicity in *in vitro* and animal models, and subchronic and chronic exposure to identified target tissues.

10.2.5

Graphene and Graphene Oxide

The graphene nanomaterial family (GNF; [212]) is expected to experience large-volume and widespread use in nanotechnology fields including medicine, drug delivery, cells, supercapacitors, batteries, and sensors [212–214]. GNF is characterized by graphene sheets, with potentially high surface area, comprised of different lateral widths, edge morphology, number of graphene layers, stiffness, surface functionalization due to oxidation/reduction preparations [pristine vs graphene oxide (GO) vs reduced graphene oxide (rGO)], compact platelets, and well-dispersed graphene sheets. Thermal exfoliation during graphene production

results in dry powders that are respirable, which indicates lung tissue as a primary GNF toxicological target. Surprisingly, little evidence exists in evaluating the GNF for potential genotoxicity and subsequent tumor-associated pathologies when compared to similar nano-sized graphene NMs (i.e., carbon nanotubes) or other weak carcinogenic nano-sized carbon (i.e., carbon black). Similar to CNTs, limited studies suggest that graphene size, surface functionalization, and dispersibility appear to dictate toxicological response. GO, rGO, and organic-coated graphene have received increased attention due to their excellent dispersibility in aqueous solutions for technological manipulation, but they also have shown increased toxicity compared to their pristine counterparts. Several recent detailed reviews on GNF highlight the large nanotechnology potential of these materials, including the biological benefits and consequences of GNF exposure [212, 214–218].

At present, published data indicate that the high surface area, sorption, and catalytic ability of GNF particle surfaces provide dramatic ROS generation or quenching capacity. These qualities are comparable to those of SWCNTs, minus the HAR morphology. At present, it is not clear whether ROS in exposed tissues generated directly from the GNF particle surface or indirectly from cellular sources (e.g., leukocyte inflammation, mitochondria) is a greater risk for DNA oxidative damage. Stacking of monolayer graphene into multilayered graphene (e.g., graphene nanoplatelets) greatly reduces the surface area and alters sheet rigidity/morphology and the potential for altering oxidative/reduction reactions [212, 216]. The bonding between and number of layers in graphene NPs is rarely measured, even though it is thought to directly impact biological effects. Packing of sheets greatly reduces the surface area and should be assessed during characterization since it may lead to conflicting results [212]. Many publications evaluating MWCNTs repeatedly acknowledge that surface area and rigidity, due to the number of graphene layers, has a dramatic impact on particle morphology and toxicity response in exposed tissues. For example, a graphene NP with a fluid shape may experience passive diffusion in cytoplasm, endocytosis, or phagocytosis, while a particle with similar size but rigid morphology may elicit frustrated phagocytosis, inflammation, and ROS generation via recruited leukocytes. Their size ranges from $<10\text{ nm}$ to $>20\text{ }\mu\text{m}$ in lateral width, which clearly impact the uptake, endosome and lysosome receptor binding, and the potential for frustrated phagocytosis [212]. A few studies suggest the potential for some small-sized graphene with planar morphology to directly interact with DNA. Graphene may bind to single-stranded DNA, during replication or transcription, which could cause DNA damage and failure of genetic inheritance and block specific protein synthesis. It has also been suggested that planar graphene may intercalate into the DNA helix, similar to aromatic compounds [219]. Clearly, systematic studies evaluating the impact of several physicochemical properties on GNF particle toxicokinetics during exposure and in biological tissue, fate, uptake route, direct and indirect genotoxicity, and subchronic effects are warranted.

10.2.5.1

In Vivo Studies

Graphene exposure studies on *in vivo* models have typically used either i.v. injection or i.t. instillation to evaluate GNF particles' fate as well as whole-body or tissue level responses. Most studies report an enhanced inflammation response with little long-term effects, although GNF particles are biopersistent and can exhibit systemic fate. An important study by Duch *et al.* [220] evaluated aggregated graphene, dispersed graphene, and GO following i.t. exposure of 50 µg per mouse. Of note, GO particles displayed uniform, very thin sheets (1 nm thick) while Pluronic-dispersed pristine graphene displayed higher variability in thickness with a mean of ~2.5 nm. GO containing hydroxyl and carbonyl surface groups produced robust and prolonged inflammation with macrophage and neutrophil infiltration followed by severe lung tissue damage. Surprisingly, less GO was found inside phagocytic vesicles than graphene. Enhanced plasma thrombin was specific to GO-exposed mice. GO exposure elevated mitochondrial respiration by lending electrons to the electron transport chain, which enhanced ROS generation. This suggests that ROS generation may partially drive the activation of inflammatory and apoptotic signaling. Conversely, aggregated graphene showed reduced effect, while synthetically dispersed (Pluronic) graphene showed a mild inflammatory response. Interestingly, only GO caused a significant increase in TUNEL positive nuclei *in vivo* and DNA fragmentation in alveolar macrophage exposure experiments *in vitro*. Minimal fibrosis occurred in all three particle exposures compared to control. Intravenous injection of GO into the tail vein of mice caused significant impacts to lung tissue at 7 and 30 days post exposure [221]. Lung, liver, and spleen were the primary targets of injected GO. GO was found in the lung closely associated with neutrophil and foamy macrophage infiltrates. At 30 days, granulomas containing GO were observed along with interstitial inflammation and thickening of alveolar septa.

Other studies support the idea that well-dispersed pristine graphene causes acute inflammation but with minimal long-term health impacts. A unique inhalation exposure screening study of numerous carbon nanomaterials [222] compared graphene sheets, graphene nanoplatelets, MWCNTs, and carbon black for their *in vivo* cytotoxicity and inflammation response in Wistar rats. Graphene sheets exhibited toxic effects at the highest dose (10 mg m⁻³), while nanoplatelets and carbon black exhibited little to no toxic response. These responses paled in comparison to MWCNTs', which exhibited responses at ≥0.5 mg m⁻³.

Graphene nanoplatelets (>5 µm diameter, 1–10 graphene layers) were respirable up to 25 µm diameter in C57Bl6 mice and elicited a robust inflammatory response in the lung (aspiration) and pleural space (i.p. injection) after 1 and 7 days compared to Printex 90 carbon black [223]. Induction of several cytokines (IL-1β, MCP-1, IL-8) and ROS via NADPH oxidase, consistent with NALP3 inflammasome activation, was noted in *in vivo* lung and *in vitro* THP-1 exposures. Frustrated phagocytosis and granulomatous lesions, similar to those reported for different CNTs [106, 125] were also found. Nanoplatelets were found in chest wall pleural tissue with wall thickening at 1 week post injection

and exhibited slower clearance than carbon black via mediastinal lymph nodes. A follow-up report at 6 weeks post aspiration indicated minimal inflammation and oxidative degradation of graphene nanoplatelets in mouse lung tissue [224]. In contrast to CNT exposure, minimal fibrosis or hyperplasia was observed along with no inflammation in the pleural space.

As a follow-up study to the Schinwald studies, a 5-day inhalation exposure to 0.018 and 0.102 mg lung burden using 550-nm-wide stacked graphene platelets found little evidence for lung tissue damage at 28 days post exposure, including no LDH or protein release, with a robust alveolar macrophage phagocytotic response [225]. Interestingly, changes in hemocytometry and blood chemistry were observed in the high-dose group. Only slight alveolar wall thickening was observed. Similar to Schinwald, the authors suspected that the minimal toxicological effect was due to the large width, stacked platelet shape, and low surface area. Expansion of these studies using graphene with different physico-chemical properties would greatly assist in identifying property-associated lung disease risk.

Little to no evidence exists in evaluating GNF's *in vivo* genotoxicity following expected exposure scenarios. Based on available *in vitro* data, computational modeling, and *in vivo* data, several potential factors may contribute to GNF's genotoxic potential in exposed tissues. Graphene with small lateral diameter shows the ability to penetrate plasma membrane, are present in cytoplasm, accumulate near nucleus, and minimally penetrate the nucleus. Given their planar morphology, direct interaction with DNA by either direct binding or intercalation in exposed epithelial or fibroblast cells should be evaluated. Large planar graphene is not expected to penetrate deep into tissues but may illicit indirect genotoxicity via ROS generation and oxidative DNA damage.

Although not as reactive in tissue as CNTs, several major lines of evidence support the potential weak carcinogenicity of GNF particles. First, carbon black, a Group 2 carcinogen, possesses similar makeup and *in vivo* fate as GNF particles [222, 224]. Second, given that graphene is more acutely reactive in exposed lung tissue [223], indirect oxidative DNA damage in lung tissue following inflammation over repeated exposure is expected. Recovery periods after a single bolus and several days' inhalation suggest transient inflammation with little fibrosis promotion. Building on this report showing acute inflammation in mouse lungs after 1 day, Schinwald *et al.* [224] reported that pristine GPs showed minimal inflammation in mouse lungs after 6 weeks, even though there was no degradation of GP in lung tissue. It remains to be tested how a prolonged, repeated exposure to GNF particle (i.e., occupational setting) affects the risk for oxidative DNA damage and initiation. GNF particles repeatedly show long biopersistence in exposed tissues, either via i.v. injection or inhalation. At present, it is unclear what types of GNF particles have the potential to either move out of the exposed lung or potentially promote tumorigenesis by stimulating pro-proliferation and other cellular signaling pathways. Interestingly, graphene i.v. injected in the tail vein accumulated in lung tissue [221]. Lastly, use of GNF in biomedical applications involving implants, grafts, and scaffolds may elicit a foreign-body tumor response [212]. These sarcomas

are typically reported following contact with biopersistent materials, regardless of composition, that possess large surface area and smooth surfaces [226] used as implants or grafts. Several types of graphene NMs possess these morphological and surface characteristics [213]. Although not initially identified, inflammatory response followed by ROS and oxidative damage to DNA may be important drivers of tumor progression in foreign-body tumors [227]. It is also may rely on direct contact of preneoplastic cells in contact with a smooth surface and a drop in cell–cell communication, resulting in uncontrolled cell growth [228]. Of interest, a recent study reported the potential involvement of mesenchymal stem cells (MSCs) in foreign-body tumorigenesis [229]. Foreign-body sarcomas usually comprise dense collagen fiber with fibroblast cellular morphology [230] and exhibit late onset [228]. MSCs and MSC-derived cells (i.e., myofibroblasts) currently constitute an intensive area of research as key regulators of interstitial pulmonary fibrotic remodeling [231, 232]. Given that CNT exposure induces stem-like cells, with known MSC markers [233], leading to fibrotic nodules [234], it raises the possibility of a role of MSCs in potential foreign-body tumorigenesis following biopersistent graphene exposure. Clearly, these issues should be addressed in systematic *in vivo* exposure studies using appropriate ROS, biopersistence, and genotoxicity assessment procedures.

10.2.5.2

In Vitro Studies

Based on limited *in vitro* data, GNF exposure to established *in vitro* cell models can result in plasma membrane penetration, endocytosis, ROS release or sequestration, and cytotoxicity. Most adverse responses, including apoptosis and cytotoxicity, are reported at high doses. To date, it appears that lateral width and surface functionalization largely dictate both cellular fate and toxic response. Other physicochemical factors that may dictate adverse response include layer number, size, stiffness, and hydrophobicity [212]. Zhang *et al.* [235] compared several-layered graphene to SWCNTs to assess the effect of graphene's shape on cytotoxicity in neuronal cells. Graphene was more potent at reducing metabolic activity at low concentration ($0.1 \mu\text{g ml}^{-1}$), while SWCNTs produced significantly more LDH and metabolic disruption at higher doses ($>1 \mu\text{g ml}^{-1}$). ROS generation coincided with caspase 3 activation and apoptosis ($\geq 10 \mu\text{g GO per milliliter}$). Exposure of pristine graphene to RAW 264.7 macrophages elicited decreased mitochondrial membrane potential, increased ROS, TGF- β release, and intrinsic Bcl-2-mediated apoptosis pathway activation [236].

Recent computational modeling studies evaluated the impact of graphene sheet size and morphology on cell membrane phospholipid dynamics and potential cytotoxicity. Using bacterial membrane as a model, Tu *et al.* [237] reported that graphene and GO sheet edge can pierce plasma membranes. Sheets also retained the ability to extract phospholipids from the membrane, modify membrane polarization, and enhance cell leakiness. The authors suspect that disruption of the plasma membrane could alter membrane-bound receptor function, resulting in activation of apoptosis. Computational models suggest that size has

an impact on graphene's fate in the cell. Small sheets penetrate cell membranes, medium-sized sheets pierce membrane at certain orientations, and large sheets get absorbed in the membrane [238].

Pristine graphene and GO exhibit greater toxicity to cell models than GNF particles that possess organic coatings or organic polymers. Chang *et al.* [239] evaluated three different size preparations of GO (160–780 nm wide) for uptake, intracellular fate, and ROS generation ability in an alveolar epithelial cell model (A549). GO was not found inside cells, but ROS following exposure did increase due to generation on the GO surface in a cell-free culture medium. Wang *et al.* [221] reported a time-dependent increase in the uptake of GO into lysosomes, mitochondria, and endoplasm of human fibroblasts, albeit at high doses ($>20 \mu\text{g ml}^{-1}$). Later time points found GO accumulating around nuclear membrane, with occasional particles inside the nucleus. Another study found that single-layered GO exhibited greater ability than SWCNTs to cause increased cell membrane damage and induction of autophagy, but failure of the autolysosome, resulting in cell death of exposed mouse peritoneal macrophages [240]. A recent report showed that GO triggered an early onset of DNA melting *in vitro* [241].

Hinzmann *et al.* [242] compared pristine GO, rGO, and unaltered GO with graphite and ultra-dispersed detonation diamond in glioblastoma multiforme cells at $50 \mu\text{g ml}^{-1}$. Although conducted in a cancer cell line, pristine and reduced GO led to high cytotoxicity compared to other particles. Interestingly, particles showing both high (pristine, rGO) and low cytotoxicity (graphite and ultra-dispersed detonation diamonds) induced DNA damage as seen by positive comet assay. Carboxyl-functionalized graphene improved hydrophilicity, enhanced cell uptake, and reduced cytotoxicity compared to unfunctionalized, hydrophobic graphene [243]. Wang *et al.* [244] examined the effect of different surface charges on GO to cause oxidative stress in lung fibroblast cells. Three types of surface-modified GO were compared to the parent material. Following exposure, ROS in the exposed cells was linked to cytotoxicity. PEG coating was more protective to fibroblasts than PEI coating or unmodified GO. The authors argue that differences in surface charge impacts agglomeration, interaction with plasma membrane, and uptake into cells. Although never assessed in the study, the findings raise the idea that surface coating of GNF may protect cells against ROS-induced oxidative damage to DNA. Similarly, Hu *et al.* [245] reported that the amount of serum in cell culture medium can reduce and minimize GO toxicity as a result of the formation of a thick protein corona.

Next, an interesting, if alarming study of rGO nanoplatelets raises the idea that small nanosized GNF particles at low doses can cause genotoxicity compared to their larger counterparts. Akhavan *et al.* [8] exposed four different sizes (11–3800 nm) of rGO nanoplatelets to human MSCs. The 11-nm rGO nanoplatelets exhibited cytotoxicity as low as $1 \mu\text{g ml}^{-1}$, while larger sized platelets showed reduced toxicity. Similarly, the 11-nm platelets caused DNA fragmentation (comet assay) and chromosome aberrations in metaphase assay as low as $0.1 \mu\text{g ml}^{-1}$ following a 1-h exposure. Of note, RNA efflux, a marker

for cell membrane damage, was negative across all particles and doses. Although the authors never directly assessed the intracellular location of the nanoplatelets, the study suggests that rGO nanoplatelets are capable of penetrating cell membranes to initiate genotoxicity at low doses while ROS generation may impart indirect oxidative damage at higher doses. Lastly, a comprehensive systems toxicology evaluation of GO versus rGO was conducted to evaluate the impact of hydrophobicity on biological interactions in HepG2 cells [246]. Although both graphene particles displayed similar toxicity endpoints (oxidative stress, DNA damage, and cell death), an omics evaluation along with particle fate analysis identified completely different mechanisms of action. Hydrophilic GO experienced cell uptake, ROS generation via NADPH oxidase, and deregulation of DNA repair and oxidative stress response genes. Signaling analysis revealed TGF- β as a key mediator of toxicological response. rGO, however, got adsorbed to the plasma membrane, thereby generating ROS via direct interactions, activating viral and innate immune response via the Toll-like receptor 4–NF- κ B pathway.

Compared to inflammation- and ROS-focused research, very limited data using *in vitro* models exist concerning those physicochemical properties, toxicokinetics factors, and mechanisms associated with GNF particle genotoxicity. Based on GNF's ability to induce inflammation and ROS in exposed cells, indirect genotoxicity via oxidative DNA damage is a distinct possibility [244]; however, this has not been systematically studied to date. A nanomaterial genotoxicity study comparing numerous nanomaterials identified graphene as having comparable, if not more potent, DNA fragmentation ability than other well-studied materials in isolated fibroblast cells [247]. De Marzi *et al.* [248] compared nano-GO (130 nm) to micrometer-sized (1320 nm) GO for DNA damage via comet assay in lung (A549), intestine (Caco2), and kidney (Vero) cells. Nano-GO was more potent at inducing DNA damage than its micrometer counterpart at 10 $\mu\text{g ml}^{-1}$. At present, GNF's ability to directly damage DNA and chromosome integrity is virtually unknown. Two recent studies, however, raise this possibility. First, exposure to r-GO nanoplatelets caused DNA fragmentation and chromosomal aberrations in human MSCs (0.1–1 $\mu\text{g ml}^{-1}$) at doses far below that exhibited ROS and cytotoxicity (1–100 $\mu\text{g ml}^{-1}$) [8]. Next, a study investigating GO particle's therapeutic ability as a DNA cleavage agent found that GO sheets with bound Cu $^{2+}$ were able to intercalate DNA, resulting in cleavage via hydrolytic and oxidative mechanisms [219]. Other GO-bound metals (Ni $^{2+}$, Zn $^{2+}$, Fe $^{3+}$) also displayed similar ability. Different metals exhibit different affinities for DNA, with often drastic consequences for gene regulation [249]. Carbon nanomaterials, either through synthesis or through environmental release, can sorb different metal ions. This study raises the possibility of direct DNA damage via GNF particle exposure if the particles are successful in moving through the cytoplasm and into the nucleus, especially during cell division. In summary, the size, surface functionalization, platelet structure, and surface morphology can impact direct or indirect genotoxicity (Figure 10.7), but more research is warranted.

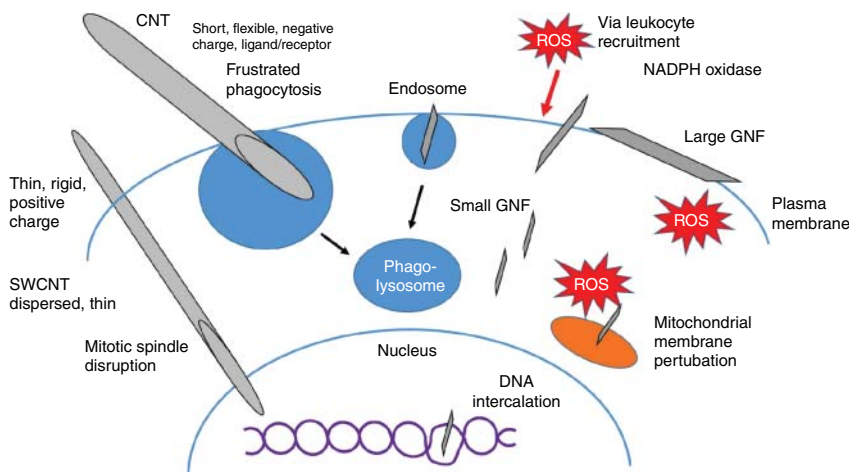


Figure 10.7 Overview of the physicochemical properties of carbon nanotubes' and graphene nanomaterial family's toxicodynamics and genotoxicity potential in target cells and tissues.

10.2.6

Carbon Nanofibers and Other Particles

Given the wide application of ECNMs in various nanotechnological applications, the types of novel ECNMs are expected to expand. In addition, based on the physicochemical properties already identified as posing significant human and environmental health hazards (e.g., pristine and long CNTs), novel second- and third-generation “safe-by-design” ECNMs are already making their way into production (e.g., biodegradable CNTs and coated CNTs). Screening each material is impossible, but through systematic studies of how their physicochemical properties impact genotoxicity and promotion mechanisms, we can effectively screen and prioritize new ECNMs for further *in vivo* testing. Recent work with CNFs compared to CNTs and asbestos shows that this strategy has merit.

CNFs share similar synthesis routes as well as morphological and chemical characteristics with MWCNTs. Their main difference is the orientation of graphene within the fiber structure. CNFs possess graphene in a cupped or stacked orientation, resulting in diameters of 40–200 nm and lengths similar to those of CNTs [22]. Airborne CNFs are known to occur during manufacturing [22, 250, 251].

10.2.6.1

In Vivo Studies

Murray *et al.* [252] evaluated the inflammatory and fibrotic potential of CNFs compared to SWCNTs and asbestos. Particle agglomeration was found to impact granuloma formation and collagen deposition. Well-dispersed CNF and asbestos

fibers did not induce granulomas, while SWCNT agglomerates displayed granulomatous lesions. CNFs showed similar leukocyte recruitment as well as ROS and inflammatory cytokine release compared to other HAR fibers. For all three particle types, effective surface area and mass dose were better predictors of adverse responses compared to other surface area metrics or particle count.

A 90-day inhalation exposure study was conducted on Showa Denko CNF with 5.8 μm mean length [253]. Rats exposed to 2.5 and 25 mg m^{-3} of the material exhibited similar inflammatory responses to CNTs, while the lower dose (0.54 mg m^{-3}) exhibited minimal effect. No fibrosis was found, although fibers persisted at 3 months post exposure, possibly due to deposited lung burden [22].

A 1-year study in mice [112] comparing CNFs to SWCNT and asbestos fibers found no tumor formation. SWCNT exposure caused significant MN and nuclear protrusions. CNF and asbestos exposure resulted in the strongest inflammation response, while SWCNT had the strongest fibrosis response. Increased frequency of KRAS mutations was seen in both CNF- and SWCNT-exposed mice.

10.2.6.2

In Vitro Studies

A few *in vitro* studies have evaluated CNFs for their neoplastic transformation potential. Darne *et al.* [254] conducted a short-term (7-day) *in vitro* neoplastic transformation assessment with 11 carbon fibers of different length and from different stages of production from polyacrylonitrile synthesis using SHE (Syrian Hamster embryo) cells. Electron paramagnetic resonance (EPR) analysis revealed no ROS formation. Subsequently, no morphological transformation compared to chrysotile asbestos positive control was observed. The authors acknowledged that short exposure duration and the high amount of protein serum (20%) in the culture medium potentially contributed to the observed null effect. Large quantities of protein potentially enlarged the protein corona, masked potential carbon binding sites, and reduced toxicity or other stimulatory effects in the exposed cells. A comparative study of CNFs versus SWCNTs and asbestos fibers [255] found that CNF exposure caused greater cytotoxicity than SWCNTs in V79 fibroblasts, while asbestos fibers showed the greatest response. CNFs produced the strongest genomic damage via DNA strand breaks, aneuploidy, and increased micronucleus frequency compared to other fibers. ROS release from exposed macrophages was strongest in CNF- and asbestos-exposed cells.

10.3

Future Challenges in Carbon Nanomaterial Carcinogenesis Risk Assessment

10.3.1

Exposure Characterization and Fate

Effective risk assessment depends on quantitatively measuring exposure concentrations and evaluating the dose–response in both acute and chronic exposure

scenarios in appropriate physiological model systems. A large volume of research has evaluated ECNMs' toxicity in numerous systems, but comparatively, we currently understand very little about exposure concentrations of ECNMs throughout their life cycle (i.e., cradle to grave). The lack of robust analytical sampling and sensitive quantitative detection technologies has proven a big hurdle to assessing ECNMs in environments with large amounts of natural carbon.

The vast majority of ECNM *in vitro* and *in vivo* toxicity studies are single exposures to achieve a modeled tissue burden. Although these models do provide useful data, they do not reflect physiologically relevant exposures (i.e., chronic low to moderate doses) expected either in the occupational or environmental settings. Inhalation chambers for *in vivo* animal models do exist and tend to show larger toxicological effects than equivalent dosing using traditional single-exposure dosing [101]. They are, however, costly and time consuming and typically reserved for either Tier II or Tier III screening [24].

Likewise, tracking of nonbiodegradable ECNMs in exposed tissues, their toxicokinetics, and ultimate fate over extended periods has proven labor intensive in past studies. Recent examples using stable isotope or fluorescent labeling of ECNMs have improved the ability to track their systemic fates in *in vivo* models and have identified new target tissues that should be assessed for adverse outcomes [e.g., 110].

10.3.2

Dosimetry

Researchers engaged in ECNM toxicity studies should first evaluate and justify their use of the chosen dose or dose range based on physiologically and relevant real-world exposure conditions. Past acute studies on ECNMs to measure their dose–response tended to use unrealistic dose ranges that could not be extrapolated to lower doses, which are 100- to 1000-fold lower. For example, noncytotoxic doses of SWCNTs in a fibroblast *in vitro* model showed enhanced proliferation and collagen deposition, which correlated well with the observed *in vivo* effects at the same deposited mass per lung surface area [256].

Currently, the question of which dose metric to use is controversial, which has resulted in a high volume of research. For ECNMs, elemental carbon mass, particle number, and effective surface area have all been proposed. An ideal dose metric should be measurable during exposure (i.e., airborne particles), during deposition/translocation, and at the site of biological effect [62]. Recently, the most useful studies adequately characterized the deposition of ECNMs since this allowed the calculation of the internal dose at the biological receptor [2, 257]. Understanding the toxicokinetics and how they influence internal dose can greatly assist in characterizing dose–response relationships for genotoxicity (or lack thereof), internal cell target, signaling pathway activation, and effects on promotion and progression in appropriate models.

10.3.3

Model Choice

Review of the literature reveals that *in vitro* cell models first established from cancer tissues (e.g., A549) are routinely used in ENM toxicity studies, primarily due to their rapid and robust growth in the laboratory. Although some information about acute toxicity of ENM exposure to these cells is useful, they serve little purpose in ENM exposure-associated neoplastic transformation or tumorigenesis studies. Some *in vivo* studies report no tumor formation following exposure in murine models that have moderate to high resistance to tumorigenesis. Both IARC and OECD have pre-validated *in vitro* cell transformation and murine tumorigenesis models with historical data to support their use on a wide variety of soluble and insoluble organic and metal xenobiotics [258, 259]. The Balb/3T3 and SHE cell lines are pre-validated models for morphological cell transformation upon exposure to known carcinogens [259, 260]. Although these mouse and hamster cell lines show good correlation with their murine *in vivo* model counterparts, they are not human cells. Thus, appropriate human-derived cell lines with a stable genotype should also be used for genotoxicity and early carcinogenic events (i.e., initiation and promotion) to provide adequate screening ability for numerous ENMs. These human cells must be carefully chosen based on the suspected ECNM exposure route, tissue dose, toxicokinetics, and eventual fate within the body [259]. With the advent, incorporation and mainstream use of genome signature profiling and Next Gen sequencing, cell models should represent a healthy phenotype (statistically) to act as an appropriate reference. As confirmed human exposure cases are reported, these models may become refined. It is important to note, however, that few of these models have been used in ENM neoplastic transformation or *in vivo* initiation/promotion studies. Future efforts should be directed toward evaluating how these established models perform in assessing unknown ENM carcinogenic effect with positive control particles (e.g., asbestos) as a measure of effect.

Great advancements have occurred in *in vitro* cell models, with monoculture cell models being quickly phased out as the primary test system. Co-culture with multiple cell types, advancements in immortalization procedures and new cell models, 3D spheroids, 3D tissue sections, microfluidic organ-on-a-chip, numerous extracellular matrix options, and air–liquid interface (ALI) systems are showing great promise in helping to bridge the gap between *in vitro* and *in vivo* exposure/effect model systems [261, 262]. These models are fairly new and relatively untested in assessing carcinogenesis-associated effects. Recent studies have highlighted that multicellular *in vitro* systems are better predictors of *in vivo* effects than a monoculture alone [263] and hold great promise in the near future. Careful design of these multicellular systems, however, needs to be effected to mimic physiological response. For example, several 3D or ALI system with A549 cells and other immune or fibroblast cell lines were employed to assess ECNM toxicity with little ROS, inflammation, or cytotoxic effect, possibly due to the cancer cells' ability to tolerate ECNMs [264, 265]. Use of more sensitive,

noncancerous airway epithelial cells, with underlying fibroblasts, would greatly add value to 3D culture and act as a bridge model between *in vitro* and *in vivo* studies. Future applications of these “bridge models” may have a distinct advantage in that they could be used to (i) predict the *in vivo* effect, (ii) study toxicokinetics in an appropriate 4D system, (iii) isolate and study specific cells via flow cytometry to assist in classifying and characterizing novel mechanisms of tumorigenesis, and (iv) reduce the time and energy needed for *in vivo* models.

10.3.4

Systematic Evaluation of Genotoxicity

Many acute exposure studies, both *in vitro* and *in vivo*, have focused on cytotoxicity and inflammation as major endpoints. The amount of studies focusing on genotoxicity palls in comparison, potentially because of the amount of conflicting results. In order to screen and identify novel ENMs for their carcinogenic potential, a systematic evaluation of numerous ENMs with different physicochemical properties with appropriate exposure models would be necessary, thereby advancing the field dramatically. Pilot studies and examples of such approaches do exist. For example, Watson *et al.* [266] designed a high-throughput comet chip assay to screen numerous ENMs. Development and validation of genotoxicity *in vitro* and *in vivo* assays for ECNMs and other ENMs is currently a major need in the ENM risk assessment framework (see below).

Novel approaches to investigate genotoxicity continue to advance and should be evaluated and potentially implemented into the ECNM toxicity screening framework. Along with the aforementioned high-throughput comet chip assay, genotoxicity studies on single cells, grown in either 2D or 3D formats, can identify and quantify single-cell genotoxicity via DNA fragmentation for use in high-throughput screening of different nanomaterials [248]. This technique could also be used on collected tissues from *in vivo* exposures by labeling a cell with a specific marker of DNA damage and performing single-cell sampling. Single-cell high-throughput polymerase chain reaction (PCR) analysis can further examine the translational impacts of potential DNA damage. Next-generation sequencing may serve as the next high-throughput genotoxicity assay for robust mutation risk assessment. Such strategies, with appropriately designed methods to capture somatic mutations, would capture numerous mutation events, thus potentially removing the use of DNA damage markers and extrapolation from animal models to assess human impact [267].

10.3.5

Role of ROS and Inflammation

Given the long history of transient and/or persistent inflammation and ROS generation following particle exposure, they can be considered strong and robust responses and should not be ignored when evaluating ENMs. Nanomaterials inherently possess high surface-to-volume ratios and particle number per unit mass. Prolonged inflammation and ROS generation can overwhelm DNA repair

mechanisms, leading to inheritance of damaged DNA, genetic instability, and possible promotion of tumorigenesis [268]. In addition, the immune system plays key roles in the promotion and progression of tumorigenesis. With the recent evidence that numerous ENMs (i) elicit DNA damage at doses below known thresholds for induction of inflammation, (ii) possess high reactivity compared to bulk counterparts, and (iii) exhibit potentially different toxicokinetics and fate in exposed tissues than bulk counterparts, future research efforts should evaluate dose-response studies to identify genotoxic, ROS generation, and inflammation thresholds in relation to tumorigenesis thresholds. Systematic studies using several ENMs with different physicochemical properties would provide data for structure/activity models for these three major processes associated with tumorigenesis. These efforts would also evaluate how the immune system responds to (fight or promote) ENM-associated tumorigenesis.

10.4

Assessment of ENM-Induced Genotoxicity and Carcinogenesis

10.4.1

Recommendations for Screening ENMs for Carcinogenic Potential

- 1) Characterize, characterize, characterize. A majority of conflicting data in genotoxicity, acute toxicity, and tumorigenesis is largely associated with inadequate physicochemical characterization. Such data is imperative to developing QSAR-like models for ENMs, given the rapid and expansive pace of nanotechnology development.
- 2) Consider exposure routes and suspected long-term exposure scenario (*dose*). Although somewhat useful as an exploratory, preliminary screen, injections of ENMs into body cavities, usually at high doses, may elicit false positives (e.g., overload) and do not incorporate the toxicokinetics and potential physicochemical changes that an ENM may experience during its uptake and internal distribution routes.
- 3) Adopt established or fully reported sample preparation and exposure methods.
- 4) Adequately justify the chosen exposure doses and characterize dosimetry. ENMs behave differently in air, liquid, or tissue. With robust characterization, the ability to model toxicokinetics and eventual internal dose is of utmost importance. Report the mass, surface area, and particle number. Avoid particle overload since this is more likely at lower mass dose due to the particles' high surface areas [269, 200–300 cm² in rats]. *In vitro* studies must justify the chosen doses and relate to *in vivo* animal model and expected or known human exposure levels.
- 5) Evaluate toxicokinetics (i.e., agglomeration, dispersion, and stability) of ENMs both during exposure and once internalized within exposed tissues.
- 6) Genotoxicity testing should be performed on low-passage, genotypically stable (i.e., p53 status) cell lines that possess low background DNA damage.

Use appropriate nontumorigenic models with either a stable genotype or gene knockdown (p53 *+/−*) to assess their predisposition for tumorigenesis. *In vitro* cell models from cancers or those sensitive to spontaneous transformation are inappropriate (unless justifiable) for carcinogenesis screening studies.

- 7) Use two or more genotoxicity tests that cover multiple forms of chromosome/DNA damage.
- 8) Use multiple particles to assess physicochemical properties, including the source unadulterated or underivatized material to provide structure/activity relationship information.
- 9) Use literature-established positive control ENMs or ultrafine particles. Well-characterized/studied UFCB, TiO₂, or crystalline silica may serve as a positive control for spherical metal/metal oxide particles. Mitsui #7 MWCNT and/or crocidolite asbestos are excellent choices for fibrous HAR ENMs. This is critical for control banding and tiered assessment approaches.
- 10) Use multiple doses to identify thresholds (NOEC, LOEC, maximum response); this is required for adequate risk assessment.
- 11) Use multiple cancer cell phenotype assays at different time points during exposure to characterize the rate of initiation, promotion, and progression of ENM-associated carcinogenesis.
- 12) Improve upon, assess, and validate multicellular and multidimensional *in vitro* models, CSCs, co-culture, spheroids, 3D tumor microenvironments; refine toxicological strategies; and reduce number of animals used to evaluate long-term health risks. When available, compare and contrast *in vitro* neoplastic transformation with *in vivo* tumorigenesis models. Integration of genotoxicity, cancer cell behavior, and toxicogenomics data from *in vitro* or 3D tissue transformation studies could one day assist in predicting *in vivo* carcinogenesis.
- 13) Evaluate the effects and mechanisms that support the tumor microenvironment. No ECNM has yet been shown as a complete carcinogen (i.e., initiation, promotion, and progression). A growing body of evidence exists, however, suggesting that carbon ENMs promote or help progress carcinogenesis through either direct interaction with genetically damaged cells (i.e., MWCNTs and UFCB) or indirectly by enhancing the tumor microenvironment (i.e., immunosuppression, extracellular matrix remodeling).
- 14) Nanotechnology continues to develop at a rapid pace, and carcinogenesis risk research should keep pace with this new development. A small subpopulation of workers is expected to come into contact with raw ECNMs. A majority of ECNM exposures to humans are more likely to occur downstream during ECNM incorporation into composites, product use, and eventual disposal. At present, exposure and toxicological assessment of ECNMs and other ENMs are switching toward life cycle assessment. In addition, second- and third-generation ECNMs continue to enter nanotechnological applications, with improved technology and safe-by-design strategies. Understanding how physicochemical properties of ECNMs

change throughout their life cycle will be imperative to the successful development of safe/prevention-by-design nanotechnologies.

10.4.2

Systematic Screening Paradigm and Workflow for ENM Carcinogenicity Risk Assessment

No documented case of ECNM-exposure-associated tumorigenesis exists. Nevertheless, it is clear that certain physicochemical properties of ECNMs elevate the risks for long-term health impacts and disease, including cancer. Recently, working groups in both the US and EU have proposed strategies to effectively screen ENMs, including ECNMs. Categorization strategies, based on (i) hazard exposure, (ii) ENM's physicochemical properties, and (iii) data from suitable and validated alternative testing strategies (ATS) would aid regulators and industry to prioritize ENMs in qualitative control banding and more quantitative tiered rankings for further costly time- and resource-consuming testing [24, 270–272]. ATS is a proposed approach to perform systematic high-throughput testing on a large number of untested chemicals (e.g., EPA ToxCast) to provide large amounts of data. It relies heavily on numerous *in vitro* assays based on toxicological mechanisms and pathways in an attempt to reduce and refine animal model use. Although the acquired ATS data can be used for understanding ENMs' structure–activity relationships and categorizing the risks, (i) the complexity of *in vivo* systems is lost for assessing both ENM toxicokinetics and dynamics, (ii) time-dependent analysis of disease progression is difficult to perform, (iii) issues exist regarding correct and relevant dosimetry, and (iv) it is necessary to design and implement multifactorial statistical procedures for adequate prediction of *in vivo* response, all of which are major obstacles [24]. Toxicogenomics and *in silico* and systems-biology approaches may allow researchers to overcome these faults. Genome signature profiling has uncovered numerous potentially relevant modes of action for numerous ENMs in both *in vitro* and *in vivo* [90, 145, 273, 274]. Comparative genomic and proteomic studies using multicellular *in vitro* tissue culture with *in vivo* models hold promise as a useful tool in toxicity testing in the near future. Tiered screening approaches using identification of hazard exposures, *in vitro* testing, ATS testing, and 90-day *in vivo* inhalation studies provide avenues to overcome the need to quickly screen and prioritize carbon and other ENMs for chronic disease risk.

Current screening assays for genotoxicity include the Ames test, comet assay, micronucleus assay during cytokinesis block, chromosome aberration, HPRT mutation assay, γ -H2AX expression, 8-hydroxydeoxyguanosine DNA adducts, and so on [275]. Numerous studies have used the comet assay to screen ENMs with conflicting results [276, 277], largely due to the differences in particle preparation, size, crystal structure, and the tested cell types [278]. Based on the great need for systematic genotoxicity assessment of numerous novel ENMs, the comet assay, micronucleus assay, γ -H2AX expression, and 8-hydroxydeoxyguanosine adduct assays provide rapid, high-throughput assay options to capture clastogenic, aneuploidy, and ROS-associated damage of chromosomes. For assessing direct DNA damage across numerous materials, the micronucleus assay has a clear

advantage since it can distinguish between clastogenic and aneuploid damage (with kinetochore staining), and is successfully being implemented in recent high-content/high-throughput imaging platforms. The remaining established assays are usually labor intensive and time consuming, but remain useful in further detailed studies of ENM genotoxicity. 8-Hydroxydeoxyguanosine is typically assayed as a DNA oxidation byproduct, but high baseline levels and nonspecific fluorophore binding are often encountered, resulting in conflicting reports. Even with these shortcomings, there is large evidence showing increased oxidative DNA damage following oral and pulmonary exposure to ECNMs, supported by *in vitro* comet assays [279]. Although these test results are generally accepted, shortcomings in studies still make it difficult to rank either ENMs or their physicochemical properties into meaningful risk groups. Like most assays, with ENMs present in the sample, proper controls with only ENM and no tissue should be used since numerous ENMs have been shown to interact with DNA once other cell structures have been removed (e.g., comet assay) [276]. Secondary tests, in addition to the primary test, should be used to adequately characterize genotoxicity across numerous particles. Nevertheless, current genotoxicity tests provide a sensitive and rapid method to systematically assess ENMs with different physicochemical properties for carcinogenesis initiation risk.

A recent OECD publication reviewed ENM genotoxicity testing strategies that are applicable for ECNMs also [280]. At present, no set guidelines are available for ENM testing. Current hurdles to achieving an effective testing strategy include a robust and adequate testing regime as well as questions as to whether single or a combination of tests should be used and whether certain classes of ENM (like ECNMs) should warrant the development of their own unique set of protocols. At present, a combined testing strategy appears to give adequate genotoxicity characterization *in vitro* [281]. The micronucleus assay (OECD TG 487), using cytochalasin B in the absence of ENM, 24-h ENM exposure, physiologically relevant protein serum levels, and p53-stable cell lines, was cited as a preferable assay at present. The comet assay can characterize both aneugenic and clastogenic DNA damage. The mammalian mutation assay (OECD TG 476) should be used instead of the Ames test since bacteria display strikingly different ENM toxicokinetics.

In vitro testing serves as an appropriate screening strategy, but may not predict *in vivo* effects since several reports show little *in vivo* toxicity although the *in vitro* tests were positive [280]. Toxicokinetics, clearance mechanisms, and inherent variability within an ENM particle class are usually confounding factors that must be characterized, thus dictating that genotoxicity endpoints must be a part of a Tier II short-term *in vivo* toxicity testing strategies. As such, improvements are needed in cell/tissue uptake assessment to identify appropriate dose metrics, low-dose effects, and dispersant effects. Researchers should understand exposure scenarios and base their *in vitro/in vivo* exposures (dose and time) to adequately model potential genotoxicity.

10.5

Concluding Remarks

Accumulated *in vivo* and *in vitro* studies have suggested genotoxicity and carcinogenic effects of ECNMs, with UFCB and MWCNTs showing human carcinogenic potential, while, currently, an overall understanding of this is lacking. Full characterization of an ECNM's properties appears to lend critical data to understand what drives genotoxicity and promotion. Technological advances in characterizing nanomaterials will help assess their exposure and their fate in the workplace and environment, as well as identify nanomaterials in biological tissues following exposure. Systematic strategies to assess genotoxicity and malignant transformation exist and await incorporation into screening and tiered assessment frameworks. Equal attention should be paid to both genotoxic and non-genotoxic ECNMs since some materials may solely promote or help progress carcinogenesis. As our understanding of carcinogenesis expands (e.g., CSCs, tumor microenvironment), the validation and incorporation of new screening and assay techniques into a comparative model framework can potentially improve cancer risk and keep pace with oncology research and clinical advancements. As the spectrum of ECNMs expands and ECNM-enabled technology use becomes widespread with second- and third-generation materials, the development for rapid and robust assessment for long-term occupational and public health risks is a pressing need. By considering the above recent advancements, it is clear that a multidisciplinary and translational approach must be developed and utilized to improve and mainstream "prevention-by-design" strategies to reduce their carcinogenic potential and safeguard beneficial ECNM nanotechnologies. It is imperative that stakeholders form a consensus on appropriate frameworks to assess the risk and develop ECNM technologies that balance technological benefit and "prevention-by-design" considerations.

Acknowledgments

TAS and LW acknowledge the support of Nanotechnology Research Center (NTRC) through No. ZXFJ. LS is supported by NTRC through No. 011N and NIOSH Intramural Grant No. ZLDA funding. YR acknowledges the support of the National Institute of Health through award No. R01-ES022968 and the National Science Foundation through award No. CBET-1434503. Special thanks are due to Aaron Erdely for his constructive comments on this work.

Disclaimer

The findings and conclusions in this report are those of the authors and do not necessarily represent the views or policy of the National Institute for Occupational Safety and Health. Mention of product name does not constitute an endorsement.

References

- Zhang, B., Zheng, X., Li, H. *et al.* (2013) Application of carbon-based nanomaterials in sample preparation: a review. *Anal. Chim. Acta*, **784**, 1–17.
- Oberdorster, G. (2010) Safety assessment for nanotechnology and nanomedicine: concepts of nanotoxicology. *J. Intern. Med.*, **267** (1), 89–105.
- Maynard, A.D. (2006) Nanotechnology: the next big thing, or much ado about nothing? *Ann. Occup. Hyg.*, **51**, 1–12.
- Johnson, D.R., Methner, M.M., Kennedy, A.J. *et al.* (2010) Potential for occupational exposure to engineered carbon-based nanomaterials in environmental laboratory studies. *Environ. Health Perspect.*, **118** (1), 49–54.
- Han, J.H., Lee, E.J., Lee, J.H. *et al.* (2008) Monitoring multiwalled carbon nanotube exposure in carbon nanotube research facility. *Inhalation Toxicol.*, **20** (8), 741–749.
- Sargent, L.M., Reynolds, S.H., and Castranova, V. (2010) Potential pulmonary effects of engineered carbon nanotubes: *in vitro* genotoxic effects. *Nanotoxicology*, **4**, 396–408.
- Muller, J., Decordier, I., Hoet, P.H. *et al.* (2008) Clastogenic and aneugenic effects of multi-wall carbon nanotubes in epithelial cells. *Carcinogenesis*, **29**, 427–433.
- Akhavan, O., Ghaderi, E., and Akhavan, A. (2012) Size-dependent genotoxicity of graphene nanoplatelets in human stem cells. *Biomaterials*, **33**, 8017–8025.
- Grosse, Y., Loomis, D., Guyton, K.Z. *et al.* (2014) Carcinogenicity of fluorodenite, silicon carbide fibres and whiskers, and carbon nanotubes. *Lancet Oncol.*, **15**, 1427–1428.
- Dresler, C. (2013) The changing epidemic of lung cancer and occupational and environmental risk factors. *Thorac. Surg. Clin.*, **23**, 113–122.
- Dey, A., Biswas, D., Saha, S.K. *et al.* (2012) Comparison study of clinicoradiological profile of primary lung cancer cases: an Eastern India experience. *Indian J. Cancer*, **49**, 89–95.
- Samet, J.M., Avila-Tang, E., Boffetta, P. *et al.* (2009) Lung cancer in never smokers: clinical epidemiology and environmental risk factors. *Clin. Cancer Res.*, **15**, 5626–5645.
- Loomis, D., Grosse, Y., Lauby-Secretan, B., El Ghissassi, F., Bouvard, V., Benbrahim-Tallaa, L., Guha, N., Baan, R., Mattock, H., Straif, K., and International Agency for Research on Cancer Monograph Working Group IARC (2013) The carcinogenicity of outdoor air pollution. *Lancet Oncol.*, **14**, 1262–1263.
- Becker, H., Herzberg, F., Schulte, A. *et al.* (2011) The carcinogenic potential of nanomaterials, their release from products and options for regulating them. *Int. J. Hyg. Environ. Health*, **214**, 231–238.
- Sargent, L.M., Porter, D.W., Staska, L.M. *et al.* (2014) Promotion of lung adenocarcinoma following inhalation exposure to multi-walled carbon nanotubes. *Part. Fibre Toxicol.*, **11**, 3.
- Nel, A.E., Madler, L., Velegol, D. *et al.* (2009) Understanding biophysico-chemical interactions at the nano-bio interface. *Nat. Mater.*, **8**, 543–557.
- Luanpitpong, S., Wang, L., and Rojanasakul, Y. (2014) The effects of carbon nanotubes on lung and dermal cellular behaviors. *Nanomedicine*, **9**, 895–912.
- Bergin, I.L. and Witzmann, F.A. (2013) Nanoparticle toxicity by the gastrointestinal route: evidence and knowledge gaps. *Int. J. Biomed. Nanosci. Nanotechnol.*, **3** (1-2), 163.
- Mercer, R.R., Scabilloni, J.F., Hubbs, A.F. *et al.* (2013) Extrapulmonary transport of MWCNT following inhalation exposure. *Part. Fibre Toxicol.*, **10**, 38.
- Donaldson, K. and Poland, C.A. (2012) Inhaled nanoparticles and lung cancer – what we can learn from conventional particle toxicology. *Swiss Med. Wkly.*, **142**, w13547.
- Erdely, A., Dahm, M., Chen, B.T. *et al.* (2013) Carbon nanotube dosimetry:

from workplace exposure assessment to inhalation toxicology. *Part. Fibre Toxicol.*, **10** (1), 53.

22. NIOSH (2013) Occupational exposure to carbon nanotubes and carbon nanofibers, in *Current Intelligence Bulletin*, vol. 65. Centers for Disease Control, United States Department of Human and Health Services.

23. Gonzalez, L., Lison, D., and Kirsch-Volders, M. (2008) Genotoxicity of engineered nanomaterials: a critical review. *Nanotoxicology*, **2**, 252–273.

24. Nel, A.E., Nasser, E., Godwin, H. *et al.* (2013) A multi-stakeholder perspective on the use of alternative test strategies for nanomaterial safety assessment. *ACS Nano*, **7** (8), 6422–6433.

25. Pott, F. and Roller, M. (2005) Carcinogenicity study with nineteen granular dusts in rats. *Eur. J. Oncol.*, **10** (4), 249–281.

26. Fung, V.A., Barrett, J.C., and Huff, J. (1995) The carcinogenic bioassay in perspective: application in identifying human cancer hazards. *Environ. Health Perspect.*, **103**, 680–683.

27. Hanahan, D. and Weinberg, R.A. (2011) Hallmarks of cancer: the next generation. *Cell*, **144**, 646–674.

28. Barrett, J.C. (1993) Mechanisms of multistep carcinogenesis and carcinogen risk assessment. *Environ. Health Perspect.*, **100**, 9–20.

29. Slaga, T.J. (1983) Overview of tumor promotion in animals. *Environ. Health Perspect.*, **50**, 3–14.

30. Gensler, H. and Bowden, G.T. (1984) Influence of 13-cis-retinoic acid on mouse skin tumor initiation and promotion. *Cancer Lett.*, **22**, 71–75.

31. Pitot, H.C., Campbell, H.A., Maronpot, R. *et al.* (1989) Critical parameters in the quantitation of the stages of initiation, promotion, and progression in one model of hepatocarcinogenesis in the rat. *Toxicol. Pathol.*, **17** (4, Pt. 1), 594–611; discussion 611–612.

32. Pitot, H.C. (1993) The molecular biology of carcinogenesis. *Cancer*, **72** (Suppl 3), 962–970.

33. Voight, M.D. (2005) Alcohol in hepatocellular cancer. *Clin. Liver Dis.*, **9**, 151–169.

34. Malkinson, A.M., Koski, K.M., Evans, W.A. *et al.* (1997) Butylated hydroxytoluene exposure is necessary to induce lung tumors in BALB mice treated with 3-methylcholanthrene. *Cancer Res.*, **57**, 2832–2834.

35. Klaassen, C. (2013) *Casarett and Doull's Toxicology*, 8th edn, McGraw-Hill.

36. Combes, R., Balls, M., Curren, R. *et al.* (1999) Cell transformation assays as predictors of human carcinogenicity. *Altern. Lab. Anim.*, **27**, 745–767.

37. Ding, L., Getz, G., Wheeler, D.A. *et al.* (2008) Somatic mutations affect key pathways in lung adenocarcinoma. *Nature*, **455**, 1069–1075.

38. Troll, W. and Wiesner, R. (1985) The role of oxygen radicals as a possible mechanism of tumor promotion. *Annu. Rev. Pharmacol. Toxicol.*, **25**, 509–528.

39. Maslov, A.Y. and Vijg, J. (2009) Genome instability, cancer and aging. *Biochim. Biophys. Acta*, **1790** (10), 963–969.

40. Moller, P., Danielsen, P.H., Jantzen, K. *et al.* (2013) Oxidatively damaged DNA in animals exposed to particles. *Crit. Rev. Toxicol.*, **43**, 96–118.

41. Sato, M., Shames, D.S., and Hasegawa, Y. (2012) Emerging evidence of epithelial-to-mesenchymal transition in lung carcinogenesis. *Respirology*, **17**, 1048–1059.

42. Diaz-Canو, S.J. (2012) Tumor heterogeneity: mechanisms and bases for a reliable application of molecular marker design. *Int. J. Mol. Sci.*, **13**, 1951–2011.

43. Azad, N., Iyer, A.K., Wang, L. *et al.* (2013) Reactive oxygen species-mediated p38 MAPK regulates carbon nanotube-induced fibrogenic and angiogenic responses. *Nanotoxicology*, **7** (2), 157–168.

44. Dalerba, P., Cho, R.W., and Clarke, M.F. (2007) Cancer stem cells: models and concepts. *Annu. Rev. Med.*, **58**, 267–284.

45. Gupta, P.B., Fillmore, C.M., Jiang, G. *et al.* (2011) Stochastic state transitions give rise to phenotypic equilibrium in populations of cancer cells. *Cell*, **146**, 633–644.

46. Shvedova, A.A., Tkach, A.V., Kisin, E.R. *et al.* (2013) Carbon nanotubes enhance metastatic growth of lung carcinoma via upregulation of myeloid-derived suppressor cells. *Small*, **9** (9–10), 1691–1695.

47. Sellers, T.A., Weaver, T.W., Phillips, B. *et al.* (1998) Environmental factors can confound identification of a major gene effect: results from a segregation analysis of a simulated population of lung cancer families. *Genet. Epidemiol.*, **15**, 251–262.

48. Clapp, R.W., Jacobs, M.M., and Loechler, E.L. (2008) Environmental and occupational causes of cancer: new evidence 2005–2007. *Rev. Environ. Health*, **23**, 1–37.

49. Donaldson, K., Aitken, R., Tran, L. *et al.* (2006) Carbon nanotubes: a review of their properties in relation to pulmonary toxicology and workplace safety. *Toxicol. Sci.*, **92**, 5–22.

50. Hussain, M.A., Kabir, M.A., and Sood, A.K. (2009) On the cytotoxicity of carbon nanotubes. *Curr. Sci.*, **96**, 664–673.

51. Pacurari, M., Castranova, V., and Vallyathan, V. (2010) Single- and multi-wall carbon nanotubes versus asbestos: are the carbon nanotubes a new health risk to humans? *J. Toxicol. Environ. Health A*, **73**, 378–395.

52. Oberdorster, G., Oberdorster, E., and Oberdorster, J. (2005) Nanotoxicology: an emerging discipline evolving from studies of ultrafine particles. *Environ. Health Perspect.*, **113**, 823–839.

53. Møller, P., Folkmann, J.K., Danielsen, P.H. *et al.* (2012) Oxidative stress generated damage to DNA by gastrointestinal exposure to insoluble particles. *Curr. Mol. Med.*, **12**, 732–745.

54. Borm, P.J., Cakmak, G., Jermann, E. *et al.* (2005) Formation of PAH-DNA adducts after in vivo and vitro exposure of rats and lung cells to different commercial carbon blacks. *Toxicol. Appl. Pharmacol.*, **205**, 157–167.

55. Oettinger, R., Drumm, K., Knorst, M. *et al.* (1999) Production of reactive oxygen intermediates by human macrophages exposed to soot particles and asbestos fibers and increase in NF- κ B p50/p105 mRNA. *Lung*, **177**, 343–354.

56. Harrison, R.M. and Yin, J. (2000) Particulate matter in the atmosphere: which particle properties are important for its effects on health? *Sci. Total Environ.*, **249** (1–3), 85–101.

57. IARC (1996) *IARC Monographs on the Evaluation of Carcinogenic Risks to Humans: Printing Processes and Printing Inks*, Carbon Black and Some Nitro Compounds, vol. 65, IARC, Lyon.

58. IARC (2010) *IARC Monographs on the Evaluation of Carcinogenic Risks to Humans*, Carbon Black, Titanium Dioxide and Talc, vol. 93, IARC, Lyon.

59. Donaldson, K., Tran, L., Jimenez, L.A. *et al.* (2005) Combustion-derived nanoparticles: a review of their toxicology following inhalation exposure. *Part. Fibre Toxicol.*, **2**, 10.

60. Renwick, L.C., Brown, D., Clouter, A. *et al.* (2004) Increased inflammation and altered macrophage chemotactic responses caused by two ultrafine particle types. *Occup. Environ. Med.*, **61**, 442–447.

61. Brown, D.M., Stone, V., Findlay, P. *et al.* (2000) Increased inflammation and intracellular calcium caused by ultrafine carbon black is independent of transition metals or other soluble components. *Occup. Environ. Med.*, **57**, 685–691.

62. Kreyling, W.G., Semmler, M., and Moller, W. (2004) Dosimetry and toxicology of ultrafine particles. *J. Aerosol Med.*, **17**, 140–152.

63. Gilmour, P.S., Ziesenis, A., Morrison, E.R. *et al.* (2004) Pulmonary and systemic effects of short-term inhalation exposure to ultrafine carbon black particles. *Toxicol. Appl. Pharmacol.*, **195**, 35–44.

64. Schreiber, N., Ströbele, M., Kopf, J. *et al.* (2013) Lung alterations following single or multiple low-dose carbon black nanoparticle aspirations in mice. *J. Toxicol. Environ. Health A*, **76**, 1317–1332.

65. Gallagher, J., Sams, R. II., Inmon, J. *et al.* (2003) Formation of 8-oxo-7,8-dihydro-2'-deoxyguanosine in rat lung

DNA following subchronic inhalation of carbon black. *Toxicol. Appl. Pharmacol.*, **190**, 224–231.

66. Bourdon, J.A., Saber, A.T., Jacobsen, N.R. *et al.* (2012) Carbon black nanoparticle instillation induces sustained inflammation and genotoxicity in mouse lung and liver. *Part. Fibre Toxicol.*, **9**, 5.

67. Bourdon, J.A., Halappanavar, S., Saber, A.T. *et al.* (2012) Hepatic and pulmonary toxicogenomic profiles in mice intratracheally instilled with carbon black nanoparticles reveal pulmonary inflammation, acute phase response, and alterations in lipid homeostasis. *Toxicol. Sci.*, **127** (2), 474–484.

68. Saber, A.T., Jacobsen, N.R., Bornholdt, J. *et al.* (2006) Cytokine expression in mice exposed to diesel exhaust particles by inhalation. Role of tumor necrosis factor. *Part. Fibre Toxicol.*, **3**, 4.

69. Jacobsen, N.R., Møller, P., Jensen, K.A. *et al.* (2009) Lung inflammation and genotoxicity following pulmonary exposure to nanoparticles in ApoE-/- mice. *Part. Fibre Toxicol.*, **6**, 2.

70. Jackson, P., Hougaard, K.S., Boisen, A.M. *et al.* (2012) Pulmonary exposure to carbon black by inhalation or instillation in pregnant mice: effects on liver DNA strand breaks in dams and offspring. *Nanotoxicology*, **6**, 486–500.

71. Kyjovska, Z.O., Jacobsen, N.R., Saber, A.T. *et al.* (2015) DNA damage following pulmonary exposure by instillation to low doses of carbon black (Printex 90) nanoparticles in mice. *Environ. Mol. Mutagen.*, **56** (1), 41–49.

72. Nikula, K.J., Snipes, M.B., Barr, E.B. *et al.* (1995) Comparative pulmonary toxicities and carcinogenicities of chronically inhaled diesel exhaust and carbon black in F344 rats. *Fundam. Appl. Toxicol.*, **25**, 80–94.

73. Heinrich, U., Fuhst, R., Rittinghausen, S. *et al.* (1995) Chronic inhalation exposure of Wistar rats and two different strains of mice to diesel engine exhaust, carbon black, and titanium dioxide. *Inhalation Toxicol.*, **7** (4), 533–556.

74. Dungworth, D.L., Mohr, U., Heinrich, U. *et al.* (1994) in *Toxic and Carcinogenic Effects of Solid Particles in the Respiratory Tract* (eds U. Mohr, D.L. Dungworth, J.L. Mauderly, and G. Oberdörster), ILSI Press, Washington, DC, pp. 75–98.

75. Heinrich, U. (1994) in *Toxic and Carcinogenic Effects of Solid Particles in the Respiratory Tract* (eds U. Mohr, D.L. Dungworth, J.L. Mauderly, and G. Oberdörster), ILSI Press, Washington, DC, pp. 57–73.

76. Reeves, A.L., Puro, H.E., Smith, R.G. *et al.* (1971) Experimental asbestos carcinogenesis. *Environ. Res.*, **4**, 496–511.

77. Mauderly, J.L. (1997) Relevance of particle-induced rat lung tumors for assessing lung carcinogenic hazard and human lung cancer risk. *Environ. Health Perspect.*, **105**, 1337–1346.

78. Valberg, P.A. and Watson, A.Y. (1996) Lung-cancer rates in carbon-black workers are discordant with predictions from rat bioassay data. *Regul. Toxicol. Pharm.*, **24**, 155–170.

79. Jacobsen, N.R., Saber, A.T., White, P. *et al.* (2007) Increased mutant frequency by carbon black, but not quartz in the lacZ and cll transgenes of Muta mouse lung epithelial cells. *Environ. Mol. Mutagen.*, **48**, 451–461.

80. Riebe-Imre, M., Aufderheide, M., Gärtner-Hübsch, S. *et al.* (1994) in *Toxic and Carcinogenic Effects of Solid Particles in the Respiratory Tract* (eds U. Mohr, D.L. Dungworth, J.L. Mauderly, G. Oberdörster, Jacobsen, *et al.*), ILSI Press, Washington, DC, pp. 519–523.

81. Driscoll, K.E., Deyo, L.C., Carter, J.M. *et al.* (1997) Effects of particle exposure and particle-elicited inflammatory cells on mutation in rat alveolar epithelial cells. *Carcinogenesis*, **18**, 423–430.

82. Kirwin, C.J., LeBlanc, J.V., Thomas, W.C. *et al.* (1981) Evaluation of the genetic activity of industrially produced carbon black. *J. Toxicol. Environ. Health*, **7**, 973–989.

83. Knaapen, A.M., Seiler, F., Schilderman, P.A. *et al.* (1999) Neutrophils cause oxidative DNA damage in alveolar

epithelial cells. *Free Radical Biol. Med.*, **27**, 234–240.

84. Don Porto, C.A., Hoet, P.H., Verschaeve, L. *et al.* (2001) Genotoxic effects of carbon black particles, diesel exhaust particles, and urban air particulates and their extracts on a human alveolar epithelial cell line (A549) and a human monocytic cell line (THP-1). *Environ. Mol. Mutagen.*, **37**, 155–163.

85. Chuang, H.C., Cheng, Y.L., Lei, Y.C. *et al.* (2013) Protective effects of pulmonary epithelial lining fluid on oxidative stress and DNA single-strand breaks caused by ultrafine carbon black, ferrous sulphate and organic extract of diesel exhaust particles. *Toxicol. Appl. Pharmacol.*, **266** (3), 329–334.

86. Mroz, R.M., Schins, R.P., Li, H. *et al.* (2008) Nanoparticle-driven DNA damage mimics irradiation-related carcinogenesis pathways. *Eur. Respir. J.*, **31**, 241–251.

87. Mroz, R.M., Schins, R.P., Li, H. *et al.* (2007) Nanoparticle carbon black driven DNA damage induces growth arrest and AP-1 and NFkappa B DNA binding in lung epithelial A549 cell line. *J. Physiol. Pharmacol.*, **58** (Suppl. 5), 461–470.

88. Jacobsen, N.R., White, P.A., Gingerich, J. *et al.* (2010) Mutation spectrum in FE1-MUTA(TM) Mouse lung epithelial cells exposed to nanoparticulate carbon black. *Environ. Mol. Mutagen.*, **52**, 331–337.

89. Tamaoki, J., Isono, K., Takeyama, K. *et al.* (2004) Ultrafine carbon black particles stimulate proliferation of human airway epithelium via EGF receptor-mediated signaling pathway. *Am. J. Physiol. Lung Cell Mol. Physiol.*, **287**, L1127–L1133.

90. Wang, L., Stueckle, T.A., Mishra, A. *et al.* (2014) Neoplastic-like transformation effect of single-walled and multiwalled carbon nanotubes compared to asbestos on human lung small airway epithelial cells. *Nanotoxicology*, **8**, 485–507.

91. van Berlo, D., Clift, M.J., Albrecht, C. *et al.* (2012) Carbon nanotubes: an insight into the mechanisms of their potential genotoxicity. *Swiss Med. Wkly.*, **5**, 142.

92. Johnston, H.J., Hutchison, G.R., Christensen, F.M. *et al.* (2010) A critical review of the biological mechanisms underlying the in vivo and in vitro toxicity of carbon nanotubes: the contribution of physicochemical characteristics. *Nanotoxicology*, **4**, 207–246.

93. Donaldson, K., Poland, C.A., Murphy, F.A. *et al.* (2013) Pulmonary toxicity of carbon nanotubes and asbestos—similarities and differences. *Adv. Drug Delivery Rev.*, **65** (15), 2078–2086.

94. Sanchez, V.C., Pietruska, J.R., Miselis, N.R. *et al.* (2009) Biopersistence and potential adverse health impacts of fibrous nanomaterials: what have we learned from asbestos? *WIREs Nanomed. Nanobiotechnol.*, **1**, 511–529.

95. Møller, P., Christoffersen, D.V., Jensen, D.M. *et al.* (2014) Role of oxidative stress in carbon nanotube-generated health effects. *Arch. Toxicol.*, **88**, 1939–1964.

96. Huncharek, M. (1995) Genetic factors in the etiology of malignant mesothelioma. *Eur. J. Cancer*, **31A**, 1741–1747.

97. Dahm, M.M., Evans, D.E., Schubauer-Berigan, M.K. *et al.* (2012) Occupational exposure assessment in carbon nanotube and nanofiber primary and secondary manufacturers. *Ann. Occup. Hyg.*, **56** (5), 542–556.

98. Dahm, M.M., Schubauer-Berigan, M.K., Evans, D.E. *et al.* (2015) Carbon nanotube and nanofiber exposure assessments: an analysis of 14 site visits. *Ann. Occup. Hyg.*, **59**, 705–723.

99. Mercer, R.R., Scabilloni, J., Wang, L. *et al.* (2008) Alteration of deposition pattern and pulmonary response as a result of improved dispersion of aspirated single-walled carbon nanotubes in a mouse model. *Am. J. Physiol. Lung Cell Mol. Physiol.*, **294** (1), L87–L97.

100. Mercer, R.R., Hubbs, A.F., Scabilloni, J.F. *et al.* (2010) Distribution and persistence of pleural penetrations by

multi-walled carbon nanotubes. *Part. Fibre Toxicol.*, **7**, 28.

101. Mercer, R.R., Scabilloni, J.F., Hubbs, A.F. *et al.* (2013) Distribution and fibrotic response following inhalation exposure to multi-walled carbon nanotubes. *Part. Fibre Toxicol.*, **10**, 33.
102. Dinu, C.Z., Bale, S.S., Zhu, G. *et al.* (2009) Tubulin encapsulation of carbon nanotubes into functional hybrid assemblies. *Small*, **5**, 310–315.
103. Cortez, B.A., Quassollo, G., Caceres, A. *et al.* (2011) The fate of chrysotile-induced multipolar mitosis and aneuploid population in cultured lung cancer cells. *PLoS One*, **6** (4), e18600.
104. Boyles, M.S., Young, L., Brown, D.M. *et al.* (2015) Multi-walled carbon nanotube induced frustrated phagocytosis, cytotoxicity and pro-inflammatory conditions in macrophages are length dependent and greater than that of asbestos. *Toxicol. in Vitro*, **29**, 1513–1528.
105. Hubbs, A.F., Mercer, R.R., Coad, J.E. *et al.* (2009) Persistent pulmonary inflammation, airway mucous metaplasia and migration of multi-walled carbon nanotubes from the lung after subchronic exposure. *Toxicologist*, **108**, 2193.
106. Porter, D.W., Hubbs, A.F., Mercer, R.R. *et al.* (2010) Mouse pulmonary dose- and time course-responses induced by exposure to multi-walled carbon nanotubes. *Toxicology*, **269**, 136–147.
107. Ryman-Rasmussen, J.P., Cesta, M.F., Brody, A.R. *et al.* (2009) Inhaled carbon nanotubes reach the subpleural tissue in mice. *Nat. Nanotechnol.*, **4**, 747–751.
108. Mercer, R.R., Hubbs, A.F., Scabilloni, J.F. *et al.* (2011) Pulmonary fibrotic response to aspiration of multi-walled carbon nanotubes. *Part. Fibre Toxicol.*, **8**, 21.
109. Porter, D.W., Hubbs, A.F., Chen, B.T. *et al.* (2013) Acute pulmonary dose–responses to inhaled multi-walled carbon nanotubes. *Nanotoxicology*, **7**, 1399.
110. Czarny, B., Georgin, D., Berthon, F. *et al.* (2014) Carbon nanotube translocation to distant organs after pulmonary exposure: insights from *in situ* (14)C-radiolabeling and tissue radioimaging. *ACS Nano*, **8** (6), 5715–5724.
111. Shvedova, A.A., Kapralov, A.A., Feng, W.H. *et al.* (2012) Impaired clearance and enhanced pulmonary inflammatory/fibrotic response to carbon nanotubes in myeloperoxidase-deficient mice. *PLoS One*, **7** (3), e30923.
112. Shvedova, A.A., Yanamala, N., Kisin, E.R. *et al.* (2014) Long-term effects of carbon containing engineered nanomaterials and asbestos in the lung: one year postexposure comparisons. *Am. J. Physiol. Lung Cell Mol. Physiol.*, **306** (2), L170–L182.
113. Fujita, K., Fukuda, M., Fukui, H. *et al.* (2014) Intratracheal instillation of single-wall carbon nanotubes in the rat lung induces time-dependent changes in gene expression. *Nanotoxicology*, **9**, 1–12.
114. Shvedova, A.A., Kisin, E., Murray, A.R. *et al.* (2008) Inhalation vs. aspiration of single-walled carbon nanotubes in C57BL/6 mice: inflammation, fibrosis, oxidative stress, and mutagenesis. *Am. J. Physiol. Lung Cell Mol. Physiol.*, **295** (4), L552–L565.
115. Manke, A., Luanpitpong, S., Dong, C. *et al.* (2014) Effect of fiber length on carbon nanotube-induced fibrogenesis. *Int. J. Mol. Sci.*, **15** (5), 7444–7461.
116. Pauluhn, J. (2010) Subchronic 13-week inhalation exposure of rats to multi-walled carbon nanotubes: toxic effects are determined by density of agglomerate structures, not fibrillar structures. *Toxicol. Sci.*, **113** (1), 226–242.
117. Jackson, M.A., Lea, I., Rashid, A. *et al.* (2006) Genetic alterations in cancer knowledge system: analysis of gene mutations in mouse and human liver and lung tumors. *Toxicol. Sci.*, **90**, 400–418.
118. Pacurari, M., Qian, Y., Porter, D.W. *et al.* (2011) Multi-walled carbon nanotube-induced gene expression in the mouse lung: association with lung pathology. *Toxicol. Appl. Pharmacol.*, **255**, 18–31.
119. Poulsen, S.S., Jacobsen, N.R., Labib, S. *et al.* (2013) Transcriptomic analysis

reveals novel mechanistic insight into murine biological responses to multi-walled carbon nanotubes in lungs and cultured lung epithelial cells. *PLoS One*, **8**, e80452.

120. Luanpitpong, S., Wang, L., Stueckle, T.A. *et al.* (2014) Caveolin-1 regulates lung cancer stem-like cell induction and p53 inactivation in carbon nanotube-driven tumorigenesis. *Oncotarget*, **5** (11), 3541–3554.

121. Chen, D., Stueckle, T.A., Luanpitpong, S. *et al.* (2015) Gene expression profile of human lung epithelial cells chronically exposed to single walled-carbon nanotubes. *Nanoscale Res. Lett.*, **10**, 12.

122. Guo, N.L., Wan, Y.W., Denvir, J. *et al.* (2012) Multiwalled carbon nanotube-induced gene signatures in the mouse lung: potential predictive value for human lung cancer risk and prognosis. *J. Toxicol. Environ. Health A*, **75**, 1129–1153.

123. Nagai, H. and Toyokuni, S. (2012) Differences and similarities between carbon nanotubes and asbestos fibers during mesothelial carcinogenesis: shedding light on fiber entry mechanism. *Cancer Sci.*, **103**, 1378–1390.

124. Poland, C.A., Duffin, R., Kinloch, I. *et al.* (2008) Carbon nanotubes introduced into the abdominal cavity of mice show asbestos-like pathogenicity in a pilot study. *Nat. Nanotechnol.*, **3** (7), 423–428.

125. Murphy, F.A., Poland, C.A., Duffin, R. *et al.* (2011) Length-dependent retention of carbon nanotubes in the pleural space of mice initiates sustained inflammation and progressive fibrosis on the parietal pleura. *Am. J. Pathol.*, **178** (6), 2587–2600.

126. Murphy, F.A., Poland, C.A., Duffin, R. *et al.* (2013) Length-dependent pleural inflammation and parietal pleural responses after deposition of carbon nanotubes in the pulmonary airspaces of mice. *Nanotoxicology*, **7**, 1157–1167.

127. Xu, J., Alexander, D.B., Futakuchi, M. *et al.* (2014) Size- and shape-dependent pleural translocation, deposition, fibrogenesis, and mesothelial proliferation by multiwalled carbon nanotubes. *Cancer Sci.*, **105** (7), 763–769.

128. Murphy, F.A., Schinwald, A., Poland, C.A. *et al.* (2012) The mechanism of pleural inflammation by long carbon nanotubes: interaction of long fibres with macrophages stimulates them to amplify pro-inflammatory responses in mesothelial cells. *Part. Fibre Toxicol.*, **9**, 8.

129. Shvedova, A.A., Kisin, E.R., Mercer, R. *et al.* (2005) Unusual inflammatory and fibrogenic pulmonary responses to single-walled carbon nanotubes in mice. *Am. J. Physiol. Lung Cell Mol. Physiol.*, **289**, L698–L708.

130. World Health Organization (2002) *IARC Monographs on the Evaluation of Carcinogenic Risk to Humans*, Man-Made Vitreous Fibres, vol. 81, IARC, Lyon.

131. Muller, J., Delos, M., Panin, N. *et al.* (2009) Absence of carcinogenic response to multiwall carbon nanotubes in a 2-year bioassay in the peritoneal cavity of the rat. *Toxicol. Sci.*, **110**, 442–448.

132. Sakamoto, Y., Nakae, D., Fukumori, N. *et al.* (2009) Induction of mesothelioma by a single intrascrotal administration of multi-wall carbon nanotube in intact male Fischer 344 rats. *J. Toxicol. Sci.*, **34** (1), 65–76.

133. Takagi, A., Hirose, A., Nishimura, T. *et al.* (2008) Induction of mesothelioma in p53^{+/−} mouse by intraperitoneal application of multi-wall carbon nanotube. *J. Toxicol. Sci.*, **33**, 105–116.

134. Takagi, A., Hirose, A., Futakuchi, M. *et al.* (2012) Dose-dependent mesothelioma induction by intraperitoneal administration of multi-wall carbon nanotubes in p53 heterozygous mice. *Cancer Sci.*, **103**, 1440–1444.

135. Pritchard, J.B., French, J.E., Davis, B.J. *et al.* (2003) The role of transgenic mouse models in carcinogen identification. *Environ. Health Perspect.*, **111**, 444–454.

136. Nagai, H., Okazaki, Y., Chew, S.H. *et al.* (2011) Diameter and rigidity of multiwalled carbon nanotubes are critical factors in mesothelial injury and carcinogenesis. *Proc. Natl. Acad. Sci. U.S.A.*, **108**, E1330–E1338.

137. Rittinghausen, S., Hackbarth, A., Creutzberg, O. *et al.* (2014) The carcinogenic effect of various multi-walled carbon nanotubes (MWCNTs) after intraperitoneal injection in rats. *Part. Fibre Toxicol.*, **11**, 59.

138. Yu, K.N., Kim, J.E., Seo, H.W. *et al.* (2013) Differential toxic responses between pristine and functionalized multiwall nanotubes involve induction of autophagy accumulation in murine lung. *J. Toxicol. Environ. Health A*, **76**, 1282–1292.

139. Xu, J., Futakuchi, M., Shimizu, H. *et al.* (2012) Multi-walled carbon nanotubes translocate into the pleural cavity and induce visceral mesothelial proliferation in rats. *Cancer Sci.*, **103** (12), 2045–2050.

140. Kobayashi, N., Naya, M., Mizuno, K. *et al.* (2011) Pulmonary and systemic responses of highly pure and well-dispersed single-wall carbon nanotubes after intratracheal instillation in rats. *Inhalation Toxicol.*, **23** (13), 814–828.

141. Shvedova, A.A., Kisin, E.R., Yanamala, N. *et al.* (2015) MDSC and TGF- β are required for facilitation of tumor growth in the lungs of mice exposed to carbon nanotubes. *Cancer Res.*, **75** (8), 1615–1623.

142. Pacurari, M., Yin, X.J., Zhao, J. *et al.* (2008) Raw single-wall carbon nanotubes induce oxidative stress and activate MAPKs, AP-1, NF- κ B, and Akt in normal and malignant human mesothelial cells. *Environ. Health Perspect.*, **116** (9), 1211–1217.

143. Azad, N., Rojanasakul, Y., and Valliyathan, V. (2008) Inflammation and lung cancer: roles of reactive oxygen/nitrogen species. *J. Toxicol. Environ. Health B Crit. Rev.*, **11**, 1–15.

144. Aschberger, K., Johnston, H.J., Stone, V. *et al.* (2010) Review of carbon nanotubes toxicity and exposure–appraisal of human health risk assessment based on open literature. *Crit. Rev. Toxicol.*, **40** (9), 759–790.

145. Li, R., Wang, X., Ji, Z. *et al.* (2013) Surface charge and cellular processing of covalently functionalized multiwall carbon nanotubes determine pulmonary toxicity. *ACS Nano*, **7** (3), 2352–2368.

146. Park, E.J., Zahari, N.E., Lee, E.W. *et al.* (2014) SWCNTs induced autophagic cell death in human bronchial epithelial cells. *Toxicol. in Vitro*, **28** (3), 442–450.

147. Funahashi, S., Okazaki, Y., Ito, D. *et al.* (2015) Asbestos and multi-walled carbon nanotubes generate distinct oxidative responses in inflammatory cells. *J. Clin. Biochem. Nutr.*, **56** (2), 111–117.

148. Manke, A., Wang, L., and Rojanasakul, Y. (2013) Pulmonary toxicity and fibrogenic response of carbon nanotubes. *Toxicol. Mech. Methods*, **23**, 196–206.

149. Fenoglio, I., Greco, G., Tornatis, M. *et al.* (2008) Structural defects play a major role in the acute lung toxicity of multiwall carbon nanotubes: physico-chemical aspects. *Chem. Res. Toxicol.*, **21** (9), 1690–1697.

150. Tsuruoka, S., Matsumoto, H., Koyama, K. *et al.* (2015) Radical scavenging reaction kinetics with multiwalled carbon nanotubes. *Carbon*, **83**, 232–239.

151. Pacurari, M., Yin, X.J., Ding, M. *et al.* (2008) Oxidative and molecular interactions of multi-wall carbon nanotubes (MWCNT) in normal and malignant human mesothelial cells. *Nanotoxicology*, **2**, 155–170.

152. Toyokuni, S. (2013) Genotoxicity and carcinogenicity risk of carbon nanotubes. *Adv. Drug Delivery Rev.*, **65** (15), 2098–2110.

153. Guo, F., Ma, N., Horibe, Y. *et al.* (2012) Nitritative DNA damage induced by multi-walled carbon nanotube via endocytosis in human lung epithelial cells. *Toxicol. Appl. Pharmacol.*, **260**, 138–192.

154. Sargent, L.M., Shvedova, A.A., Hubbs, A.F. *et al.* (2009) Induction of aneuploidy by single-walled carbon nanotubes. *Environ. Mol. Mutagen.*, **50**, 708–717.

155. Sargent, L.M., Hubbs, A.F., Young, S.H. *et al.* (2012) Single-walled carbon nanotube-induced mitotic disruption. *Mutat. Res.*, **745**, 28–37.

156. Rodriguez-Fernandez, L.I., Valiente, R., Gonzalez, J. *et al.* (2012) Multiwalled carbon nanotubes display microtubule biomimetic properties in vivo, enhancing microtubule assembly

and stabilization. *ACS Nano*, **6** (8), 6614–6625.

157. Siegrist, K.J., Reynolds, S.H., Kashon, M.L. *et al.* (2014) Genotoxicity of multi-walled carbon nanotubes at occupationally relevant doses. *Part. Fibre Toxicol.*, **11**, 6.

158. Salisbury, J.L., D'Assoro, A.B., and Lingle, W.L. (2004) Centrosome amplification and the origin of chromosomal instability in breast cancer. *J. Mammary Gland Biol. Neoplasia*, **9**, 275–283.

159. Jackson, P., Kling, K., Jensen, K.A. *et al.* (2015) Characterization of genotoxic response to 15 multiwalled carbon nanotubes with variable physicochemical properties including surface functionalizations in the FE1-Muta(TM) mouse lung epithelial cell line. *Environ. Mol. Mutagen.*, **56**, 183–203.

160. Kato, T., Totsuka, Y., Ishino, K. *et al.* (2013) Genotoxicity of multi-walled carbon nanotubes in both *in vitro* and *in vivo* assay systems. *Nanotoxicology*, **7**, 452–461.

161. Balls, M. and Clothier, R. (2010) A FRAME response to the draft report on alternative (non-animal) methods for cosmetics testing: current status and future prospects—2010. *Altern. Lab. Anim.*, **38**, 345–353.

162. Corvi, R., Aardema, M.J., Gribaldo, L. *et al.* (2012) ECVAM prevalidation study on *in vitro* cell transformation assays: general outline and conclusions of the study. *Mutat. Res.*, **744** (1), 12–19.

163. Ponti, J., Broggi, F., Mariani, V. *et al.* (2013) Morphological transformation induced by multiwalled carbon nanotubes on Balb/3T3 cell model as an *in vitro* end point of carcinogenic potential. *Nanotoxicology*, **7**, 221–233.

164. Wang, L., Luanpitpong, S., Castranova, V. *et al.* (2011) Carbon nanotubes induce malignant transformation and tumorigenesis of human lung epithelial cells. *Nano Lett.*, **11**, 2796–2803.

165. Wu, P., Yuan, S.S., Ho, C.C. *et al.* (2013) Focal amplification of HOXD-harboring chromosome region is implicated in multiple-walled carbon nanotubes-induced carcinogenicity. *Nano Lett.*, **13**, 4632–4641.

166. Thurnherr, T., Brandenberger, C., Fischer, K. *et al.* (2011) A comparison of acute and long-term effects of industrial multiwalled carbon nanotubes on human lung and immune cells *in vitro*. *Toxicol. Lett.*, **200**, 176–186.

167. Jean, D., Thomas, E., Manie, E. *et al.* (2011) Syntenic relationships between genomic profiles of fiber-induced murine and human malignant mesothelioma. *Am. J. Pathol.*, **178**, 881–894.

168. Stueckle, T.A., Mishra, A., Derk, R. *et al.* (2013) Identification of novel exposure and lung cancer gene markers for carbon nanotube exposed human lung epithelial cells [abstract]. *Toxicologist*, **426**, 91.

169. Pongrakhananon, V., Luanpitpong, S., Stueckle, T.A. *et al.* (2015) Carbon nanotubes induce apoptosis resistance of human lung epithelial cells through FLICE-inhibitory protein. *Toxicol. Sci.*, **143** (2), 499–511.

170. Luanpitpong, S., Wang, L., Castranova, V. *et al.* (2014) Induction of stem-like cells with malignant properties by chronic exposure of human lung epithelial cells to single-walled carbon nanotubes. *Part. Fibre Toxicol.*, **11**, 22.

171. Lohcharoenkal, W., Wang, L., Stueckle, T.A. *et al.* (2013) Chronic exposure to carbon nanotubes induces invasion of human mesothelial cells through matrix metalloproteinase-2. *ACS Nano*, **7**, 7711–7723.

172. Lohcharoenkal, W., Stueckle, T.A., Wang, L. *et al.* (2014) Role of H-Ras/ERK signaling in carbon nanotube-induced neoplastic transformation of human mesothelial cells. *Front. Physiol.*, **5**, 222.

173. Nielsen, G.D., Roursgaard, M., Jensen, K.A. *et al.* (2008) In vivo biology and toxicology of fullerenes and their derivatives. *Basic Clin. Pharmacol. Toxicol.*, **103**, 197–208.

174. Aschberger, K., Johnston, H.J., Stone, V. *et al.* (2010) Review of fullerene toxicity and exposure-appraisal of a human health risk assessment, based on open literature. *Regul. Toxicol. Pharmacol.*, **58**, 455–473.

175. Johnston, H.J., Hutchison, G.R., Christensen, F.M. *et al.* (2010) The

biological mechanisms and physico-chemical characteristics responsible for driving fullerene toxicity. *Toxicol. Sci.*, **114**, 162–182.

176. Shinohara, N., Matsumoto, K., Endoh, S. *et al.* (2009) In vitro and in vivo genotoxicity tests on fullerene C60 nanoparticles. *Toxicol. Lett.*, **191**, 289–296.

177. Takada, H., Kokubo, K., Matsubayashi, K. *et al.* (2006) Antioxidant activity of supramolecular water-soluble fullerenes evaluated by beta-carotene bleaching assay. *Biosci. Biotechnol., Biochem.*, **70**, 3088–3093.

178. Witte, P., Beuerle, F., Hartnagel, U. *et al.* (2007) Water solubility, antioxidant activity and cytochrome C binding of four families of exohedral adducts of C60 and C70. *Org. Biomol. Chem.*, **5**, 3599–3613.

179. Markovic, Z. and Trajkovic, V. (2008) Biomedical potential of the reactive oxygen species generation and quenching by fullerenes (C60). *Biomaterials*, **29**, 3561–3573.

180. Hu, Z., Guan, W., Wang, W. *et al.* (2007) Synthesis of β -alanine C60 derivative and its protective effect on hydrogen peroxide-induced apoptosis in rat pheochromocytoma cells. *Cell Biol. Int.*, **31**, 798–804.

181. Sayes, C.M., Marchione, A.A., Reed, K.L. *et al.* (2007) Comparative pulmonary toxicity assessments of C60 water suspensions in rats: few differences in fullerene toxicity in vivo in contrast to in vitro profiles. *Nano Lett.*, **7** (8), 2399–2406.

182. Baker, G.L., Gupta, A., Clark, M.L. *et al.* (2008) Inhalation toxicity and lung toxicokinetics of C60 fullerene nanoparticles and microparticles. *Toxicol. Sci.*, **101** (1), 122–131.

183. Fujita, K., Morimoto, Y., Ogami, A. *et al.* (2009) Gene expression profiles in rat lung after inhalation exposure to C(60) fullerene particles. *Toxicology*, **258** (1), 47–55.

184. Morimoto, Y., Hirohashi, M., Ogami, A. *et al.* (2010) Inflammogenic effect of well-characterized fullerenes in inhalation and intratracheal instillation studies. *Part. Fibre Toxicol.*, **14** (7), 4.

185. Park, E.J., Kim, H., Kim, Y. *et al.* (2010) Carbon fullerenes (C60s) can induce inflammatory responses in the lung of mice. *Toxicol. Appl. Pharmacol.*, **244** (2), 226–233.

186. Roursgaard, M., Poulsen, S.S., Kepley, C.L. *et al.* (2008) Polyhydroxylated C60 fullerene (fullerenol) attenuates neutrophilic lung inflammation in mice. *Basic Clin. Pharmacol. Toxicol.*, **103**, 386–388.

187. Jiao, F., Qu, Y., Zhou, G. *et al.* (2010) Modulation of oxidative stress by functionalized fullerene materials in the lung tissues of female C57/BL mice with a metastatic Lewis lung carcinoma. *J. Nanosci. Nanotechnol.*, **10**, 8632–8637.

188. NIEHS NTP (2012) NTP Range-Finding Report: Immunotoxicity of C60 Fullerene in Female Wistar Han Rats (CASRN 99685-96-8), <http://ntp.niehs.nih.gov/testing/types/imm/abstract/i20710i20407/index.html> (accessed 20 April 2015).

189. NIEHS NTP (2012) NTP Range-Finding Report: Immunotoxicity of C60 Fullerene in Female B6C3F1 Mice (CASRN 99685-96-8), <http://ntp.niehs.nih.gov/testing/types/imm/abstract/i20710i20407/index.html> (accessed 20 April 2015).

190. Yamago, S., Tokuyama, H., Nakamura, E. *et al.* (1995) In vivo biological behaviour of a water-miscible fullerene: ^{14}C labelling, absorption, distribution, excretion and acute toxicity. *Chem. Biol.*, **2**, 385–389.

191. Bullard-Dillard, R., Creek, K.E., Scrivens, W.A. *et al.* (1996) Tissue sites of uptake of ^{14}C labelled C60. *Bioorg. Chem.*, **24**, 376–385.

192. Gharbi, N., Pressac, M., Hadchouel, M. *et al.* (2005) [60]Fullerene is a powerful antioxidant in vivo with no acute or subacute toxicity. *Nano Lett.*, **5**, 2578–2585.

193. Folkmann, J.K., Risom, L.R., Jacobsen, N.R. *et al.* (2009) Oxidatively damaged DNA in rats exposed by oral gavage to C60 fullerenes and single-walled carbon nanotubes. *Environ. Health Perspect.*, **117**, 703–708.

194. Totsuka, Y., Higuchi, T., Imai, T. *et al.* (2009) Genotoxicity of nano/microparticles in *in vitro* micronuclei, *in vivo* comet and mutation assay system. *Part. Fibre Toxicol.*, **6**, 23.

195. Ema, M., Tanaka, J., Kobayashi, N. *et al.* (2012) Genotoxicity evaluation of fullerene C60 nanoparticles in a comet assay using lung cells of intratracheally instilled rats. *Regul. Toxicol. Pharm.*, **62** (3), 419–424.

196. Jacobsen, N.R., Pojana, G., White, P. *et al.* (2008) Genotoxicity, cytotoxicity, and reactive oxygen species induced by single-walled carbon nanotubes and C60 fullerenes in the FE1-MutaTM mouse lung epithelial cells. *Environ. Mol. Mutagen.*, **49**, 476–487.

197. Liu, Y., Jiao, F., Qiu, Y. *et al.* (2009) Immunostimulatory properties and enhanced TNF- α mediated cellular immunity for tumor therapy by C60(OH)20 nanoparticles. *Nanotechnology*, **20** (41), 415102.

198. Zogovic, N.S., Nikolic, N.S., Vranjes-Djuric, S.D. *et al.* (2009) Opposite effects on nanocrystalline fullerene (C60) on tumor cell growth *in vitro* and *in vivo* and a possible role of immunosuppression in the cancer-promoting activity of C(60). *Biomaterials*, **30** (36), 6940–6946.

199. Wang, D., Sun, L., Liu, W. *et al.* (2009) Photoinduced DNA cleavage by α -, β -, and γ -cyclodextrin- bicapped C60 supramolecular complexes. *Environ. Sci. Technol.*, **43**, 5825–5829.

200. Zhao, B., He, Y.Y., Bilski, P.J. *et al.* (2008) Pristine (C60) and hydroxylated [C60(OH)24] fullerene phototoxicity towards HaCaT keratinocytes: type I vs type II mechanisms. *Chem. Res. Toxicol.*, **21** (5), 1056–1063.

201. Babynin, E.V., Nuretdinov, I.A., Gubskaya, V.P. *et al.* (2002) Study of mutagenic activity of fullerene and some of its derivatives using His $^{+}$ reversions of *salmonella typhimurium* as an example. *Russ. J. Genet.*, **38** (4), 453–457.

202. Sera, N., Tokiwa, H., and Miyata, N. (1996) Mutagenicity of the fullerene C60-generated singlet oxygen dependent formation of lipid peroxides. *Carcinogenesis*, **17** (10), 2163–2169.

203. Mrdanović, J., Šolajić, S., Bogdanović, V. *et al.* (2009) Effects of fullerol C60(OH)24 on the frequency of micronuclei and chromosome aberrations in CHO-K1 cells. *Mutat. Res.*, **680**, 25–30.

204. Xu, A., Chai, Y., Nohmi, T. *et al.* (2009) Genotoxic responses to titanium dioxide nanoparticles and fullerene in gpt delta transgenic MEF cells. *Part. Fibre Toxicol.*, **6**, 3.

205. Dhawan, A., Taurozzi, J.S., Pandey, A.K. *et al.* (2006) Stable colloidal dispersions of C60 fullerenes in water: evidence for genotoxicity. *Environ. Sci. Technol.*, **40**, 7394–7401.

206. Niwa, Y. and Iwai, N. (2006) Genotoxicity in cell lines induced by chronic exposure to water soluble fullerenes using micronucleus test. *Environ. Health Prev. Med.*, **11**, 292–297.

207. Sayes, C.M., Fortner, J.D., Guo, W. *et al.* (2004) The differential cytotoxicity of water-soluble fullerenes. *Nano Lett.*, **4**, 1881–1887.

208. Sayes, C.M., Gobin, A.M., Ausman, K.D. *et al.* (2005) Nano-C60 cytotoxicity is due to lipid peroxidation. *Biomaterials*, **26**, 7587–7595.

209. Rouse, J.G., Yang, J., Barron, A.R. *et al.* (2006) Fullerene-based amino acid nanoparticle interactions with human epidermal keratinocytes. *Toxicol. in Vitro*, **20**, 1313–1320.

210. Kamat, J.P., Devasagayam, T.P.A., Priyadarshini, K.I. *et al.* (2000) Reactive oxygen species mediated membrane damage induced by fullerene derivatives and its possible biological implications. *Toxicology*, **155**, 55–61.

211. Xia, T., Kovochich, M., Brant, J. *et al.* (2006) Comparison of the abilities of ambient and manufactured nanoparticles to induce cellular toxicity according to an oxidative stress paradigm. *Nano Lett.*, **6** (8), 1794–1807.

212. Sanchez, V.C., Jachak, A., Hurt, R.H. *et al.* (2012) Biological interactions of graphene-family nanomaterials: an interdisciplinary review. *Chem. Res. Toxicol.*, **25** (1), 15–34.

213. Soldano, C., Mahmood, A., and Dujardin, E. (2010) Production, properties and potential of graphene. *Carbon*, **48**, 2127–2150.

214. Zhang, Y., Petibone, D., Xu, Y. *et al.* (2014) Toxicity and efficacy of carbon nanotubes and graphene: the utility of carbon-based nanoparticles in nanomedicine. *Drug Metab. Rev.*, **46** (2), 232–246.

215. Guo, X. and Mei, N. (2014) Assessment of the toxic potential of graphene family nanomaterials. *J. Food Drug Anal.*, **22** (1), 105–115.

216. Nezakati, T., Cousins, B.G., and Selfallan, A.M. (2014) Toxicology of chemically modified graphene-based materials for medical application. *Arch. Toxicol.*, **88**, 1987–2012.

217. Seabra, A.B., Paula, A.J., de Lima, R. *et al.* (2014) Nanotoxicity of graphene and graphene oxide. *Chem. Res. Toxicol.*, **27** (2), 159–168.

218. Yang, K., Li, Y., Tan, X. *et al.* (2013) Behavior and toxicity of graphene and its functionalized derivatives in biological systems. *Small*, **9** (9–10), 1492–1503.

219. Ren, H., Wang, C., Zhang, J. *et al.* (2010) Dna cleavage system of nano-sized graphene oxide sheets and copper ions. *ACS Nano*, **4**, 7169–7174.

220. Duch, M.C., Budinger, G.R., Liang, Y.T. *et al.* (2011) Minimizing oxidation and stable nanoscale dispersion improves the biocompatibility of graphene in the lung. *Nano Lett.*, **11** (12), 5201–5207.

221. Wang, K., Ruan, J., Song, H. *et al.* (2010) Biocompatibility of graphene oxide. *Nanoscale Res. Lett.*, **6**, 8.

222. Ma-Hock, L., Strauss, V., Treumann, S. *et al.* (2013) Comparative inhalation toxicity of multi-wall carbon nanotubes, graphene, graphite nanoplatelets and low surface carbon black. *Part. Fibre Toxicol.*, **10**, 23.

223. Schinwald, A., Murphy, F.A., Jones, A. *et al.* (2012) Graphene-based nanoplatelets: a new risk to the respiratory system as a consequence of their unusual aerodynamic properties. *ACS Nano*, **6**, 736–746.

224. Schinwald, A., Murphy, F., Askounis, A. *et al.* (2014) Minimal oxidation and inflammogenicity of pristine graphene with residence in the lung. *Nanotoxicology*, **8**, 824–832.

225. Shin, J.H., Han, S.G., Kim, J.K. *et al.* (2015) 5-day repeated inhalation and 28-day post-exposure study of graphene. *Nanotoxicology*, **9** (8), 1023–1031.

226. IARC (1999) *Monographs on the Evaluation of Carcinogenic Risks to Humans*, Surgical Implants and Other Foreign Bodies, vol. 74, International Agency for Research on Cancer/World Health Organization, Lyon.

227. Okada, F. (2007) Beyond foreign-body-induced carcinogenesis: impact of reactive oxygen species derived from inflammatory cells in tumorigenic conversion and tumor progression. *Int. J. Cancer*, **121**, 2364–2372.

228. Kirkpatrick, C.J., Alves, A., Kohler, H. *et al.* (2000) Biomaterial-induced sarcoma: a novel model to study pre-neoplastic change. *Am. J. Pathol.*, **156**, 1455–1467.

229. Choi, J., Curtis, S.J., Roy, D.M. *et al.* (2010) Local mesenchymal stem/progenitor cells are a preferential target for initiation of adult soft tissue sarcomas associated with p53 and Rb deficiency. *Am. J. Pathol.*, **177**, 2645–2658.

230. Blanchard, K.T., Barthel, C., French, J.E. *et al.* (1999) Transponder-induced sarcoma in the heterozygous p53+/- mouse. *Toxicol. Pathol.*, **27**, 519–527.

231. Bonner, J.C. (2010) Mesenchymal cell survival in airway and interstitial pulmonary fibrosis. *Fibrogenesis Tissue Repair*, **3**, 15.

232. Pierro, M. and Thebaud, B. (2010) Mesenchymal stem cells in chronic lung disease: culprit or savior? *Am. J. Physiol. Lung Cell Mol. Physiol.*, **298**, L732–L734.

233. Marriott, S., Baski, r.R.S., Gaskill, C. *et al.* (2014) ABCG2^{pos} lung mesenchymal stem cells area novel pericyte subpopulation that contributes to fibrotic remodeling. *Am. J. Physiol., Cell Physiol.*, **307**, C684–C698.

234. Luangpitpong, S., Wang, L., Castranova, V. *et al.* (2014) Induction of stem-like cells with fibrogenic properties by

carbon nanotubes and its role in fibrogenesis. *Nano Lett.*, **14** (6), 3110–3116.

235. Zhang, Y., Ali, S.F., Dervishi, E. *et al.* (2010) Cytotoxicity effects of graphene and single-wall carbon nanotubes in neural phaeochromocytoma-dervied PC12 cells. *ACS Nano*, **4**, 3181–3186.

236. Li, Y., Liu, Y., Fu, Y. *et al.* (2012) The triggering of apoptosis in macrophages by pristine graphene through the MAPK and TGF-beta signaling pathways. *Biomaterials*, **33**, 402–411.

237. Tu, Y., Lv, M., Xiu, P. *et al.* (2013) Destructive extraction of phospholipids from Escherichia coli membranes by graphene nanosheets. *Nat. Nanotechnol.*, **8**, 594–601.

238. Dallavalle, M., Calvaresi, M., Bottoni, A. *et al.* (2015) Graphene can wreak havoc with cell membranes. *ACS Appl. Mater. Interfaces*, **7**, 4406–4414.

239. Chang, Y., Yang, S.T., Liu, J.H. *et al.* (2011) In vitro toxicity evaluation of graphene oxide on A549 cells. *Toxicol. Lett.*, **200**, 201–210.

240. Wan, B., Wang, Z.X., Lv, Q.Y. *et al.* (2013) Single-walled carbon nanotubes and graphene oxides induce autophagosome accumulation and lysosome impairment in primarily cultured murine peritoneal macrophages. *Toxicol. Lett.*, **221**, 118–127.

241. Ivask, A., Voelcker, N.H., Seabrook, S.A. *et al.* (2015) DNA melting and genotoxicity induced by silver nanoparticles and graphene. *Chem. Res. Toxicol.*, **28** (5), 1023–1035.

242. Hinzmann, M., Jaworski, S., Kutwin, M. *et al.* (2014) Nanoparticles containing allotropes of carbon have genotoxic effects on glioblastoma multiforme cells. *Int. J. Nanomed.*, **9**, 2409–2417.

243. Sasidharan, A., Panchakarla, L.S., Chandran, P. *et al.* (2011) Differential nano-bio interactions and toxicity effects of pristine versus functionalized graphene. *Nanoscale*, **3**, 2461–2464.

244. Wang, A., Pu, K., Dong, B. *et al.* (2013) Role of surface charge and oxidative stress in cytotoxicity and genotoxicity of graphene oxide towards human lung fibroblast cells. *J. Appl. Toxicol.*, **33** (10), 1156–1164.

245. Hu, W., Peng, C., Lv, M. *et al.* (2011) Protein corona-mediated mitigation of cytotoxicity of graphene oxide. *ACS Nano*, **5**, 3693–3700.

246. Chatterjee, N., Eom, H.J., and Choi, J. (2014) A systems toxicology approach to the surface functionality control of graphene-cell interactions. *Biomaterials*, **35**, 1109–1127.

247. Qiao, Y., An, J., and Ma, L. (2013) Single cell array based assay for in vitro genotoxicity study of nanomaterials. *Anal. Chem.*, **85**, 4107–4112.

248. De Marzi, L., Ottaviano, L., Perrozzi, F. *et al.* (2014) Flake size-dependent cyto and genotoxic evaluation of graphene oxide on in vitro A549, Caco2 and vero cell lines. *J. Biol. Regul. Homeost. Agents*, **28**, 281–289.

249. Ryu, H.W., Lee, D.H., Won, H.R. *et al.* (2015) Influence of toxicologically relevant metals on human epigenetic regulation. *Toxicol. Res.*, **31** (1), 1–9.

250. Methner, M.M., Birch, M.E., Evans, D.E. *et al.* (2007) Identification and characterization of potential sources of worker exposure to carbon nanofibers during polymer composite laboratory operations. *J. Occup. Environ. Hyg.*, **4** (12), D125–D130.

251. Methner, M., Hodson, L., Dames, A. *et al.* (2010) Nanoparticle emission assessment technique (NEAT) for the identification and measurement of potential inhalation exposure to engineered nanomaterials— part B: results from 12 field studies. *J. Occup. Environ. Hyg.*, **7** (3), 163–176.

252. Murray, A.R., Kisin, E.R., Tkach, A.V. *et al.* (2012) Factoring-in agglomeration of carbon nanotubes and nanofibers for better prediction of their toxicity versus asbestos. *Part. Fibre Toxicol.*, **9**, 10.

253. Delorme, M.P., Muro, Y., Arai, T. *et al.* (2012) Ninety-day inhalation toxicity study with a vapor grown carbon nanofiber in rats. *Toxicol. Sci.*, **128** (2), 449–460.

254. Darne, C., Terzetti, F., Coulais, C. *et al.* (2010) In vitro cytotoxicity and transforming potential of industrial carbon dust (fibers and particles) in syrian hamster embryo (SHE) cells. *Ann. Occup. Hyg.*, **54** (5), 532–544.

255. Kisin, E.R., Murray, A.R., Sargent, L. *et al.* (2011) Genotoxicity of carbon nanofibers: are they potentially more or less dangerous than carbon nanotubes or asbestos? *Toxicol. Appl. Pharmacol.*, **252** (1), 1–10.

256. Wang, L., Castranova, V., Mishra, A. *et al.* (2010) Dispersion of single-walled carbon nanotubes by a natural lung surfactant for pulmonary in vitro and in vivo toxicity studies. *Part. Fibre Toxicol.*, **7**, 31.

257. Cohen, J.M., Teeguarden, J.G., and Demokritou, P. (2014) An integrated approach for the in vitro dosimetry of engineered nanomaterials. *Part. Fibre Toxicol.*, **11**, 20.

258. Benigni, R. (2012) Alternatives to the carcinogenicity bioassay for toxicity prediction: are we there yet? *Expert Opin. Drug Metab. Toxicol.*, **8**, 4.

259. Creton, S., Aardema, M.J., Carmichael, P.L. *et al.* (2012) Cell transformation assays for prediction of carcinogenic potential: state of the science and future research needs. *Mutagenesis*, **27**, 93–101.

260. OECD (2007) Detailed review on cell transformation assays for detection of chemical carcinogens, in *OECD Environment, Health and Safety, Series on Testing and Assessment*, vol. 31. OECD, Paris, France, 1–164.

261. Lee, J., Lilly, G.D., Doty, R.C. *et al.* (2009) In vitro toxicity testing of nanoparticles in 3D cell culture. *Small*, **5** (10), 1213–1221.

262. Bhise, N.S., Ribas, J., Manoharan, V. *et al.* (2014) Organ-on-a-chip platforms for studying drug delivery systems. *J. Controlled Release*, **190**, 82–93.

263. Snyder-Talkington, B.N., Dong, C., Zhao, X. *et al.* (2015) Multi-walled carbon nanotube-induced gene expression in vitro: concordance with in vivo studies. *Toxicology*, **328**, 66–74.

264. Endes, C., Schmid, O., Kinnear, C. *et al.* (2014) An in vitro testing strategy towards mimicking the inhalation of high aspect ratio nanoparticles. *Part. Fibre Toxicol.*, **11**, 40.

265. Chortarea, S., Clift, M.J., Vanhecke, D. *et al.* (2015) Repeated exposure to carbon nanotube-based aerosols does not affect the functional properties of a 3D human epithelial airway model. *Nanotoxicology*, **9** (8), 983–993.

266. Watson, C., Ge, J., Cohen, J. *et al.* (2014) High-throughput screening platform for engineered nanoparticle-mediated genotoxicity using CometChip technology. *ACS Nano*, **8**, 2118–2133.

267. Maslov, A.Y., Quispe-Tintaya, W., Gobacheva, T. *et al.* (2015) High-throughput sequencing in mutation detection: a new generation of genotoxicity tests? *Mutat. Res.* doi: 10.1016/j.mrfmmm.2015.03.014

268. Morimoto, Y., Izumi, H., and Kuroda, E. (2014) Significance of persistent inflammation in respiratory disorders induced by nanoparticles. *J. Immunol. Res.*, **2014**, 962871.

269. Tran, C.L., Buchanan, D., Cullen, R.T. *et al.* (2000) Inhalation of poorly soluble particles. II. Influence of particle surface area on inflammation and clearance. *Inhalation Toxicol.*, **12**, 1113–1126.

270. Kumar, A. and Dhawan, A. (2013) Genotoxic and carcinogenic potential of engineered nanoparticles: an update. *Arch. Toxicol.*, **87**, 1883–1900.

271. Godwin, H., Nameth, C., Avery, D. *et al.* (2015) Nanomaterial categorization for assessing risk potential to facilitate regulatory decision-making. *ACS Nano*, **9**, 3409–3417.

272. Nel, A.E. (2013) Implementation of alternative test strategies for the safety assessment of engineered nanomaterials. *J. Intern. Med.*, **274** (6), 561–577.

273. Snyder-Talkington, B., Pacurari, M., Dong, C. *et al.* (2013) Systematic analysis of multiwalled carbon nanotube-induced cellular signaling and gene expression in human small airway epithelial cells. *Toxicol. Sci.*, **133** (1), 79–89.

274. Husain, M., Saber, A.T., Guo, C. *et al.* (2013) Pulmonary instillation of low doses of titanium dioxide nanoparticles in mice leads to particle retention and gene expression changes in the absence of inflammation. *Toxicol. Appl. Pharmacol.*, **269** (3), 250–262.

275. Singh, S., Manshian, B., Jenkins, G.J. *et al.* (2009) Nanogenotoxicology: the DNA damaging potential of engineered nanomaterials. *Biomaterials*, **30**, 3891–3914.

276. Karlsson, H.L. (2010) The comet assay in nanotoxicology research. *Anal. Bioanal. Chem.*, **398**, 651–666.

277. Magdolenova, Z., Collins, A., Kumar, A. *et al.* (2014) Mechanisms of genotoxicity. A review of in vitro and in vivo studies with engineered nanoparticles. *Nanotoxicology*, **8**, 233–278.

278. Møller, P., Jensen, D.M., Christoffersen, D.V. *et al.* (2015) Measurement of oxidative damage to DNA in nanomaterial exposed cells and animals. *Environ. Mol. Mutagen.*, **56** (2), 97–110.

279. Møller, P., Hemmingsen, J.G., Jensen, D.M. *et al.* (2015) Applications of the comet assay in particle toxicology: air pollution and engineered nanomaterials exposure. *Mutagenesis*, **30** (1), 67–83.

280. OECD (2014) *Genotoxicity of Manufactured Nanomaterials: Report of the OECD Expert Meeting*, Series on the Safety of Manufactured Nanomaterials, vol. 43. OECD, Paris, France, p. 1–37.

281. Landsiedel, R., Kapp, M.D., Schulz, M. *et al.* (2009) Genotoxicity investigations on nanomaterials: methods, preparation, and characterization of test material, potential artifacts and limitations-many questions, some answers. *Mutat. Res.*, **681**, 241–258.